NASA Contractor Report 177595

High Efficiency Pump for Space Helium Transfer

Robert Hasenbein, Michael G. Izenson, Walter L. Swift, and Herbert Sixsmith

CONTRACT NAS2-12950
December 1991

National Aeronautics and
Space Administration

NASA Contractor Report 177595

High Efficiency Pump for Space Helium Transfer

Robert Hasenbein, Michael G. Izenson, Walter L. Swift, and Herbert Sixsmith

Creare Inc.
P.O. Box 71
Hanover, NH 03755

Prepared for
Ames Research Center
CONTRACT NAS2-12950
December 1991

National Aeronautics and
Space Administration

Ames Research Center
Moffett Field, California 94035-1000

TABLE OF CONTENTS

LIST OF FIGURES

LIST OF FIGURES (Continued)

LIST OF TABLES

1. SUMMARY

A centrifugal pump has been developed for the efficient transfer of liquid helium in space. The pump can be used to refill cryostats on orbiting satellites which use liquid helium for refrigeration at extremely low temperatures. The pump meets the head and flow requirements for on-orbit helium transfer: a flow rate of 800 L/hr at a head of 128 J/kg. The design head and flow are met with zero net positive suction head, which is the condition in an orbiting helium supply Dewar. The calculated mass transfer efficiency is 0.99. Steel ball bearings are used with nylon/fiberglass/teflon composite retainers to provide solid lubrication. These bearings have demonstrated the longest life in liquid helium endurance tests under simulated pumping conditions.

Important elements of this development effort are:

1) screening test on several types of candidate bearings,

2) pump tests in several fluids at temperatures between 4 and 300 K, and

3) a comparison of pump performance with and without an inducer.

The technology developed in this project has application for terrestrial liquid cryogenic facilities, as well as on-orbit transfer of cryogenic rocket propellants.

2. INTRODUCTION

This is the final technical report of a Phase II SBIR project performed by Creare Inc. for NASA Ames Research Center. The goal of this project is to develop a mechanical pump for the efficient transfer of liquid helium in space. Helium transfer is necessary to refill depleted cryostats on board orbiting satellites which use liquid helium for passive refrigeration at extremely low temperatures. We have designed, built, and demonstrated a centrifugal pump to accomplish liquid helium transfer with high reliability and efficiency.

The main accomplishments of this project are:

1. *Design and fabrication.* We have designed and fabricated a centrifugal pump for liquid helium transfer in space. The pump is made up of an a.c. induction motor, a centrifugal impeller, a helical inducer, two ball bearings, and a pump housing.

2. *Demonstrated operation.* We have demonstrated that the pump meets its design specifications for head and flow by testing the pump in liquid helium. Calculations show that the pump will achieve a mass transfer efficiency of 0.99 when used for on-orbit helium transfer.

3. *Bearing test data.* The pump design is simple and reliable. To assess the reliability of the bearings, we tested a variety of ball bearings at cryogenic temperatures and selected the most robust for service in the transfer pump. The bearings are composed of 440C stainless steel balls and races with nylon/ fiberglass/teflon composite retainers. They have operated reliably in liquid helium for 24 hours.

Centrifugal pumps have been used successfully in liquid helium. Ludtke (1975), Steward (1986), and Daney and Ludtke (1987) at the National Bureau of Standards (now the National Institute of Standards and Technology) have tested a centrifugal pump in liquid helium and reported its operating characteristics in normal and superfluid liquid helium. The tests at NIST (NBS) have shown the potential for cavitation free operation in normal liquid helium even with negative values of net positive suction head. The NIST pump included a helical inducer for improved performance at low NPSH. The researchers at NIST have accumulated significant experience using ball bearings for the liquid helium pump. One set of bearings has operated successfully in that pump for 70 hours at rotating speeds of 5000-7000 rpm. Sixsmith and Giarratano (1970) have also tested a centrifugal pump with ball bearings in liquid helium.

The basic bearing concept has already been proven by several workers. Wilson et al. (1961) at NBS identified bearings with stainless steel balls and raceways with plastic-composite retainers as promising candidates. Brewe, Scibbe and Anderson (1966) also report good performance from tests of steel bearings with composite retainers. Retainers are typically a polymer such as Rulon or PTFE to provide solid lubrication and a structural material like fiberglass to provide strength.

This SBIR project builds upon and extends previous efforts in the areas of pump efficiency and reliability. The transfer pump developed in this project has an overall efficiency of 0.45, compared to 0.30 for previous pumps. Increased efficiency is the result

of higher rotating speeds, which increases the specific speed of the impeller compared to the earlier NIST design. The bearings used in the pump have been run in liquid helium and tested extensively for signs of wear. We have selected the most robust bearings from a field of four candidate designs, including advanced materials and surface treatments.

The remainder of this report describes the pump and its development in more detail. Section 3 describes the transfer pump, presents key performance data, shows that the design requirements have been met, and demonstrates that the pump achieves high mass transfer efficiency. Section 4 documents the testing and development effort. The final pump design is based on fundamental fluid mechanical considerations as well as test experience with several different pump housings and impellers. Bearings for the pump have been selected based on results of endurance tests on a variety of designs, including several advanced materials and surface treatments. Section 5 discusses the results of this project in the general context of pump performance, transfer of cryogens in space, and pump performance at low available suction head.

3. DESCRIPTION AND OPERATION OF THE PUMP

The liquid helium transfer pump is a straightforward mechanical design. The pump has a centrifugal impeller which imparts energy to the liquid and a helical inducer for improved performance at low values of net positive suction head. The pump is powered by an a.c. induction motor cooled by the liquid helium in the supply Dewar. The pump shaft is held in position by solid-lubricated ball bearings. The pump operates submerged in the liquid helium supply. The design flow rate is 800 L/hr (222×10^{-6} m^3/s) with a head of 128 J/kg at an impeller rotational speed of 12,000 rpm (200 Hz). This performance is achieved with a net positive suction head of zero at the elevation of the inducer.

Figure 3.1 is a schematic of the liquid helium transfer pump showing the main components and the liquid helium flow path. The impeller and inducer are mounted on the end of a shaft which is supported by bearings inside the motor. The motor is fastened to the outside of the pump housing where it is cooled by the liquid helium in the supply tank. The pump is 4.54 inches (11.5 cm) in overall diameter and 3.4 inches (8.7 cm) in length.

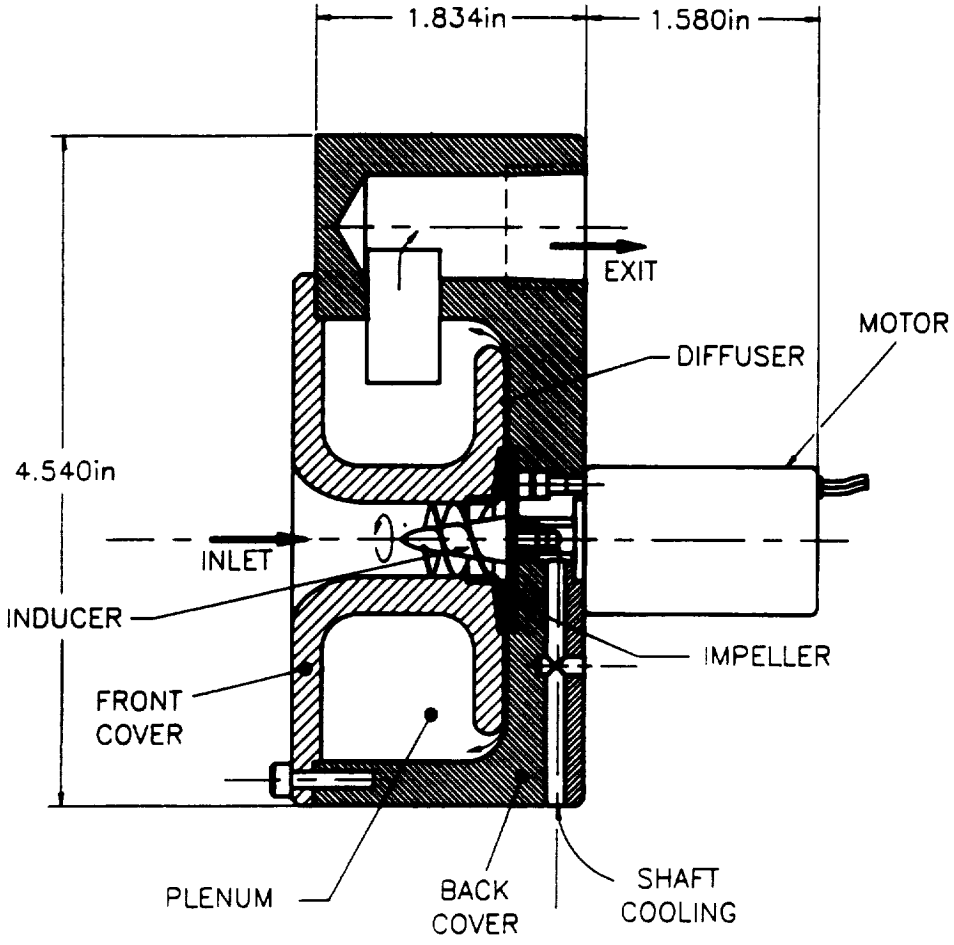

Figure 3.1. LIQUID HELIUM TRANSFER PUMP

Liquid helium from the supply Dewar flows into the pump through the inlet. The liquid first enters the inducer and then flows into the centrifugal impeller. The inducer is resistant to flow blockage from cavitation and imparts a small amount of head to the inlet stream to reduce the tendency of the pump to cavitate in the centrifugal impeller. The impeller then provides most of the pressure rise through the pump as a result of centrifugal forces. The liquid helium next flows radially away from the impeller through the diffuser region between the front and back covers, then enters the plenum which surrounds the inlet. As the helium decelerates in the diffuser and plenum, its kinetic energy is (partially) converted into increased pressure. From the plenum, the liquid helium enters the fluid exit and leaves the pump.

Figure 3.2 is a photograph of the transfer pump showing an exploded view of the main components. From left to right, they are the pump front cover, inducer, centrifugal impeller, pump back cover, and motor.

3.1 Design Specifications

The transfer pump meets design specifications for a mission to refill a large, depleted liquid helium cryostat on-board an orbiting satellite. NASA Ames Research Center (Kittel, 1986) has defined the mission scenario and performed analysis to specify design requirements for the transfer pump. Lee (1987) presents specific design requirements for refilling the cryostat on board the Space Infrared Telescope Facility (SIRTF). We have adopted the SIRTF refill requirements as the design basis for the transfer pump. A liquid helium resupply Dewar is filled on Earth and then sent to orbit. The transfer pump operates inside the resupply Dewar where it receives helium from a liquid acquisition device and delivers high-pressure helium to a transfer line. The liquid helium flows through the transfer line into the receiving Dewar on-board the satellite. The volume of the receiving Dewar is on the order of 4000 L.

Table 3.1 summarizes the design specifications for the transfer pump. They are:

1. *Hydraulic requirements.* The hydraulic requirements for liquid helium transfer are based on analyses of the SIRTF refill mission performed by NASA. The first phase of the refill is cooldown, in which the temperature of the receiver Dewar is reduced by boiling liquid helium. The flow rate in this phase is limited to 150 L/hr to control the cooling rate of the SIRTF mirror. There is a relatively large pressure drop of 23 kPa in the transfer line due to two-phase flow. Once the receiver Dewar is cold, rapid refilling begins. In this phase, the flow rate is 800 L/hr and the pressure drop in the transfer line is 16 kPa. The net positive suction head at the inlet of the transfer pump is zero, since the fluid in the supply Dewar is saturated and there are insufficient body forces on orbit to provide any significant pressure.

NPSH is the difference in static head between the liquid at the pump inlet and saturated vapor. At low NPSH, pumps must be designed to avoid cavitation in the impeller which may reduce the generated head or even stop all liquid flow.

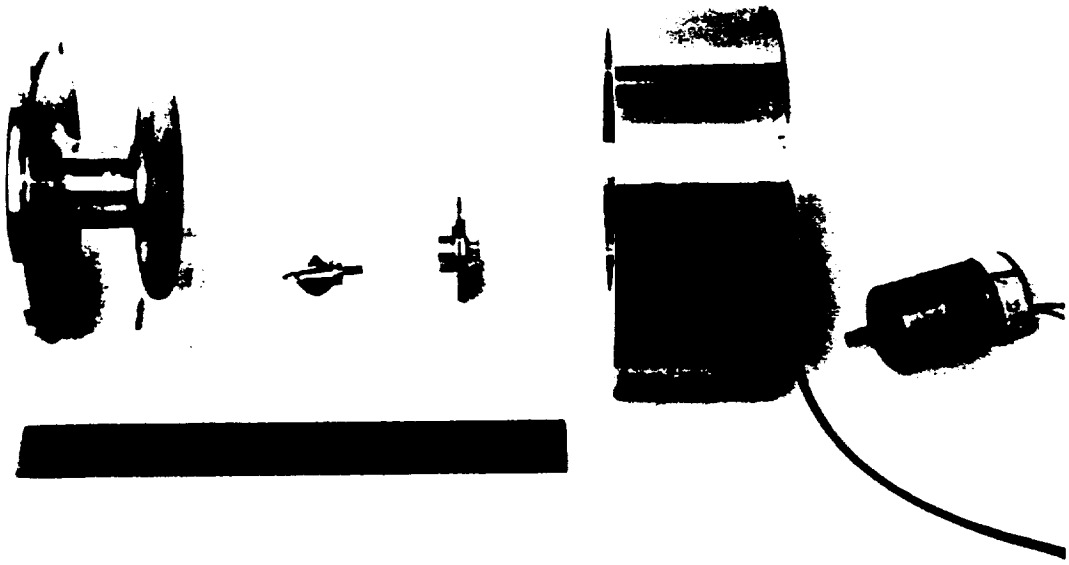

Figure 3.2. TRANSFER PUMP

Table 3.1 DESIGN REQUIREMENTS FOR LIQUID HELIUM TRANSFER IN SPACE	
Hydraulic requirements:	
Flow rate for cooldown (L/hr):	150
Pressure rise for cooldown (kPa):	23
Flow rate for cold transfer (L/hr):	800
Pressure rise for cold transfer (kPa):	16
Available net positive suction head:	0
Mass transfer efficiency:	0.99
Reliability:	Assured operation for 500 hours
Interface:	
Power supply:	3-phase a.c. 115 V L-N ≤ 600 Hz 4-wire Y conf.

2. *Efficiency*. The transfer pump must accomplish the refilling mission with minimal loss of helium. Inefficiency in the pump will add excessive energy to the liquid helium and result in additional boiloff. However, the amount of energy required to pump the liquid is so small compared to the heat of vaporization that the mass transfer efficiency is quite insensitive to the pump's mechanical efficiency. We have selected a target of 0.99 mass transfer efficiency for the transfer pump at rated conditions.

Figure 3.3 shows how the mass transfer efficiency depends on the pump efficiency. The pump efficiency is the pumping power delivered to the fluid (flow rate × pressure rise) divided by the total power input to the pump. Curves are shown for constant pump power and constant flow rate. At the design point flow rate of 800 L/hr, the transfer pump has demonstrated an efficiency of 0.45 which implies a mass transfer efficiency of 0.99 . In these calculations, the mass transfer efficiency is the ratio of mass flow into the receiver Dewar to the total of the mass flow into the receiver plus the boiloff mass.

3. *Reliability*. The transfer pump must operate with high reliability since it is a critical mission component. A single transfer mission is expected to require 15-20 hours of continuous operation. The key components of the transfer pump which affect reliability are the bearings. Bearings used in the transfer pump have demonstrated reliable operation in liquid helium tests for 24 hours of operation without a single failure. Detailed post-test examinations of these bearings show no sign of imminent failure after 24 hours of cryogenic operations. With a simple change of bearings between missions, the pump should operate reliably for a large number of missions.

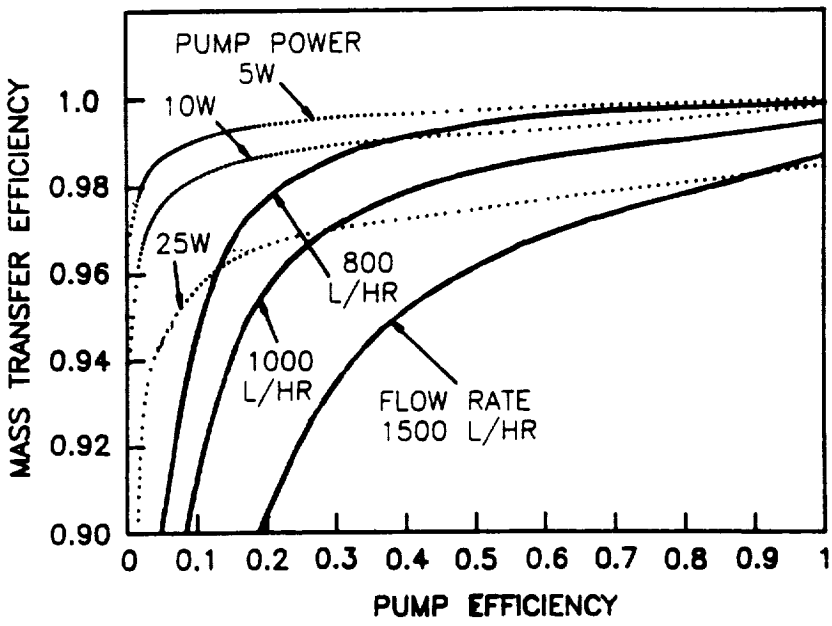

Figure 3.3. RELATIONSHIP BETWEEN MASS TRANSFER EFFICIENCY AND PUMP EFFICIENCY

Reliability specifications for the Superfluid Helium On-Orbit Transfer (SHOOT) experiment present a goal of assured operation for 500 hours. Five hundred-hour tests of many bearings were beyond the scope of this project. However, we have examined bearings in detail after 24 hour cryogenic tests and identified the most promising candidates for future development.

4. *Interface requirements*. The mechanical and electrical interfacing requirements for the transfer pump are adopted from the requirements for the planned SHOOT experiment (Superfluid Helium On-Orbit Transfer--NASA/ARC, 1987). The pump electrical power supply must be three-phase alternating current with a frequency up to 600 Hz. Voltage must be 115 V L-N.

3.2 Pump Operating Characteristics

The pump operating characteristics satisfy the design specifications for liquid helium transfer: head and flow requirements are met for both the cooldown and cold transfer phases of the refill operation with an available NPSH of zero. Pump operation has been measured in a series of tests in liquid helium. The test facility and procedures are fully described in Section 4.1.

Figure 3.4 presents pump performance data from tests in liquid helium. The figure shows pump characteristic curves, in which the head generated by the pump is plotted as a function of the flow rate. Characteristic curves are presented for two different pump rotating speeds: 12,000 and 8,000 rpm. Head is the energy per unit mass which the pump imparts to the liquid and is measured in units of J/kg. The flow rate is the net flow measured at the exit of the pump, and thus does not include any small liquid flow which may leak from the pump. Also shown in the figure are the two design points corresponding to cold transfer and cooldown for refilling the SIRTF Dewar. The design point head and flow rate have been achieved for both phases of the refilling mission.

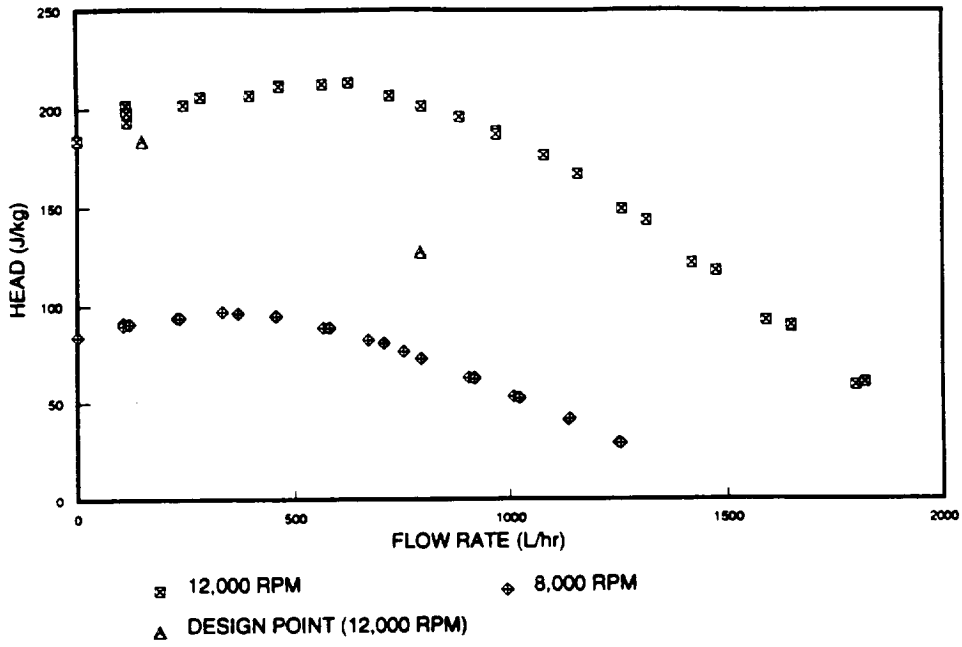

Figure 3.4. TRANSFER PUMP PERFORMANCE DATA, LIQUID HELIUM TESTS

Figure 3.5 presents the pump performance data in dimensionless form. Head has been reduced to a head coefficient and the flow rate is expressed as a flow coefficient. As expected, the data from tests at different pump speeds collapse to a single homologous pump curve. The flow coefficient, φ, is the radial velocity of the liquid divided by the tangential velocity of the impeller evaluated at the exit of the impeller:

$$\varphi \equiv \frac{C_{m2}}{U_2} = \frac{Q}{\pi^2 D_2^{\,2} b_2 N} \tag{3.1}$$

where
- C_{m2} = meridional (radial) velocity at impeller exit (m/s),
- U_2 = impeller tangential velocity at impeller exit (m/s),
- Q = total pump flow rate (m^3/s),
- D_2 = impeller diameter (m),
- b_2 = blade height at impeller exit (m), and
- N = pump rotational speed (rev/sec).

The head coefficient, ψ, is the head rise across the pump normalized by dividing by the square of the impeller tangential velocity:

$$\psi \equiv \frac{g_o H}{U_2^{\,2}} = \frac{g_o H}{\pi^2 N^2 D_2^{\,2}} \tag{3.2}$$

where g_oH = fluid head at impeller exit (J/kg).

Since the performance measured at two different pump speeds can be reduced to a single dimensionless performance curve, conventional centrifugal pump scaling applies to the transfer pump: the flow rate varies directly with the rotating speed and the head varies with the square of the rotating speed. The collapsed curve also gives confidence that the test instrumentation functions properly over a range of test parameters.

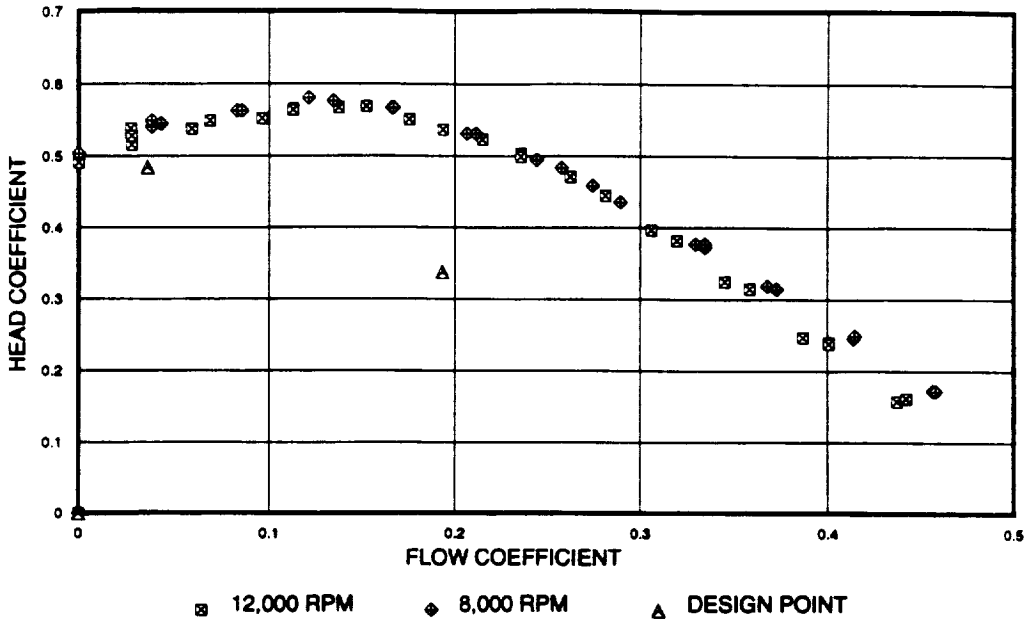

Figure 3.5. HOMOLOGOUS PERFORMANCE CURVES REDUCED FROM LHe DATA

The nominal rotating speed of the pump is 12,000 rpm. At this speed the pump achieves the flow rate and head specifications for cooldown and cold transfer to the SIRTF Dewar. We have also found that this speed results in acceptable bearing performance. At 12,000 rpm, the pump bearings are able to operate in liquid helium for 24 hours with no effect on pump performance.

Figure 3.6 shows pump performance as a function of the net positive suction head at the inducer inlet. The data show that the pump is effective even at NPSH levels less than zero (in the tests, the saturated liquid level was below the elevation of the impeller). Thus, the transfer pump meets the design requirement of effective pumping with zero available NPSH.

3.3 Bearings

The helium transfer pump uses two solid-lubricated ball bearings to carry axial and radial shaft loads. Section 4.2 details the bearing development effort. Figure 3.7 is a photograph of the bearings which are recommended for the transfer pump, which consist of 440C stainless steel balls and raceways with a fiberglass/teflon/nylon composite retainer. Similar technology has already been demonstrated in a centrifugal pump tested at the National Institute of Standards and Technology (Ludtke, 1975). In this project, we have extended the technology of cryogenic ball bearings by testing a range of bearing types including advanced materials and surface treatments, obtaining detailed endurance data, and identifying the bearings with the potential for highest reliability.

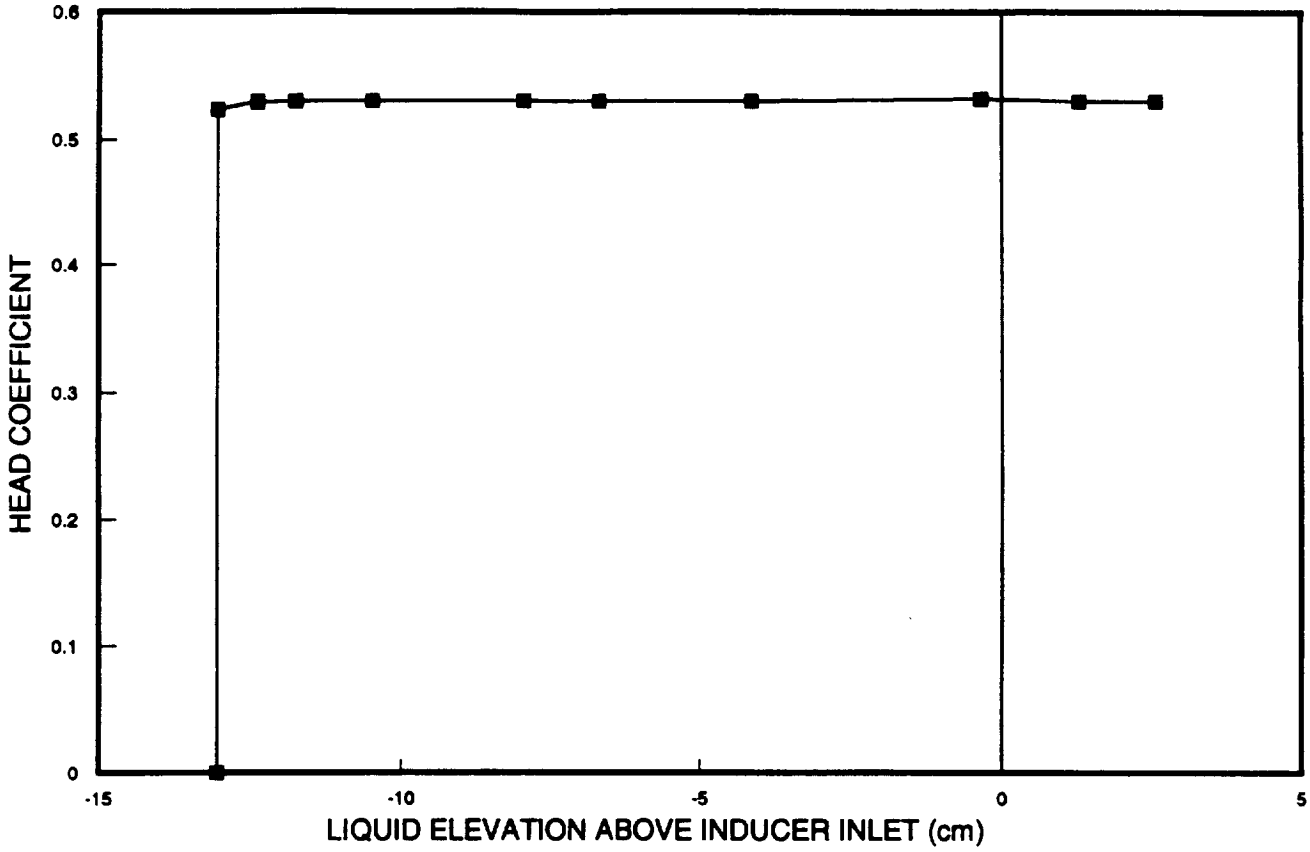

Figure 3.6. TRANSFER PUMP PERFORMANCE AT LOW NPSH

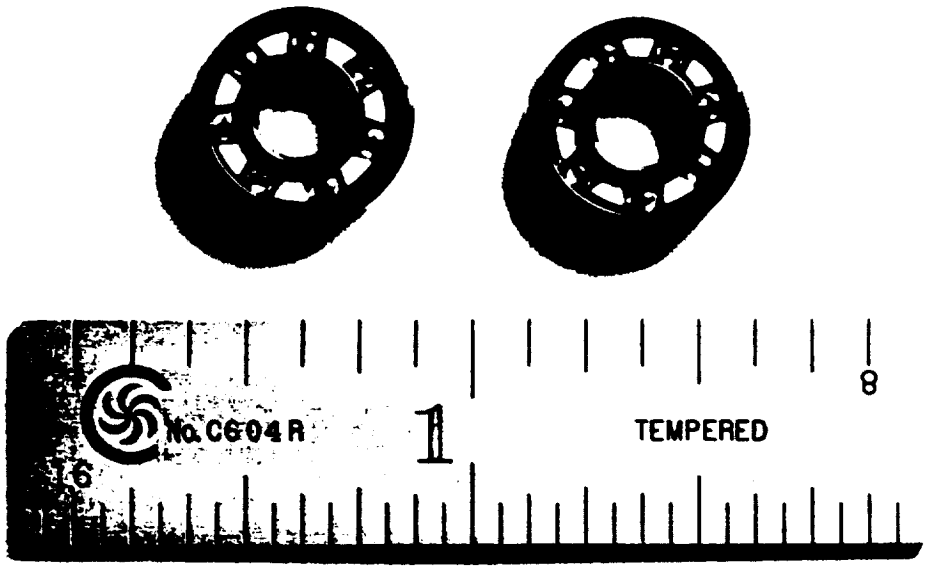

Figure 3.7. TRANSFER PUMP BEARINGS

3.4 Motor and Power Supply

The pump is powered by a three-phase, a.c. squirrel cage induction motor. An induction motor is selected due to its simplicity and lack of commutating electrical connections. Graphite brushes in commutators have very short lifetimes in dry environments in which no moisture is available for lubrication. The specific motor recommended for the transfer pump is a commercial product manufactured by Eastern Air Devices, product number E10GHP. Maximum current is 0.08 Amps and the voltage is 115 V_{L-L}. Housing, end caps, and shaft are fabricated from 416-stainless steel; laminations are 4750 steel. Power is supplied to this motor from a three-phase power supply.

4. TESTING AND DEVELOPMENT

The transfer pump has been built and demonstrated in an extensive development and testing program. Pump development involved an evolution of impeller designs. A preliminary pump was developed for demonstration of cryogenic operation and verification of instrument performance leading to the final transfer pump design described in Section 3. The evolution of this design proceeded on the basis of numerous bench-top and cryogenic tests to characterize the performance of the pumps and identify ways to improve the design. Development of bearings for the pump began with a survey of the existing state-of-the-art in cryogenic ball bearings. The most promising candidates were selected for screening tests in liquid helium. The bearing, which performed best in the screening tests, has been subjected to endurance testing under simulated pumping conditions in liquid helium.

4.1 Pump Testing and Development

This section describes the design and development effort which has produced the transfer pump described in Section 3. The main elements of this effort are:

- Impellers,
- The transfer pump inducer, and
- The cryogenic test facility.

Development of the impellers has proceeded in several stages, from the Phase I preliminary design through intermediate and final designs. Each new design has been guided by test results and increasing sophistication of the design models. The transfer pump inducer has been tested with the final impeller design. The design of the inducer is based on empirical data from the literature and fundamental fluid mechanic considerations. The test facility allowed for measurement of pump performance in liquid helium under prototypical conditions for space helium transfer as well as "bench top" tests using ambient air as the working fluid. The facility has provided data to guide the pump design and to demonstrate its performance.

4.1.1 Impellers

The pump impeller has evolved through three design phases, beginning with the preliminary design produced in Phase I of this project, progressing to intermediate designs used for initial bench-top and cryogenic tests, and ending with the final impeller design.

Early in Phase II, the preliminary pump design was modified slightly as a result of more detailed design studies. The purpose of this intermediate pump design was to quickly provide a simple impeller which could be used with the motor and housing to obtain early experience using the pump and test facility. Two intermediate impellers were fabricated, one with straight vanes and one with drilled holes for flow passages. Following tests with the intermediate impellers, the final impeller was designed with curved blades and a lower rotating speed. Speed was reduced to 12,000 rpm to improve bearing performance, for it was found that the ball bearings suffered rapid degradation at speeds of 21,000 rpm. Curved blades were adopted to more precisely control fluid flow in order to increase the fluid dynamic efficiency.

Figure 4.1 shows the impeller designs. The first is the preliminary design produced in Phase I of this project. Next are two intermediate impeller designs, one with drilled holes for flow passages and another with straight vanes. The fourth impeller is the final design used in the helium transfer pump. Table 4.1 lists the main design data for the three vaned impellers. (The drilled impeller was used mainly for verification of operation. Detailed fluid-dynamic design calculations have not been performed.)

Preliminary design from Phase I. The preliminary impeller design (or Impeller 1) is based on considerations of pump efficiency and specific speed and the design requirements for helium transfer in space. The objective of this design is to achieve maximum efficiency while meeting the head and flow requirements for the SIRTF refill mission.

Basic design parameters were selected by choosing a specific speed to maximize efficiency, then using the SIRTF refill requirements to set the rotating speed of the impeller. The specific speed is a shape factor defined for an impeller at its best efficiency point (BEP). It is a dimensionless parameter which is defined as:

$$N_s \equiv \frac{\omega \, Q^{0.5}}{(g_o H)^{0.75}} \tag{4.1}$$

where ω = pump rotational speed (rad/s),
Q = pump flow rate (m^3/s), and
g_oH = pump head (J/kg).

To maximize hydraulic efficiency, a specific speed of 0.90 was chosen for the preliminary design. Data from a wide range of pumps (Shepherd, 1956) suggest that maximum hydraulic efficiency is obtained for specific speeds near this value. Values for the flow rate ($Q = 222 \times 10^{-6}$ m^3/s) and head ($g_oH = 128$ J/kg) were selected from the SIRTF refill mission requirements for cold transfer. These values were used in Equation 4.1 to obtain the pump speed of 2300 rad/sec (which is equal to 22,000 rpm).

Impeller 1 was also predicted to meet the cooldown head and flow requirements. Characteristic data from other pumps' specific speeds close to 0.9 show that the cooldown flow requirements will also be met for a pump with a design point corresponding to cold transfer. This pump data is reported by Kamath and Swift (1982), Donsky (1961) and Kamath et al. (1982).

The diameter of Impeller 1 was determined using Euler's equation for pump head, reasonable assumptions about pump efficiency and inlet swirl, and empirical relations for the exit velocity. Euler's equation is:

$$\frac{g_o H}{\eta_p} = U_2 C_{u2} - U_1 C_{u1} \tag{4.2}$$

where U_2 = blade velocity at impeller exit,
C_{u2} = fluid tangential velocity at impeller exit,
U_1 = blade velocity at impeller inlet,
C_{u1} = fluid tangential velocity at impeller inlet,
η_p = pump efficiency.

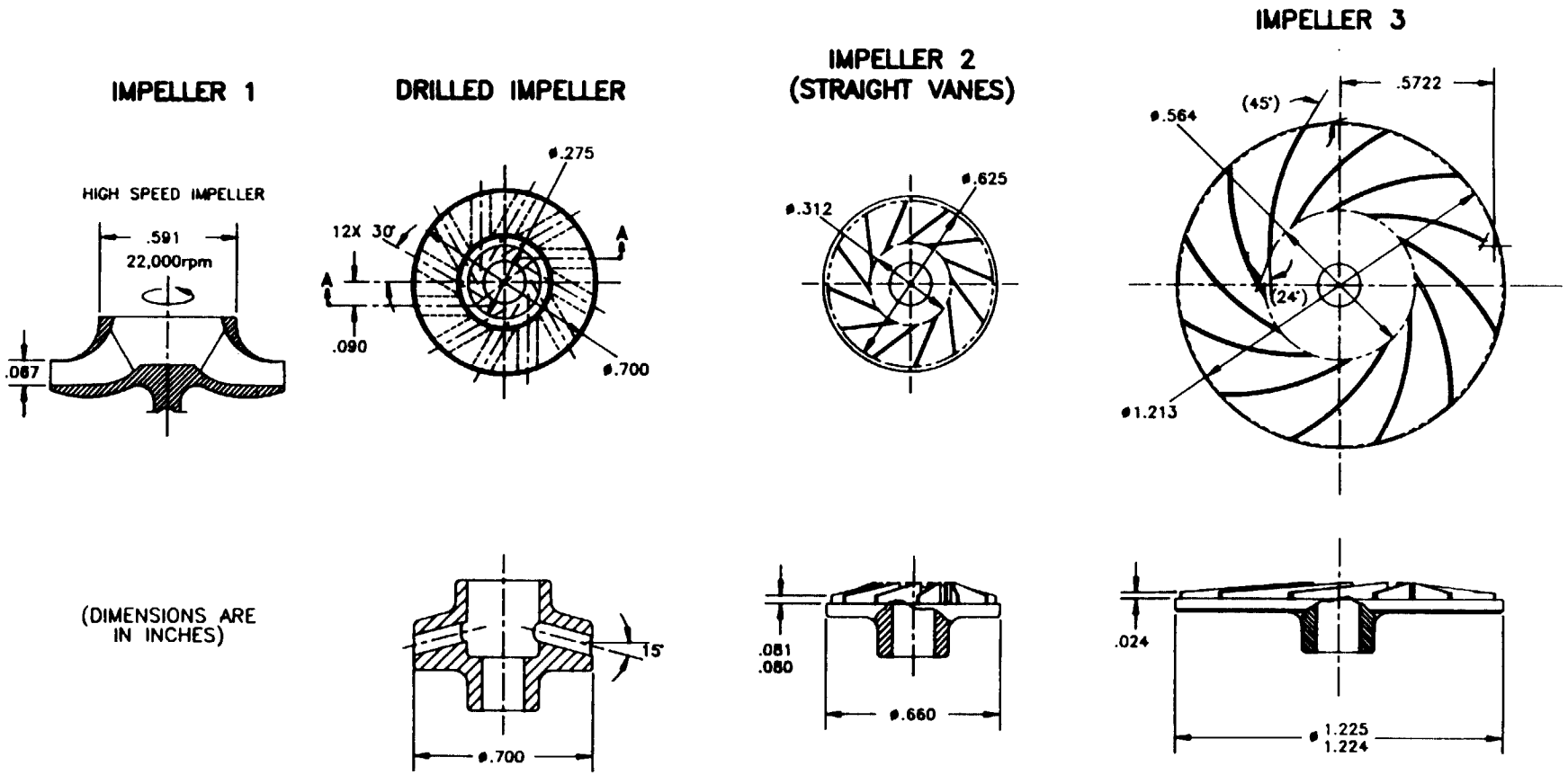

Figure 4.1. IMPELLER DESIGNS

Table 4.1. DESIGN DATA FOR TRANSFER PUMP IMPELLERS			
PARAMETER	PHASE I DESIGN (#1)	INTERMEDIATE DESIGN (STRAIGHT VANES) (#2)	FINAL DESIGN (#3)
Impeller:			
Exit diameter (cm)	1.5	1.588	3.08
Exit height (mm)	1.7	0.76	0.84
Inlet diameter (cm)	-	0.711	1.432
Inlet height (mm)	-	2.03	1.6
Exit blade angle (°)[1]	-	25.9	45.0
Inlet blade angle (°)[1]	-	62.0	65.0
Design speed (rpm)	22,000	22,000	12,000
Flow rate (L/hr)	800	780	800
Pressure rise (kPa)	16	16	18.6
Head (J/kg)	128	128	149
Efficiency (%)	75	60	55
Specific speed	0.90	0.89	0.49
1 - Blade angles are measured from a radial plane. 2 - Specific speed is dimensionless and uses angular velocity.			

To size the preliminary impeller, a pump efficiency of 0.6 was assumed and the inlet swirl (C_{u1}) was assumed to be zero. Empirically, it is known that for well-designed pumps the fluid tangential velocity is about 60% of the blade velocity at the impeller exit. With these assumptions and data, Equation 4.2 can be solved for the blade velocity at the impeller exit which, in combination with the known rotating speed, sets the impeller diameter. Blade height was selected to provide enough flow area at the impeller exit to achieve the desired exit velocity at the design point flow rate.

Drilled impeller. The drilled impeller is a simple part used primarily to verify mechanical operation of the pump and proper functioning of the test instruments. This impeller is simple to machine and provides a flow rate and pressure rise in the range of prototypical values. Early bench tests with this impeller proved operation of the pump and test facility in room-temperature air.

The impeller has 12 circular flow passages which are backswept at an angle of 30° at their inner diameter. The impeller diameter (0.700 inches) is selected to yield approximately the design pump head and flow rate using Equation 4.2.

The drilled impeller was tested in air at room temperature to verify mechanical operation of the pump and motor and to confirm operation of the test instruments. Figure 4.2 shows dimensionless performance curves measured in air at speeds of 12,000, 16,000 and 20,000 rpm. Head and flow coefficients for this impeller are smaller than for the final design due to the relatively low flow area and high losses in the small flow passages. Following these successful tests we began tests on the straight-vaned, intermediate design (Impeller 2).

Intermediate straight-vaned impeller. The purpose of this impeller (Impeller 2) was to provide reasonable performance and early experience with the pump assembly and test facility at cryogenic conditions. Simple design models were used which could be tested against pump performance data. Extensive tests in a variety of fluids provided key design data for the final impeller.

Table 4.1 lists the main design parameters for Impeller 2. The inlet and exit diameters of the impeller are 0.71 and 1.59 cm, respectively. The rotating speed is 22,000 rpm. There are 12 straight vanes with an exit angle of 25.9° (measured from a radial plane). The blades are 2.03 mm high at the inlet and 0.76 mm high at the exit.

Design of Impeller 2 began with the head and flow requirements for SIRTF refill and the speed calculation from Impeller 1. Speed remains the same because Impeller 2 has the same specific speed as the preliminary impeller for maximum hydraulic efficiency. The objective of the intermediate design was to specify details of the impeller geometry which meet the SIRTF refill requirements with good efficiency and also satisfy several additional constraints. These additional constraints are simplicity of fabrication and empirical "good design practice" for centrifugal pumps.

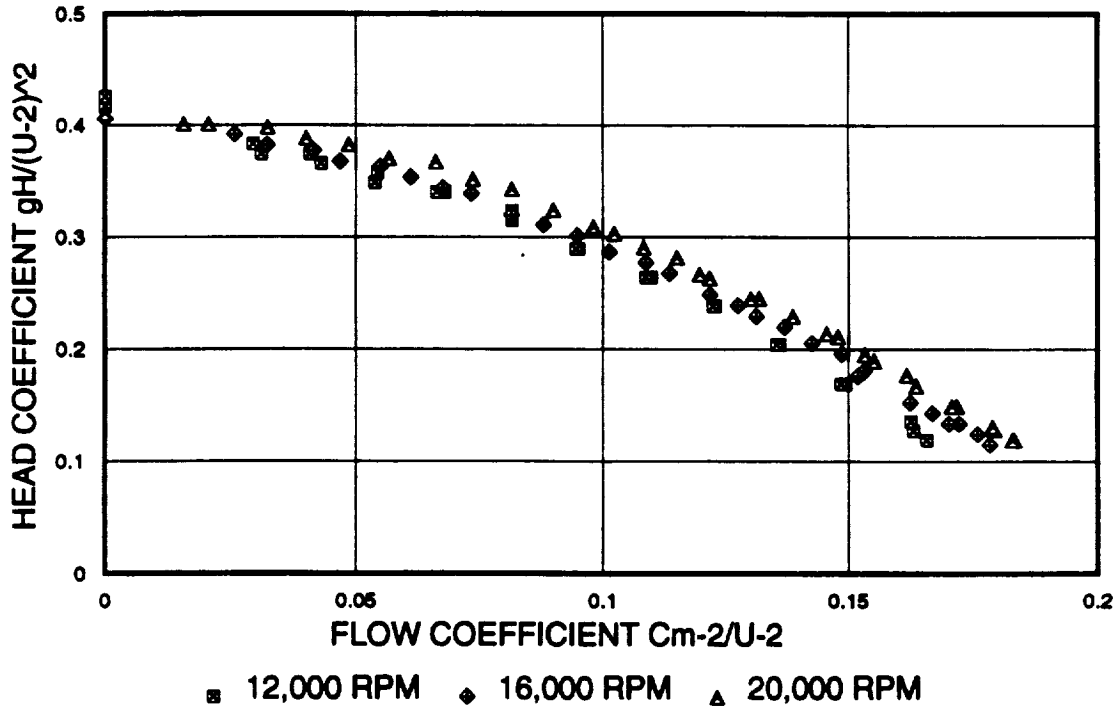

Figure 4.2. PERFORMANCE OF THE DRILLED IMPELLER IN AIR AT 300 K

Impeller geometry is specified by considering the relations between fluid and impeller velocities. Then the Euler Equation 4.2 is used to relate these velocities to the head generated by the impeller. Figure 4.3 presents vector diagrams of the fluid and impeller velocities at the inlet and exit. It is common design practice at the inlet to assume that there is negligible swirl in the fluid, so C_1 is perpendicular to U_1. At the exit of the impeller, fluid velocities are estimated by assuming a "slip factor" of 0.10. Slip is the term used to describe the phenomena in which liquid leaves the impeller at an angle less than the blade angle. The figure shows an "ideal" relative velocity at the impeller exit, W_2^*, which leaves the impeller at the impeller exit angle (β_2). The expected exit velocity W_2 is calculated by adding a tangential slip equal to the impeller tip velocity multiplied by the slip factor (0.1). In this way, the fluid velocity at the exit is related to the geometry of the impeller.

Figure 4.4 shows results of these design calculations for Impeller 2. Figure 4.4a shows the impeller tip velocity (U_2) required for two values of head as a function of the ratio C_{u2}/U_2. Figure 4.4b shows the impeller diameter required to reach these tip speeds at pump rotating speeds of 20,000, and 24,000 rpm. So for any combination of impeller diameter and rotating speed, Figure 4.4b indicates the resulting tip speed. The tip speed and the design head in Figure 4.4a correspond to a unique velocity ratio C_{u2}/U_2. The velocity ratio is related to the impeller blade design through the velocity triangles of Figure 4.3.

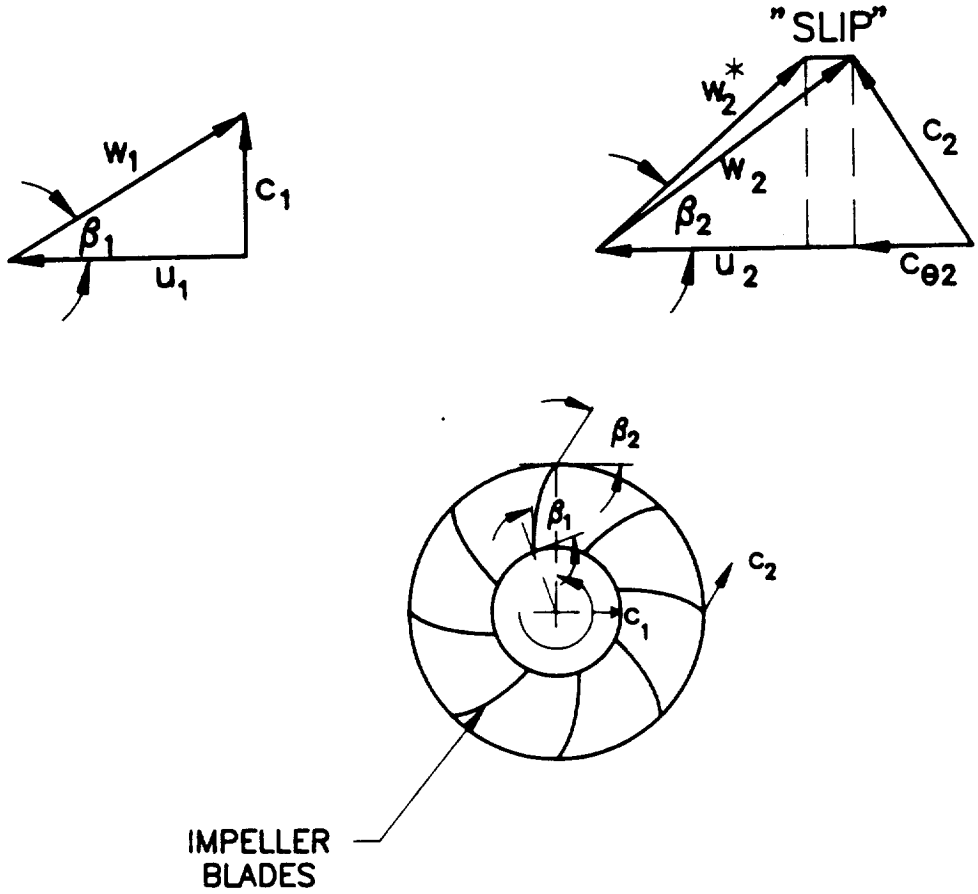

Figure 4.3. FLUID AND IMPELLER VELOCITY TRIANGLES

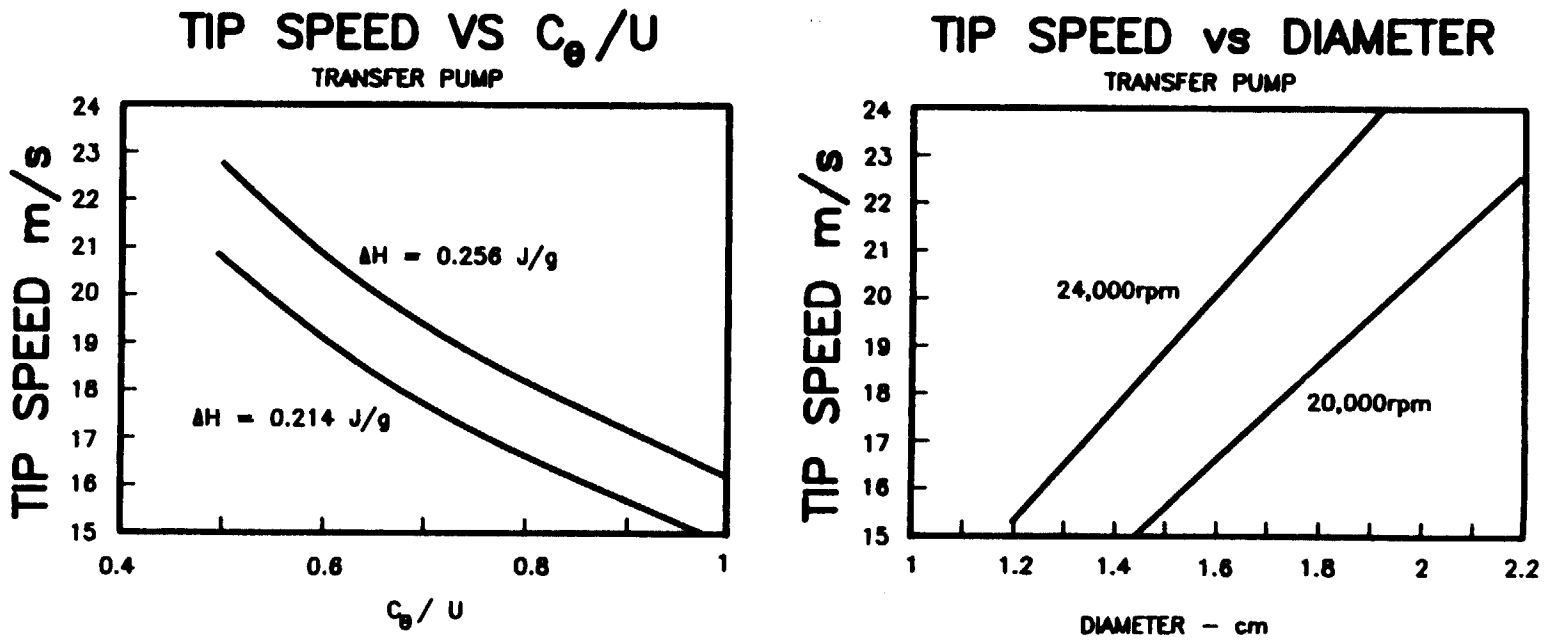

Figure 4.4. DESIGN CALCULATIONS FOR IMPELLER 2

The final design parameters for Impeller 2 were selected based on these calculations and three additional considerations: 1) impeller blades are straight for ease of fabrication, 2) the exit swirl (C_{u2}/C_{m2}) is approximately equal to 2, and 3) the diffusion ratio in the impeller (W_2/W_1) is equal to about 0.7. The last two design conditions are selected based on past design experience with pumps of similar specific speed. The resulting design parameters are listed in Table 4.1.

Impeller 2 was tested in a variety of working fluids at temperatures from 4 K to 300 K. The objectives of these tests were to:

- provide data for design of the final pump impeller,
- refine design of the pump housing and motor before the final impeller was ready,
- provide experience using the test facility at cryogenic conditions and indicate potential limitations of the test instruments.

The test series for Impeller 2 met all these objectives. Design models for the final impeller were based on performance data from Impeller 2. Results from these tests pointed out deficiencies in the design of the intermediate pump housing (motor cooling produced two-phase flow at the pump exit which could not be measured accurately at first by the test instrumentation) and the pump housing was altered to solve the problem.

Figures 4.5, 4.6, 4.7 and 4.8 show the performance of Impeller 2 measured in air (300 K), cold nitrogen vapor (194 K) and liquid helium (4.2 K), respectively.

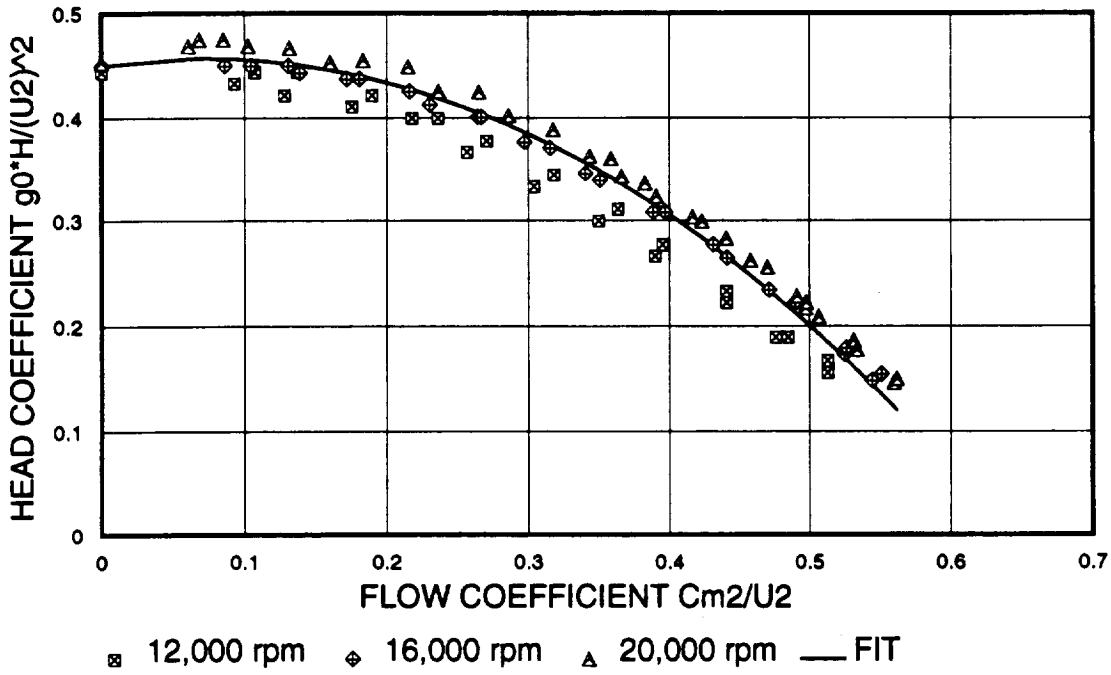

Figure 4.5. PERFORMANCE OF IMPELLER 2 IN AIR TESTS AT 300 K

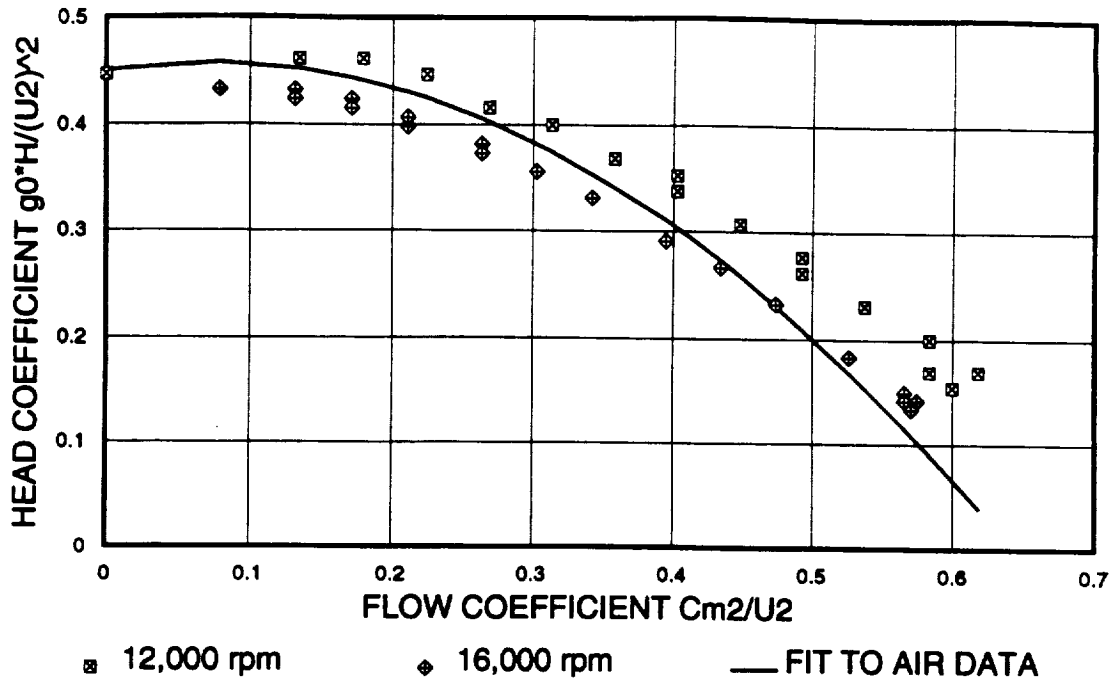

Figure 4.6. PERFORMANCE OF IMPELLER 2 IN COLD (194 K) NITROGEN VAPOR

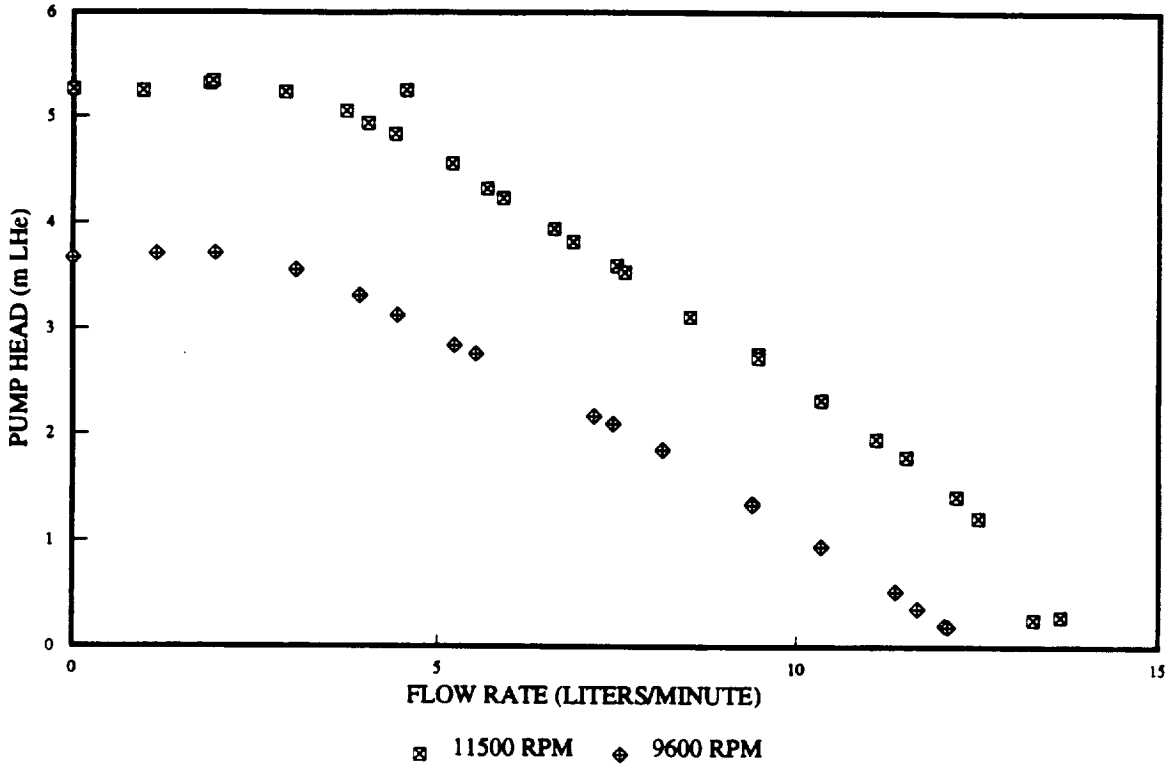

Figure 4.7. PERFORMANCE OF IMPELLER 2 IN LIQUID HELIUM

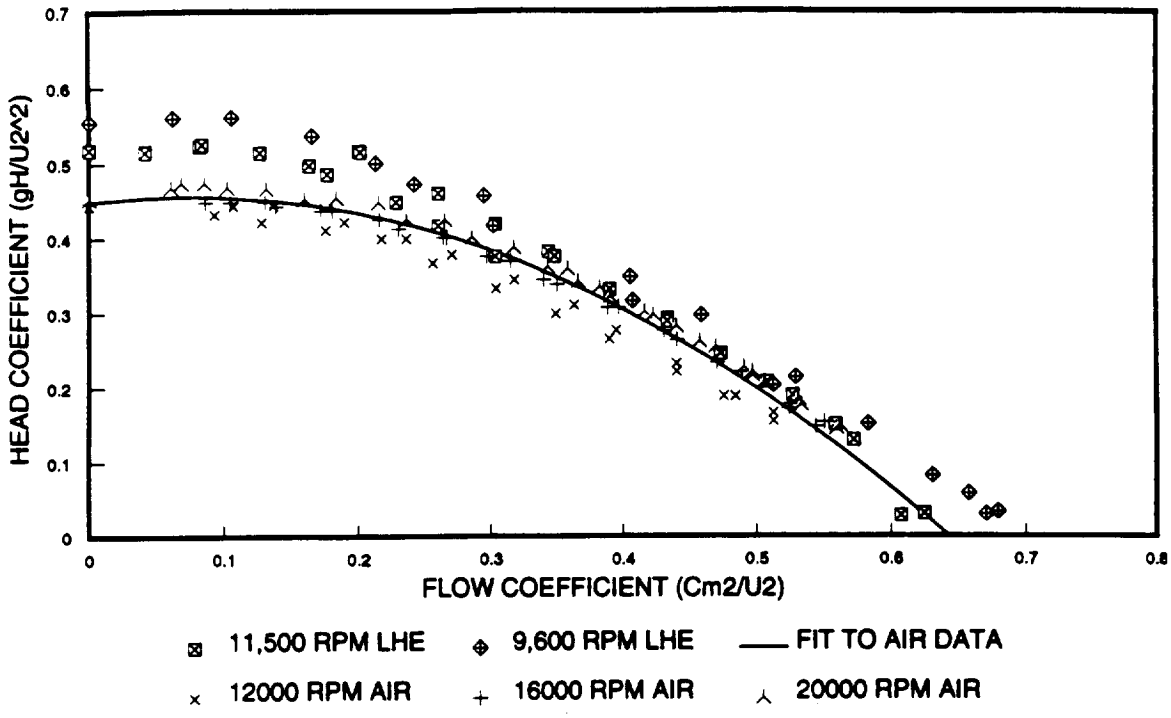

Figure 4.8. DIMENSIONLESS CHARACTERISTIC DATA FOR IMPELLER 2 (LIQUID HELIUM AND AIR DATA)

Preliminary bench-top tests were run in air to verify mechanical operation of the pump and to provide baseline data. Figure 4.5 shows air data at pump speeds of 12,000, 16,000 and 20,000 rpm. The data are reduced and presented as dimensionless flow and head coefficients (defined in Equations 3.1 and 3.2). The reduced dimensionless data fall mainly along the same curve, which has been fit with the parabola shown in the figure to simplify comparison with additional data.

Tests were next run with the pump in cold nitrogen vapor (roughly 200 K) to observe the effects of cold operation in the cryogenic test facility separately from the effects of operation in liquid. Figure 4.6 presents the results of the cold nitrogen tests. Dimensionless data are shown which are reduced from tests at pump speeds of 12,000 and 16,000 rpm. Also shown is the parabolic fit to the air tests data. The cold nitrogen data scales as expected with the bench-top air data. To measure pump head in this test, the cryogenic pressure transducer (described in the section on the test facility) was used at the far low end of its operating range. Thus, there is significant uncertainty in the head data for this test.

Final tests of Impeller 2 pumped liquid helium at 4.2 K. Data were recorded at rotating speeds of 11,500 and 9,600 rpm. Figure 4.7 shows the pump head measured as a function of flow rate at these two speeds. Figure 4.8 presents the liquid helium data in dimensionless form along with the data from the bench tests with air. Agreement between the dimensionless data shows that the pump scales properly, and the test facility instrumentation functions well with both gas and liquid working fluids and temperatures from 4.2 to 300 K.

The performance of Impeller 2 was assessed by comparing the measured head coefficient with the "theoretical" value for the same flow coefficient. Figure 4.9 shows the Euler efficiency of Impeller 2, which is the ratio of the actual to the theoretical maximum pump head. The theoretical value is obtained using Euler's Equation 4.2 to calculate the head assuming that the flow leaves the impeller with no slip. Maximum efficiencies in the range of 0.50-0.60 are obtained for flow coefficients in the range 0.0-0.2.

Figure 4.10 shows the effects of cavitation at low NPSH on the performance of Impeller 2. Flow rate was held constant and the pump head was measured as the NPSH was reduced (i.e., the level of the liquid helium bath decreased due to boiloff). The pump head remained constant until very low values of NPSH were reached (roughly within 1 mm of the impeller elevation).

Final impeller. The objectives in the design of the final impeller (Impeller Number 3) were to: 1) reduce the rotating speed to improve bearing reliability, and 2) refine the impeller design using test data from Impeller 2. The design speed for Impeller 3 was reduced to 12,000 rpm because results of cryogenic bearings tests (Section 4.2) indicated that bearings deteriorated rapidly at speeds of 21,000 rpm. Detailed design of the impeller vanes used test data from Impeller 2 to evaluate loss coefficients in the impeller. Liquid helium tests have shown that the final impeller satisfies the design requirements for liquid helium transfer.

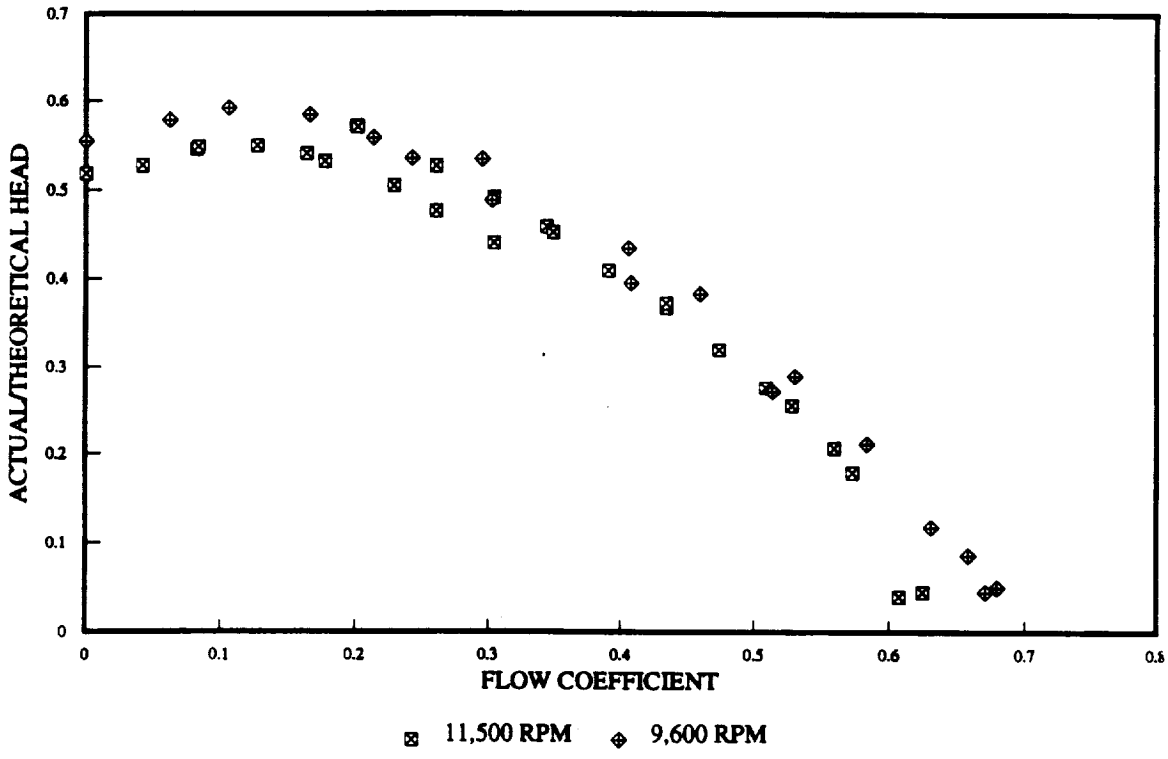

Figure 4.9. EULER EFFICIENCY OF IMPELLER 2 IN LIQUID HELIUM

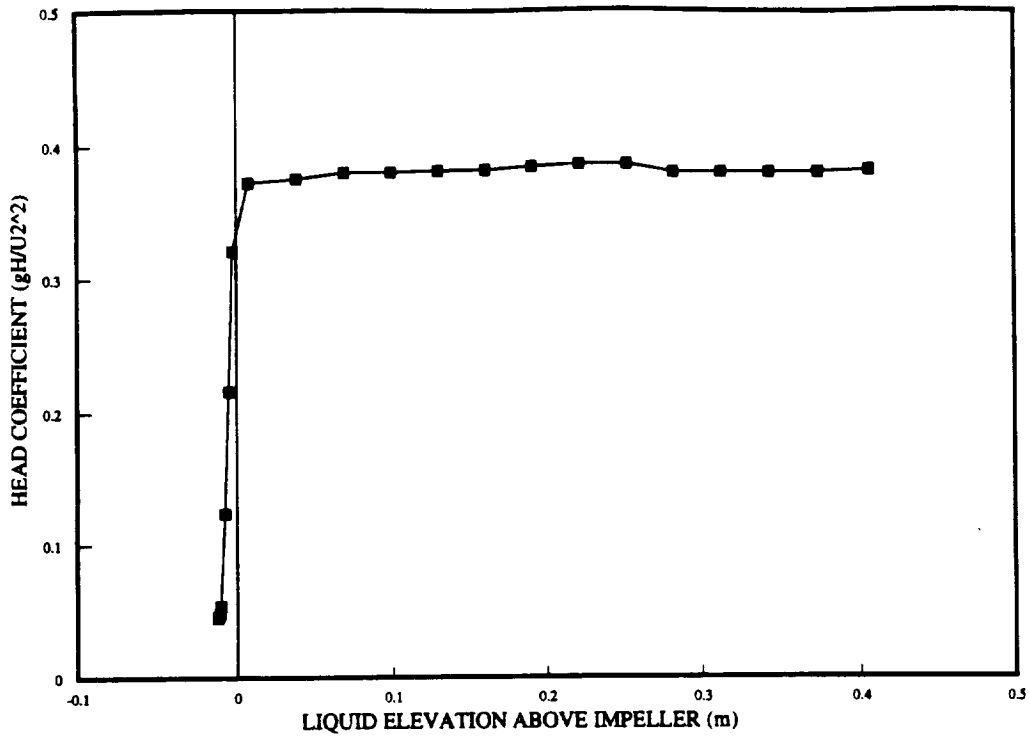

FIGURE 4.10. EFFECTS OF CAVITATION AT LOW NPSH ON PERFORMANCE OF IMPELLER 2

Table 4.1 lists the key design parameters for Impeller 3. The outer diameter has been increased to 3.08 cm. There are twelve curved blades with an inlet angle of 65° and an exit angle of 45°. The diameter of the blades at the inlet is 1.43 cm. Blade height is 0.16 cm at the inlet and 0.084 cm at the exit. Since the design head and flow rate remain constant but the rotating speed is reduced, the specific speed has also gone down. The specific speed of Impeller 3 is 0.49, roughly half the value for previous impellers.

The design models for Impeller 3 are similar to those used for Impeller 2 but also account for additional hydraulic losses in the impeller. The pump head calculated from the Euler equation is modified by two additional head loss terms. Inefficiency in the diffuser is modeled by a diffuser recovery coefficient (C_d) which accounts for kinetic energy which is not recovered as static pressure:

$$\Delta(g_oH)_d = (1-C_d)\frac{C_2^2}{2} \qquad (4.3)$$

where $\Delta(g_oH)_d$ = head loss due to inefficient pressure recovery in the diffuser,
C_2 = absolute fluid velocity at the impeller exit.

Friction losses inside the impeller are modeled by an impeller loss factor, C_f:

$$\Delta(g_oH)_f = C_f\frac{W_1^2}{2} \qquad (4.4)$$

where $\Delta(g_oH)_f$ = head loss due to friction in the impeller, and
W_1 = relative fluid velocity at the impeller inlet.

The total head generated by the pump is then calculated with a modified Euler equation:

$$g_oH = \eta_h (U_2C_{u2} - U_1C_{u1}) - \Delta(g_oH)_d - \Delta(g_oH)_f \qquad (4.5)$$

where the hydraulic efficiency (η_h) now accounts for leakage. The exit tangential velocity (C_{u2}) was evaluated from velocity triangles in the same manner as Impeller 2. Instead of a constant slip factor at the impeller exit, Wiesner's correlation (Wiesner, 1967) was used in which the slip depends on the exit blade angle.

The loss coefficients C_d, C_f and η_h were evaluated using data from the tests of Impeller 2. Values for the loss coefficients were used to predict performance of the earlier impeller and compared to the performance data. The values of these coefficients which yielded best agreement were $\eta_h = 0.78$, $C_d = 0.4$ and $C_f = 0.6$. Figure 4.11 shows that these coefficients successfully model the performance of Impeller 2.

Figure 4.12 shows the performance predicted by the design model for Impeller 3. At a rotating speed of 12,000 rpm the model predicts a head of 149 J/kg at the design point flow rate of 800 L/hr. Overall hydraulic efficiency is calculated to be 0.55.

Performance data for Impeller 3 are presented in Figures 4.13 through 4.16.

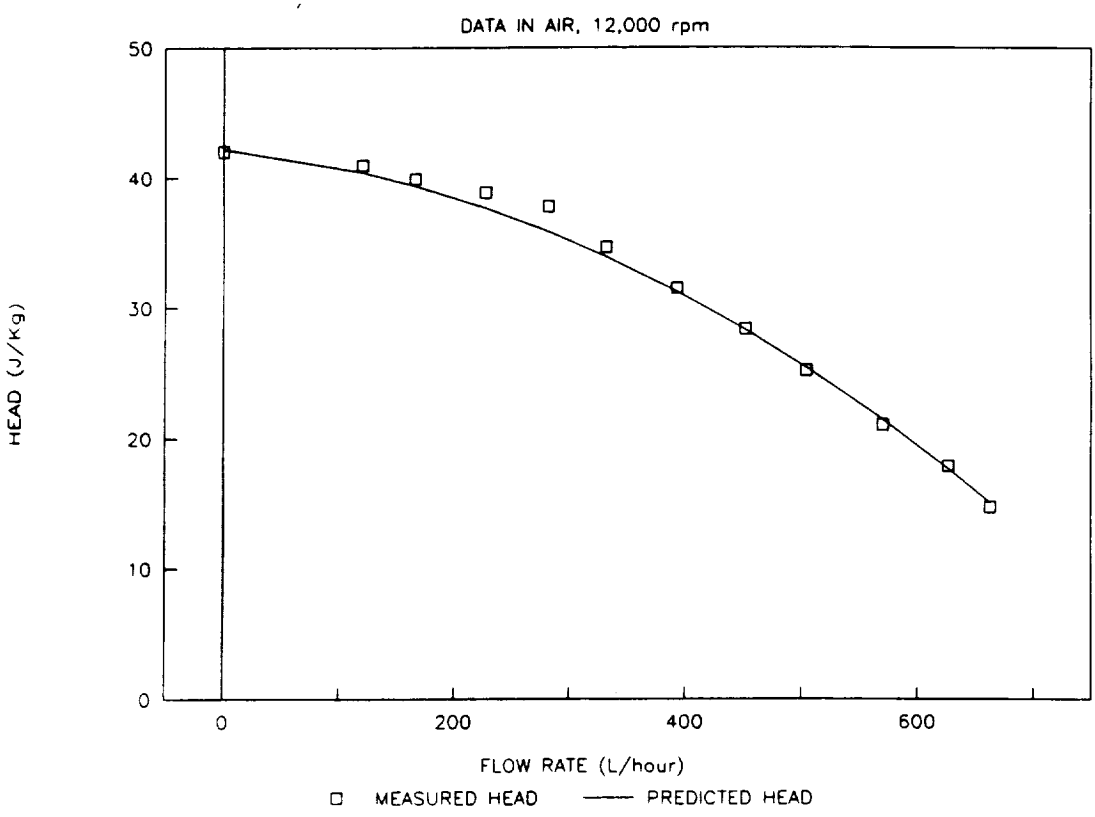

Figure 4.11. IMPELLER DESIGN MODEL FIT TO PERFORMANCE DATA FROM IMPELLER 2

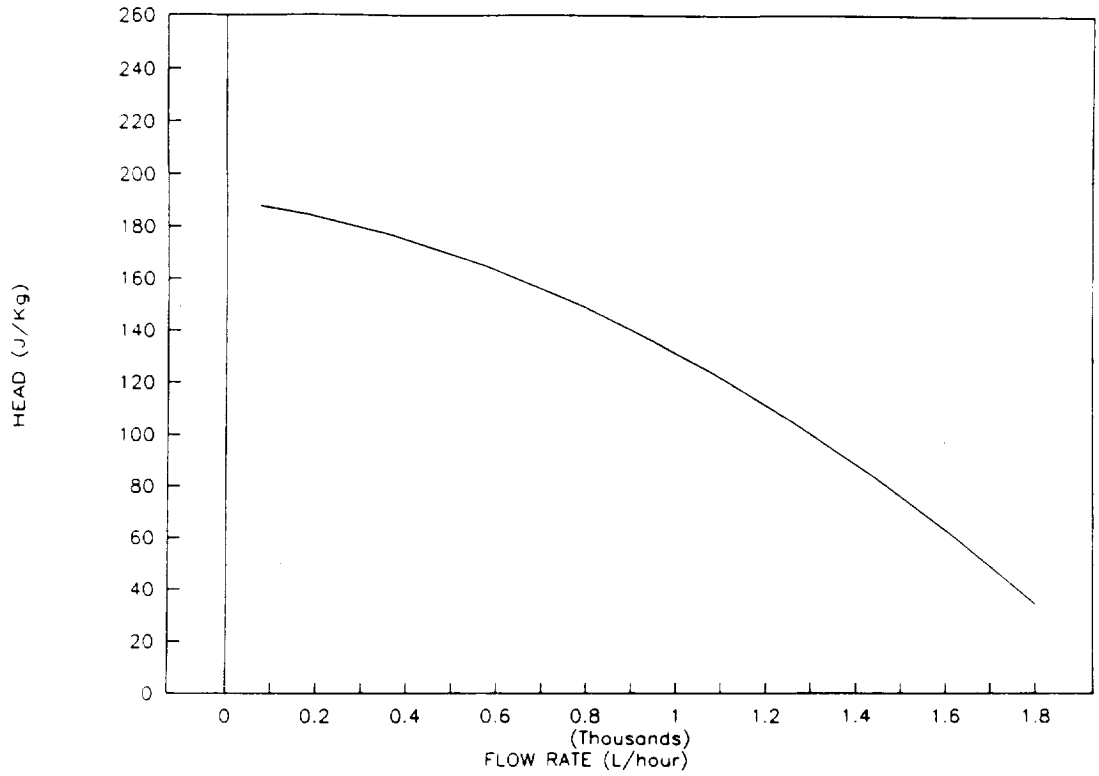

Figure 4.12. PREDICTED HYDRAULIC PERFORMANCE FOR IMPELLER 3

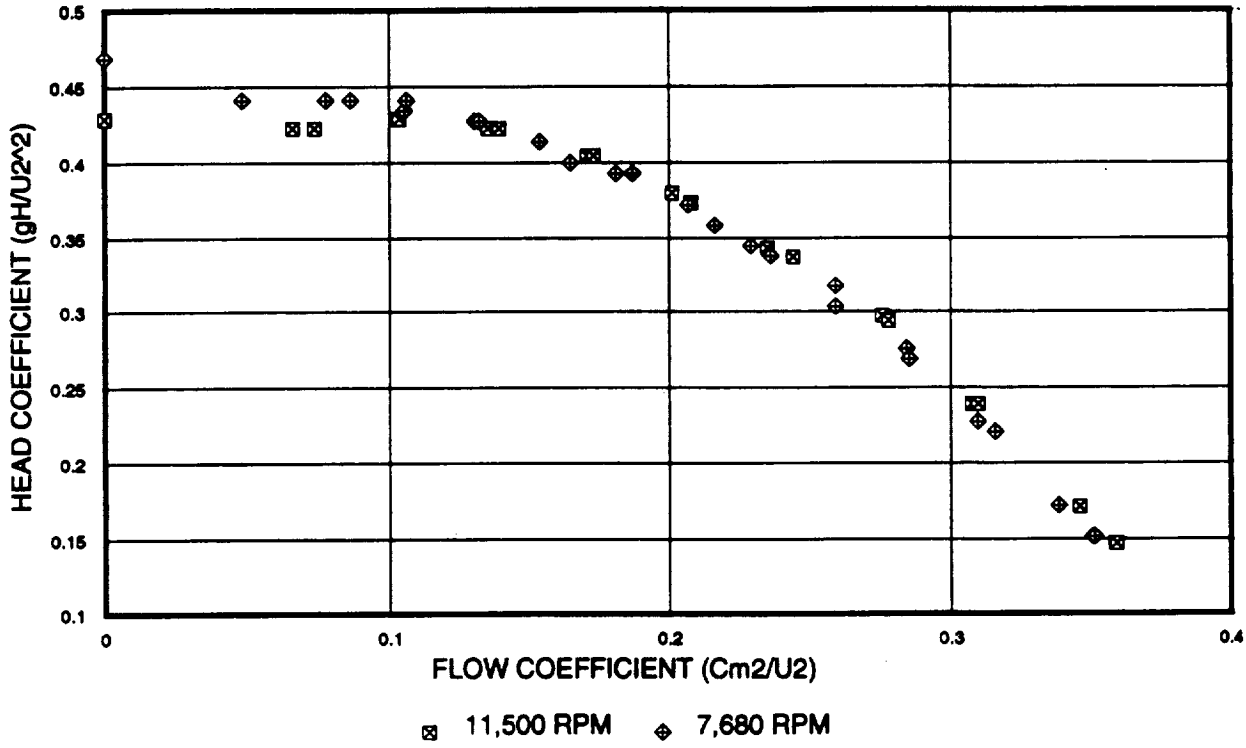

Figure 4.13. PERFORMANCE DATA FOR IMPELLER 3 - AIR AT 300 K

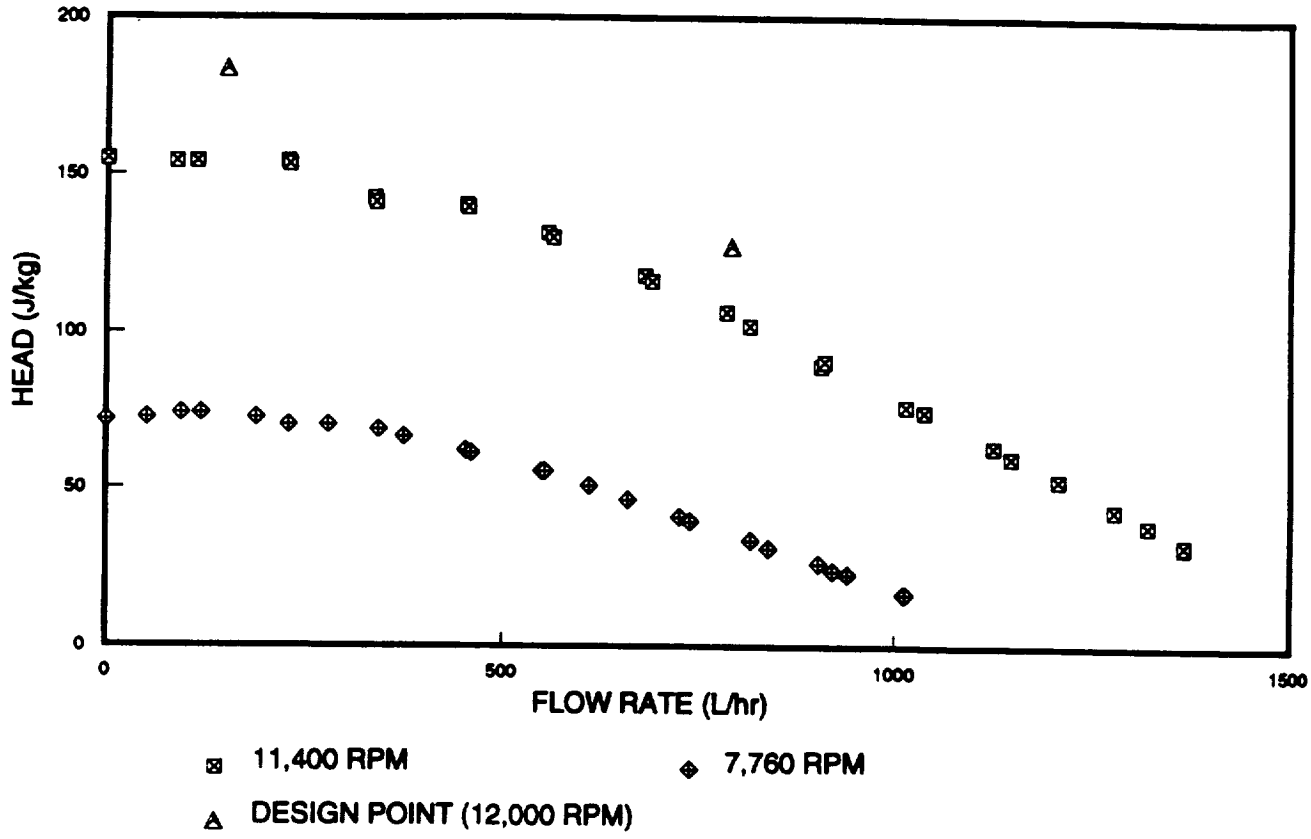

Figure 4.14. PERFORMANCE OF IMPELLER 3 - LHe AT 4.2 K

(15a)

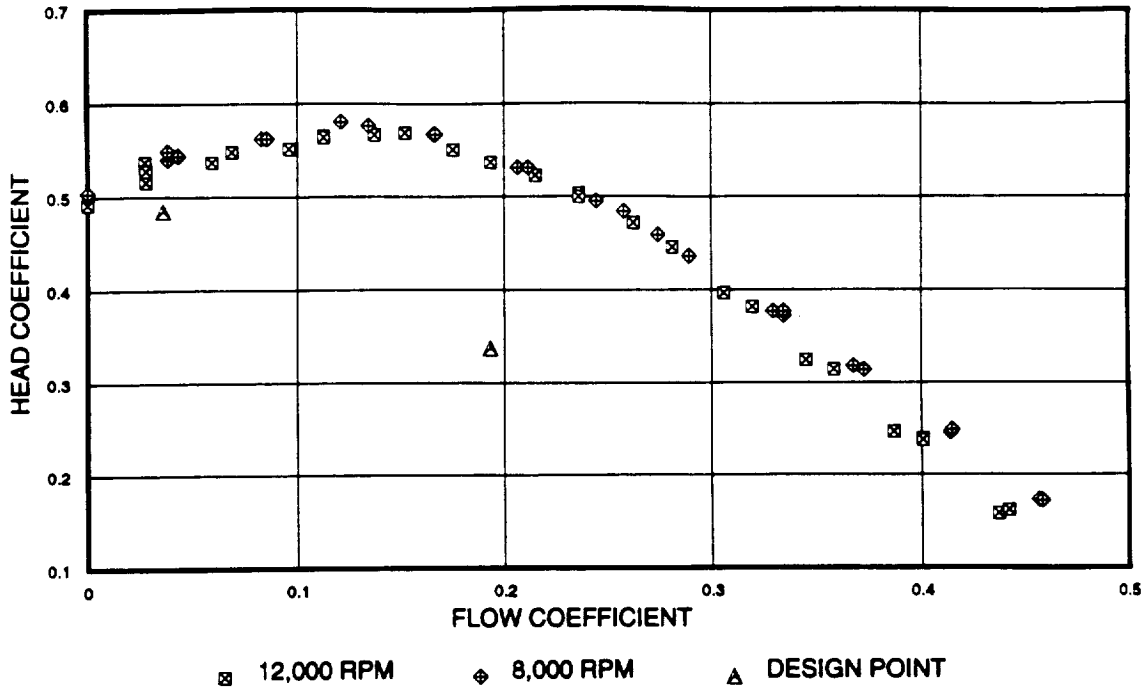

(15b)

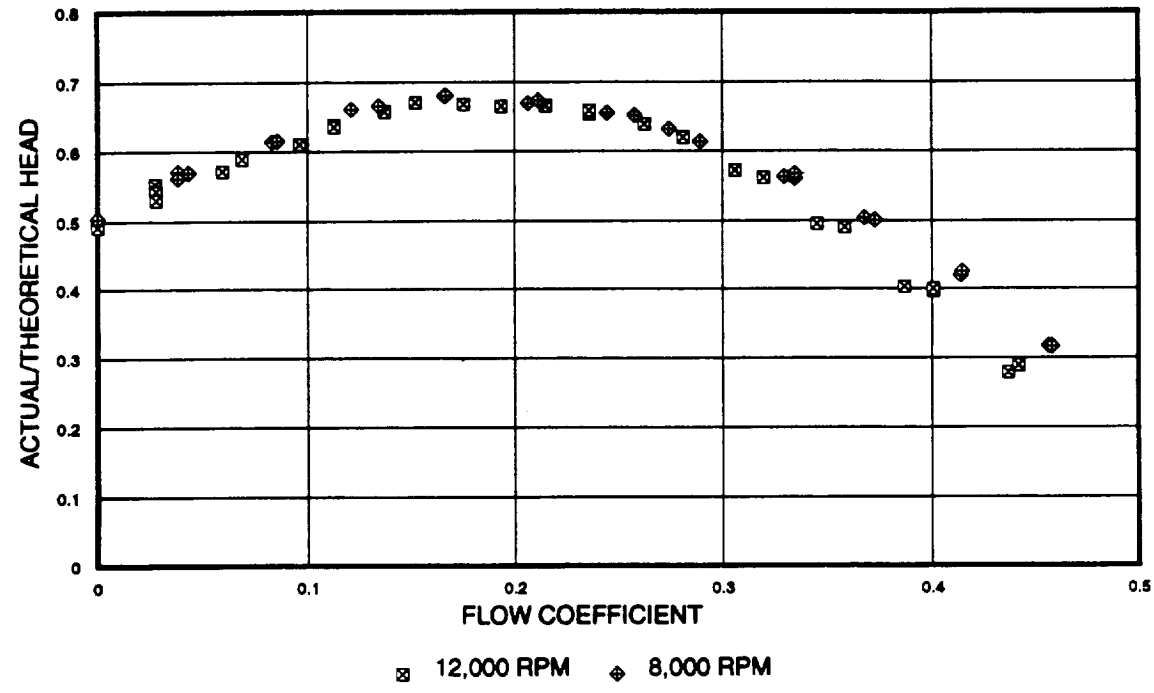

Figure 4.15. DIMENSIONLESS FLOW CHARACTERISTICS AND EULER EFFICIENCY FOR IMPELLER 3 - LHe AT 4.2 K

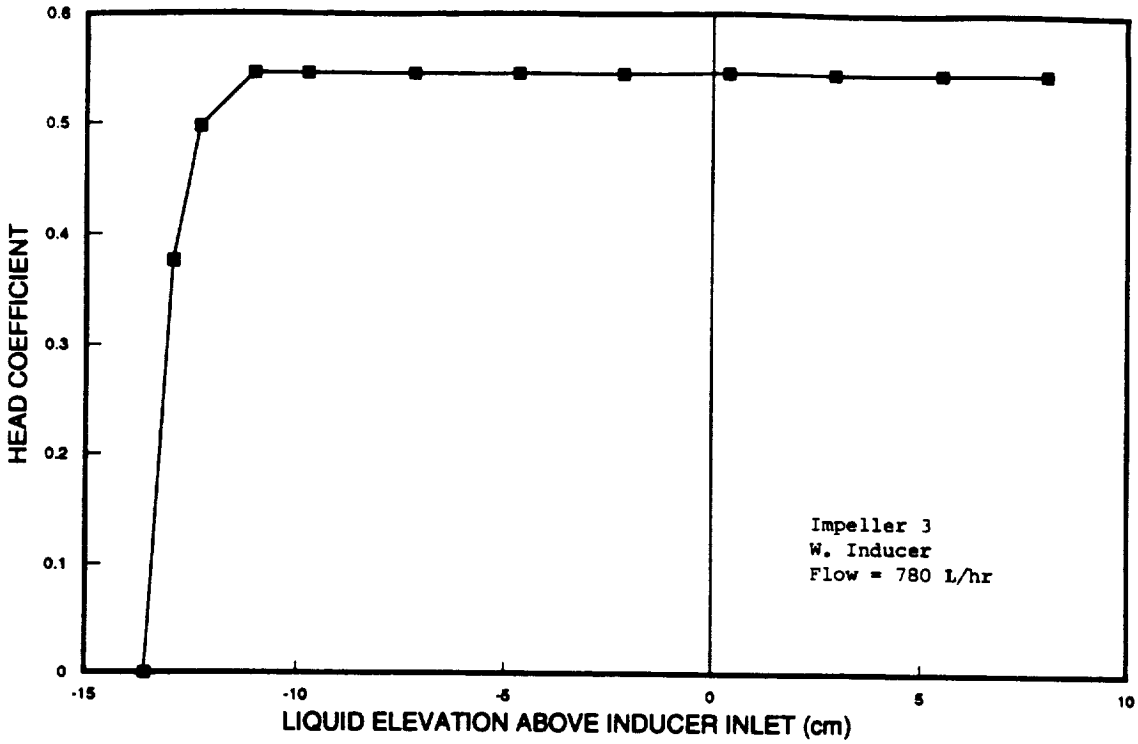

Figure 4.16. TRANSFER PUMP PERFORMANCE WITH NO INDUCER AT LOW NPSH

Figure 4.13 shows performance data for Impeller 3 in air. Performance was measured at rotating speeds of 11,500 and 7,680 rpm and reduced to dimensionless form. Figure 4.14 shows performance data measured in liquid helium at rotating speeds of 12,000 and 8,000 rpm. Also shown are the two design points corresponding to cooldown and cold transfer in the SIRTF refill mission. Note that the pump achieves both design points.

Figure 4.15 presents dimensionless performance data for Impeller 3 in liquid helium. In 4.15a the pump characteristic curves are reduced to head and flow coefficients, and Figure 4.15b plots the Euler efficiencies at both pump speeds. There is good correspondence between the dimensionless performance curves at the two pump speeds.

Figure 4.16 shows the performance of Impeller 3 at low NPSH without the inducer. The pump maintained steady head until the liquid level was 13.6 cm beneath the impeller inlet (a long inlet tube was attached to the pump inlet for these tests).

4.1.2 Inducer

A key design requirement for the transfer pump is operation with zero NPSH, which is the condition inside an orbiting helium supply Dewar. An inducer has been developed to improve the performance of the transfer pump at low values of NPSH. The inducer is a helical, axial flow impeller which is resistant to head degradation by cavitation. It is positioned upstream of the centrifugal impeller and rotates on the same shaft. The purpose of the inducer is to impart a small amount of head to the fluid so that the centrifugal impeller does not cavitate.

Figure 4.17 is a schematic of the transfer pump inducer. Key design features are summarized in Table 4.2. The inducer consists of two long blades wrapped about a central hub to form a double-helix with increasing pitch. The outer diameter of the blades is 1.27 cm (0.50 inches). The inlet angle is at 17.3°, and the exit angle is 32.40°. These angles are measured with respect to planes which are perpendicular to the axis of the inducer.

The inducer works because of its unique blade geometry. It is able to impart a small amount of head to the liquid while remaining resistant to interruption of flow by cavitation. Figure 4.18 illustrates the velocity triangles at the inlet and exit of the inducer. Because the blades have an increasing pitch, the fluid velocity at the exit has a component in the tangential direction. This swirl results in increased head, as shown in Euler's Equation 4.2. The inducer's blades are quite long so the differential pressure across them is small. As a result, cavitation is not widespread. Furthermore, any vapor cavities which may form due to local cavitation in the inducer do not significantly block the flow of liquid. This is quite different than in a centrifugal impeller, where cavitation first occurs at the inlet where the flow area is smallest.

The design of the transfer pump inducer was based on Euler's equation and the fluid/impeller velocity triangles. The inducer blades were designed to provide a head of 12 J/kg at the exit. This is roughly one-tenth the total pump head, which was reported in the literature to result in good performance in tests at low NPSH. This head requirement determined the exit angle. The inlet angle was set by the requirement for "shockless" entry--that is, the relative velocity W_1 should correspond with the blade angle β_1 as shown in Figure 4.18 (Vlaming).

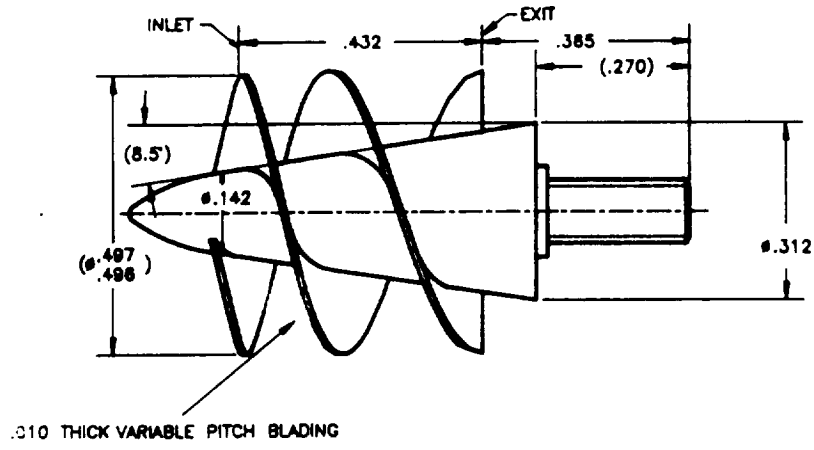

Figure 4.17. SCHEMATIC OF INDUCER

Table 4.2. INDUCER DESIGN FOR HELIUM TRANSFER PUMP	
Rotating speed (rpm)	12,000
Number of blades	2
Blade outer diameter (cm)	1.27
Blade angle at inlet	17.3°
Blade angle at exit	32.4°
Axial length of blades (cm)	1.10

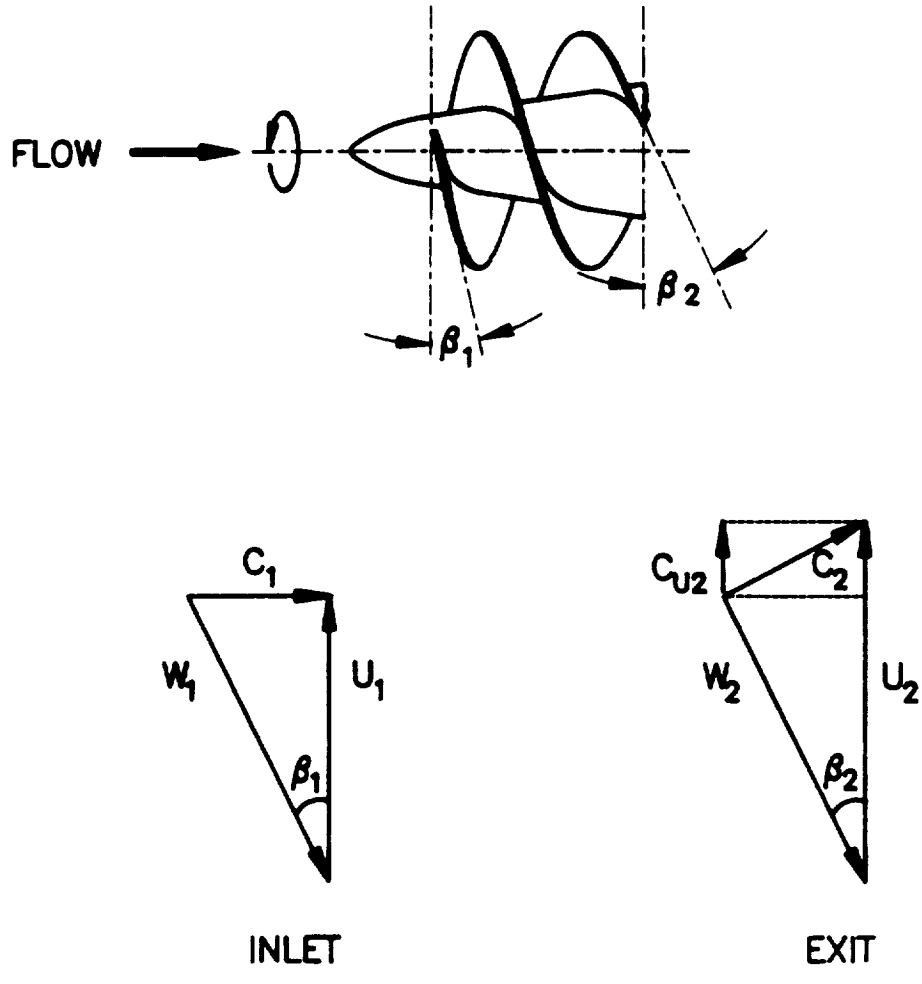

Figure 4.18. VELOCITY TRIANGLES AT INLET AND EXIT OF INDUCER

Figure 4.19 shows the performance of the transfer pump (with Impeller 3) at low NPSH including the inducer. The design requirement for pumping at rated conditions at 0 NPSH is exceeded. The pump with the inducer maintained a steady head until the liquid level was 13 cm beneath the leading edges of the inducer blade. At this point, the liquid level in the supply Dewar no longer reached the pump inlet and flow stopped. The ultimate operating limit due to cavitation could not be determined.

4.1.3 Test facility and procedures

A facility for cryogenic pump tests has been built for this project. The facility consists of a cryostat (the same cryostat used for the bearing tests) and a pump assembly. The cryostat is a vacuum-insulated Dewar for liquid helium which is surrounded by a second vacuum-insulated Dewar, which contains liquid nitrogen during tests. The pump assembly includes the pump and all test instrumentation. The facility provides pump performance characteristics and cavitation data in liquid helium.

Cryostat. Figure 4.20 shows the cryostat used for pump tests. The cryostat consists of a vacuum-jacketed Dewar for liquid helium which is suspended inside a vacuum-jacketed Dewar containing liquid nitrogen. The nitrogen acts to absorb most of the heat leak from the circumference of the Dewars. The glass Dewars are silvered for radiation shielding. Two strips on opposite sides of the Dewars are unsilvered to allow viewing the pump during operation. A wooden box encloses the Dewar and provides support for the glass vessels.

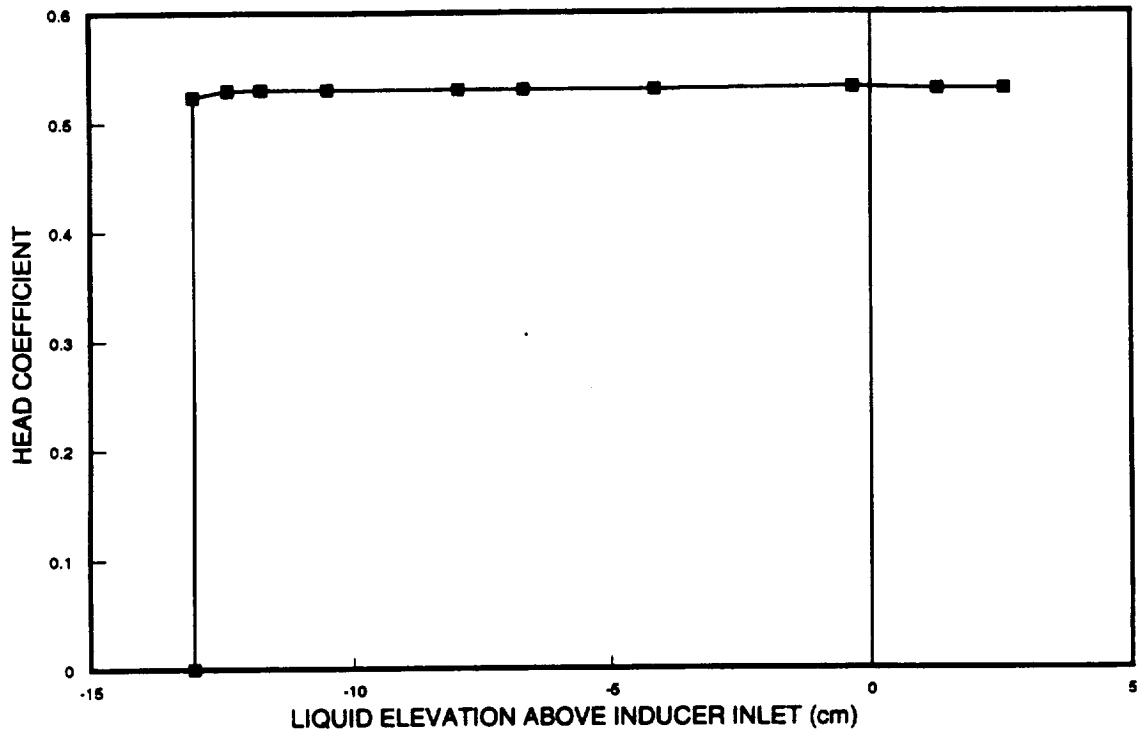

Figure 4.19. TRANSFER PUMP PERFORMANCE (IMPELLER 3) WITH INDUCER AT LOW NPSH

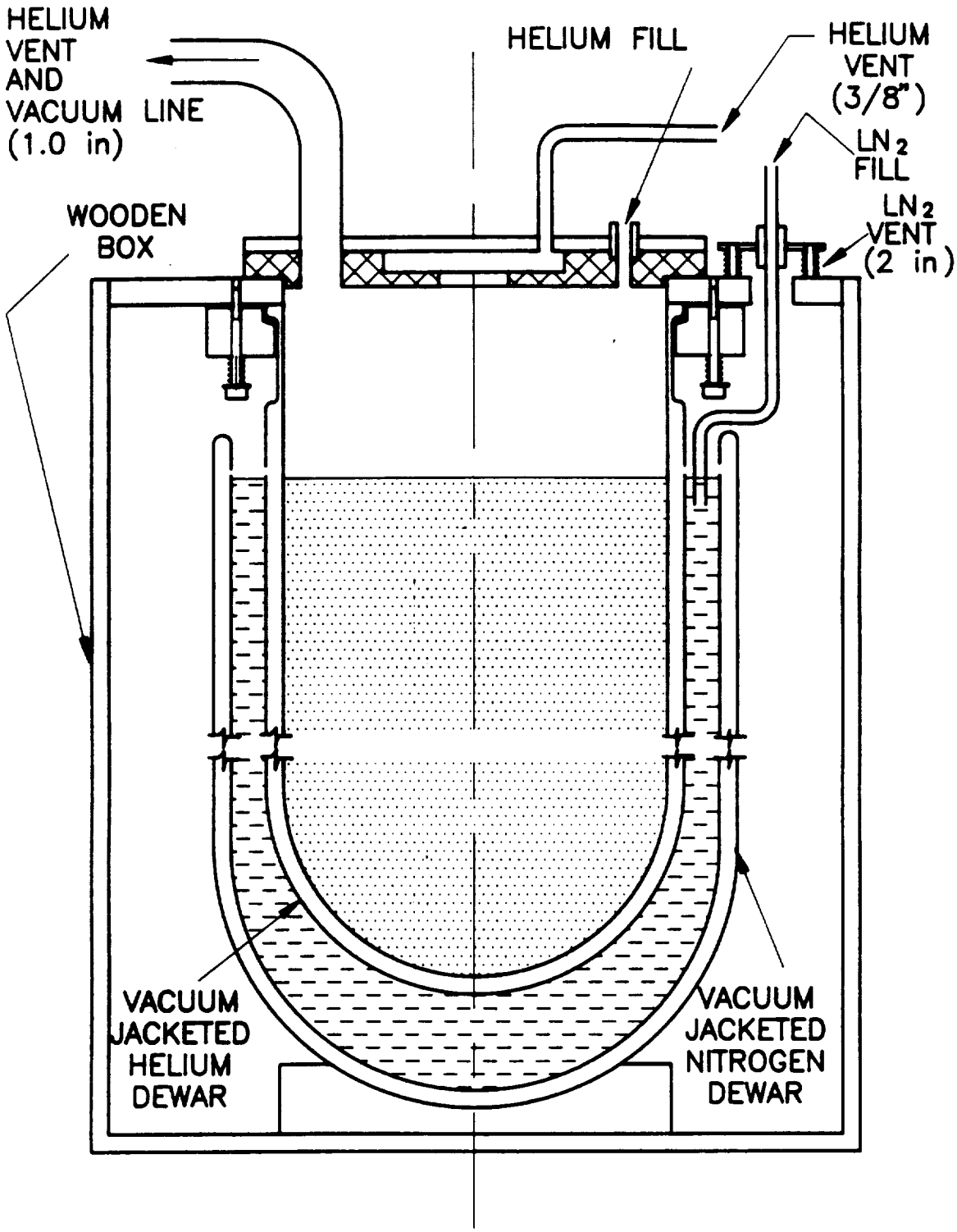

Figure 4.20. SCHEMATIC OF CRYOSTAT/LIQUID HELIUM BATH

Pump assembly. The pump and all test instruments are suspended from a flange which seals the top of the LHe Dewar during a cryogenic test. Figure 4.21a is a photograph of the pump test assembly, and Figure 4.21b is a schematic of the test's assembly which identifies the main components.

The transfer pump was placed at the lowest elevation and its inlet faced downwards towards the bottom of the Dewar. During cryogenic operation, flow left the pump and flowed into a vertical tube containing flow and pressure instrumentation. The flow rate was measured by a turbine meter, and the pump head was measured by a differential pressure transducer. One leg of this transducer was coupled directly to the pump outlet tube; the other was open to the LHe bath at the same elevation.

Liquid helium left the metering tube through an angle control valve and returned to the surrounding bath. Flow through the pump was controlled by adjusting the control valve.

Instrumentation. The pump assembly included several instruments for measuring performance. They were:

- a differential pressure transducer to measure pump head,
- a turbine meter to measure flow rate,
- a capacitance probe to measure pump rotating speed, and
- a liquid helium level meter to measure NPSH.

1) Differential pressure transducer. A differential pressure transducer was used to measure pump head during cryogenic tests with liquid helium. The transducer operated completely submerged in liquid helium, so that pressure taps leading to an external transducer were unnecessary. The transducer was purchased from Keller PSI and calibrated at room temperature and 4.2 K. The pressure range was 30 psid. For pump tests, the pressure leg of the transducer was connected to the pump discharge tube and the reference leg was open to the surrounding helium bath (at the same elevation).

The pump head during tests with warm air was too small to measure with the differential pressure transducer. For these tests, pump head was measured with a slant-tube manometer. A pressure tap from the pump discharge led to the pressure side of the manometer. In this way, accurate measurement of the pump discharge pressure was possible down to 0.01 inches of water (2.5 Pa).

2) Turbine meter. A turbine flow meter was purchased from Flow Technology Inc. to measure the flow rate from the pump. The meter consisted of a short flow section in which a small, six-bladed turbine rotated at a speed which was roughly proportional to the liquid flow rate. A magnetic pickoff located alongside the meter counted the frequency at which the turbine blades passed and produced a signal which indicated the flow rate. We performed extensive calibrations of the turbine meter at ambient and cryogenic temperatures. The meter accurately measures the liquid flow rate provided the liquid is single-phase.

We also found that in liquid nitrogen the turbine meter does not accurately measure the flow. Because the meter operates properly in liquid helium, and because liquid helium is much less prone to cavitation than liquid nitrogen, we believe that the problem with measuring LN_2 flow is due to cavitation in the turbine meter.

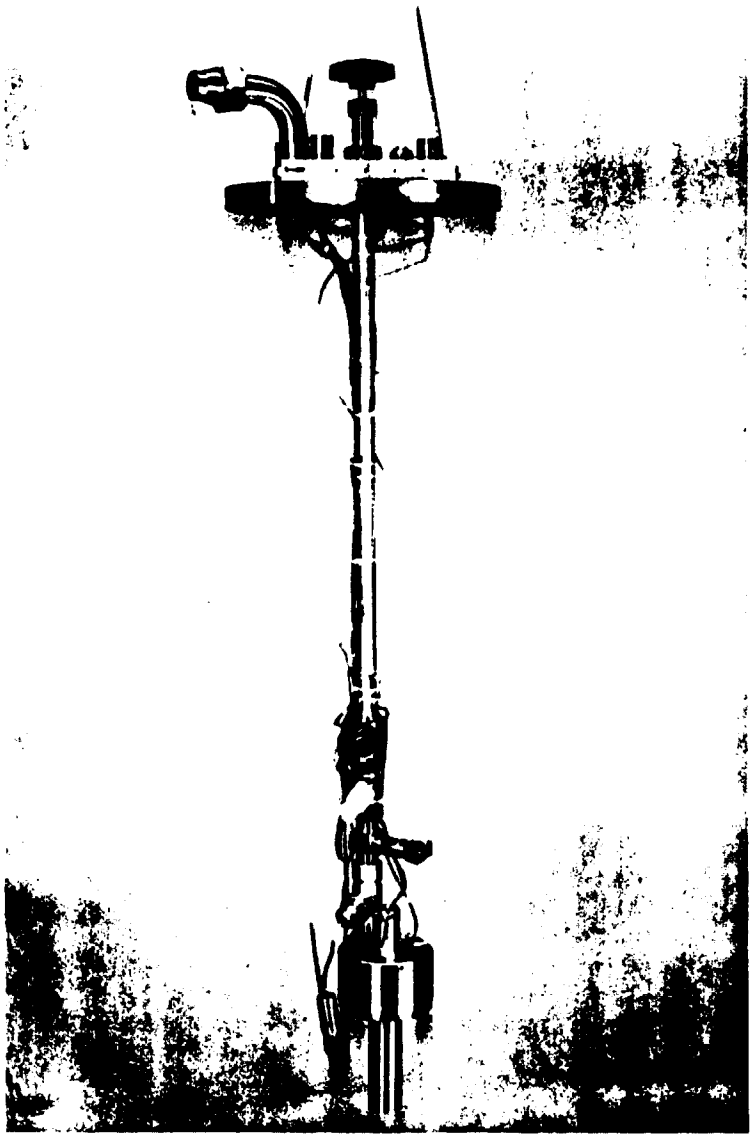

Figure 4.21a. PUMP TEST ASSEMBLY

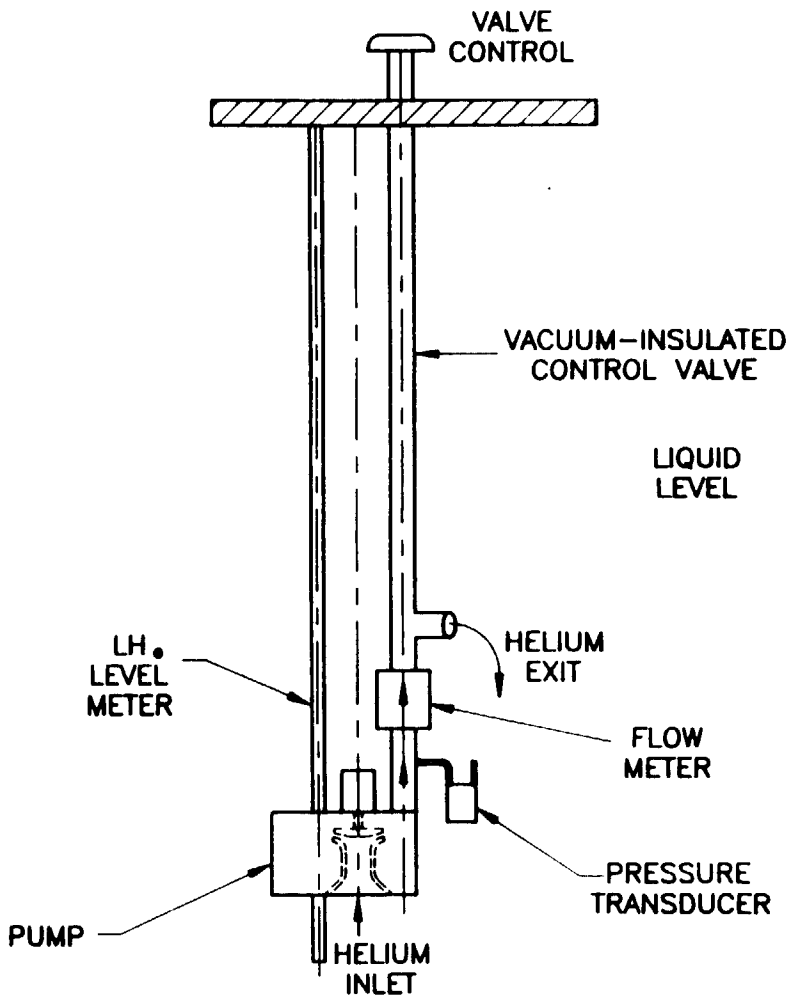

Figure 4.21b. SCHEMATIC OF PUMP TEST ASSEMBLY

3) Capacitance probe. Capacitance probes were used to measure the rotating speed of the pump. A capacitance probe is an electrode, in series with a capacitor, positioned in close proximity with a rotating element. If the capacitor is charged through a high-value resistor, then changes in capacitance between the pump and electrode can be detected as a change in voltage across the resistor. The rotating element is shaped so that the capacitance between it and the electrode changes with rotation. Thus, the voltage across the resistor provides a signal whose frequency is proportional to the rotating speed of the pump.

For the intermediate impellers, the capacitance probe was placed close to the exit of the impeller. A signal was registered each time an impeller blade (or drilled hole) passed the probe. In this case, the rotating frequency was 1/12'th the frequency of the voltage changes registered by the probe (there were 12 blades and 12 holes in the impellers). For the final impeller, two shallow holes were drilled in the back side of the impeller and the capacitance probe was located at the corresponding radius. A signal was obtained at twice the rotating frequency.

4) Liquid helium level meter. A liquid helium level meter was used to measure the depth of the liquid helium bath during cavitation tests. The meter was purchased from American Magnetics, Inc. It consists of a strip of superconducting material and a long filament heater, enclosed in a tube which hangs vertically into the liquid helium bath. The tube has many penetrations which allow liquid inside. The portion of superconductor which is in contact with liquid is beneath its transition temperature and offers no electrical resistance. The portion above the liquid level is heated above the transition temperature by the filament, and thus is resistive to current flow. Thus, the electrical resistance of the superconductor is proportional to the liquid helium level.

Pump characteristic tests. Pump characteristic tests were run to obtain head/flow performance data for the transfer pump. These tests were run with cryogenic liquids and room-temperature air.

Before running a cryogenic test, the facility, pump, and instruments were carefully cleaned with solvents. The cryostat was sealed and then evacuated and purged with high purity helium to remove contaminants which would freeze out in liquid helium.

Pump tests began after cleaning and purging. Liquid helium and nitrogen were added to the cryostats. The helium level in the inner Dewar was kept well above the pump inlet (roughly 18 inches) so that the operating characteristics could be observed with no effects of possible cavitation at low NPSH. The rotating speed of the pump was set by observing the output of the capacitance probe and adjusting the frequency of the motor controller. Once the desired speed was obtained, a head/flow characteristic curve was recorded. The control valve was opened fully and the head and flow rate at this point were recorded. Then, the control valve was closed partially and the next head/flow point was recorded. This continued until the valve was fully closed and the pump head at zero flow was recorded. Then we took a second set of flow/head points with the same pump speed as the valve was turned to full open. Data from bench tests in air were obtained in the same manner.

Following this procedure the pump speed was adjusted to the next desired level and another head/flow characteristic was recorded.

After the head/flow pump characteristics were obtained, we began tests of pump performance at low NPSH.

Tests of pump performance at low NPSH. The liquid helium in the test Dewar is in thermodynamic equilibrium with the helium vapor which covers it. Thus, the liquid helium is saturated, and the net positive suction head for the pump is provided only by the gravity head of the liquid. Thus, the NPSH at the pump inlet is equal to the difference in elevation between the inducer inlet and the liquid surface, less the velocity head of the liquid in the pump inlet. The liquid level alone is a conservative (i.e., high) measure of NPSH.

To obtain pump performance data as a function of NPSH, the liquid helium is allowed to evaporate from the inner Dewar without replenishment. The level drops gradually and pump performance is monitored. The position of the control valve and the pump speed are kept constant throughout this test so that the pump operates at the nominal design point. Head remains constant until cavitation begins in the pump. At the onset of cavitation, the head begins to drop. As the level of the liquid helium bath continues to fall, the severity of cavitation increases and head decreases still further. Pump head and the level of the liquid helium bath are recorded periodically. NPSH is calculated by subtracting the velocity head of the fluid in the pump inlet from the elevation difference.

To allow the pump to continue operating after the liquid level has dropped beneath the pump inlet, an extended inlet tube was attached to the pump for these tests.

4.2 Bearing Testing and Development

The liquid Helium transfer pump requires a journal bearing capable of moderately high speeds that can operate for long periods of time in a liquid or gaseous helium environment at temperatures near 4.2 Kelvin. The most reliable performance was achieved by bearings with 440C stainless steel balls and raceways with nylon/teflon/fiberglass composite retainers. These bearings were then tested for endurance in liquid helium under simulated pumping conditions. They have operated reliably for 24 hours at speeds of 12,000 rpm and axial loads of 2 lb_f.

The operating environments of bearings can be compared using their "DN" values, which represent the product of speed in rpm and diameter in millimeters. For the helium transfer pump, DN values of 105,000 were projected for early pump designs (which had a rotating speed of 22,000 rpm). For the final pump design, DN = 57,000 with a rotating speed of 12,000 rpm.

A substantial amount of work has been performed on the development of ball bearings for use in liquid hydrogen and liquid oxygen, most recently for Space Shuttle Main Engine (SSME) turbopumps (DN values up to 2 million at 40,000 rpm). Similar work has been performed for the development of ball bearings for gyros for operation at high speed in vacuum. There are some significant differences in the needs of the bearings for the SSME and the liquid helium pump. The SSME pump bearings are running at extremely high DN values (up to 2 million) at high loads (Hertzian stresses as high as 500 Kpsi) with a desired life on the order of 7.5 hours in either an oxidizing (LOX or GOX) or reducing (LH_2 or GH_2) environments and at temperatures of 20 K to 100 K. The liquid helium pump is operating at a much lower DN value of 50,000-100,000 and Hertzian stress in the vicinity of 200 Kpsi with a target life of 500 hours, operating in an inert environment at 4.2 K.

It has been determined, through review of the literature and consultation with bearing manufacturers, that no off-the-shelf bearing can be purchased which meets the requirements of the liquid helium transfer pump with a high degree of certainty. So an experimental development program was initiated to obtain and test several different configurations of bearings with the objective of determining which bearing performs the best in the operating environment of the liquid helium transfer pump. Screening tests were performed on four bearing configurations, including conventional solid-lubricated bearings as well as bearings with advanced ball and retainer materials and raceway surface treatments.

4.2.1 Background and Overview

Operation at cryogenic temperatures requires the use of dry or un-lubricated bearings because conventional lubricants harden at cryogenic temperatures. There are two basic types of wear resistant coatings used (Spalvins, 1978): hard, wear resistant coatings such as carbides, nitrides and silicides, and soft lubricating coatings. There are three classes of solid lubricating coatings (Gould and Roberts, 1989): soft metals (Au, Ag, Pb, etc.), lamellar solids (MoS_2, NbS_2, etc.), and polymers (PTFE, polyimides, etc.). For the needs of this project, it was decided to try four different bearing configurations, using various combinations of the above wear resistant approaches.

Because of the long life desired for these bearings, a statistical study could not be performed within the scope of the project to create a data base that would demonstrate that a bearing could operate for 500 hours (Abernathy, et al., 1983). Therefore, an experimental program was designed, with the cooperation of Miniature Precision Bearing Corp., Keene, NH, in which bearings would be tested at prototypical conditions, for a limited period of time (by Creare), and the bearings would be inspected (by MPB) to determine the degree and nature of the wear, so that bearings with the best and worst chances of success could be identified.

4.2.2 Selection of Bearing and Retainer Materials

Three different manufacturers were identified as sources of bearings for the Liquid Helium Transfer Pump. A total of four different bearing configurations were tested. Table 4.3 below gives the manufacturers, ball, race and retainer materials. Bearing combinations were chosen to utilize each of the three classes of solid lubricants and the wear resistant materials.

Bearing number one, the MPB bearing, is a standard R3 oil lubricated bearing design with the oil left out and extra clearance designed into the bearing. The MCK retainer is made of Nylon, PTFE (teflon) and glass fiber. Because it is basically a standard bearing without the lubrication, it was chosen as the baseline bearing for performance comparison. 440C is used for the balls and races because of its corrosion resistance and because it is the standard material for instrument bearings. This bearing utilizes its polymer retainer to provide solid lubricant. The MCK retainer combines the solid lubricating properties of teflon and the greater strength and wear resistance of nylon. However, no literature was found documenting the use of Nylon, or Nylon, PTFE, glass composites for cryogenic bearing applications, so the performance of this bearing was unpredictable before testing.

Bearing number two, manufactured by FAG, is designed to test the effectiveness of a lamellar solid (in this case MoS_2) as a lubricant and to test a polyimide retainer. The MoS_2 was sputter coated onto the races by Lube Co. (process 905) and burnished by a glass beading process. The burnishing process is supposed to increase the adhesion of the MoS_2 to the raceway. The retainer is a polyimide composite with 15% MoS_2 (Dupont Vespel, SP-3).

Table 4.3. TEST BEARINGS					
Bearing	Manufacturer	Race Mat'l	Ball Mat'l	Retainer Material	Race Treatment
1	MBP	440C	440C	MCK (nylon, PTFE, glass composite)	None
2	FAG	440C	440C	Vespel (SP-3) (Polyimide, 15% M_oS_2)	MoS_2 burnished on to races
3	Barden	440C	440C	Teflon/Glass/ M_oS_2	None
4	MPB	440C	Si_3N_4	Leaded Bronze	Lead Ion Plated

Polyimide composites, along with PTFE, are frequently used to provide dry lubrication in bearings and have been shown to work at high temperatures (Devine and Kroll, 1964). With the MoS_2 in the material, a transfer film of polyimide and MoS_2 should rub off onto the balls by friction and get transferred to the races. In this way, a continuous supply of dry lubricant should be available. The balls and races of this bearing are of 440C stainless steel. Radial clearance is set at 0.0005-0.0008 inch.

Bearing number three, manufactured by Barden Bearing, is an off-the-shelf dry-lubricated bearing designed for cryogenic use. This bearing is rated from -185 °C to 302°C (88 - 575 K). So operation in liquid helium (4 K) represents an extension of the design operating range. The lubricating mechanism for this bearing is the same as for other retainer-supplied dry-lubricant bearings. The balls rub small quantities of the retainer/lubricant off and deposit the material onto the raceway. The retainer is a "highly compressed material of Teflon-coated, super-fine glass fibers, impregnated with MoS_2" (The Barden Corp., 1965) Ball and race materials are of AISI 440C stainless steel, hardened and heat treated. Radial clearance in this bearing is set at 0.0005-0.0008 inch or greater to provide compensation for thermal differentials.

Bearing number four, manufactured by MPB, was our "best shot" bearing. Based on research performed by Creare and MPB, a combination of materials was chosen to provide the best performance regardless of cost. The bearing races are of 440C and are ion implanted with lead. The lead was applied at the European Space Technology Laboratory (ESTL) in England. The lead implanted coating is designed to provide a dry lubricant of soft metal. Previous researchers have found that bearings with lead-containing cages and lubricated with ion-plated

lead films showed good torque performance when cooled from 300 to 20 K (Gould and Roberts, 1989). The retainer for this bearing consisted of a leaded bronze. Leaded bronze was chosen because of its assumed greater strength than PTFE or polyimide, and because retainer failure is a common mode of unlubricated bearing failure. The lead in the bronze is intended to help provide lubricant transfer over the life of the bearing. The ball material chosen was silicon nitride Si_3N_4.

Silicon nitride balls were selected to increase the wear resistance of the bearing. There are four principal types of metallic wear: adhesive, abrasive, corrosive, and surface fatigue or pitting (Spalvins, 1978). In instrument bearings operating in a clean, inert environment, abrasive and corrosive wear are largely not an issue (though bearing debris can cause abrasion in the same or other nearby bearings as wear occurs). Typically, adhesive wear is the primary cause of bearing degradation in instrument bearings. Adhesive wear is the formation of microwelds at the metal to metal interfaces such as between the balls and races (Fletcher, 1990). Eventually, adhesive wear leads to increased surface roughness, increased torque and ultimately bearing failure. Experience with ceramic coatings and ceramic bearing elements has shown that they substantially decrease the occurrence of adhesive wear because dissimilar materials are less prone to adhesion.

4.2.3 Test Descriptions

Bearing tests were developed for the purpose of demonstrating the suitability of the different bearing designs for operation in liquid helium. A review of Weibull analysis (Abernathy, et al., 1983) showed that performing a statistical study, in which large numbers of bearings are tested until failure and the failure data is used to estimate reliability, was not feasible. The statistical study was beyond the scope of this project because 1) the cost of performing the tests would be very high, and 2) the duration required for the tests is quite long (over 500 hours). Therefore, a test program was developed that would enable the bearings to be run for short periods of time and then be inspected. An inspection program was developed to identify the severity and nature of wear and to determine the causes of such wear.

Test Facilities

Two separate test facilities were developed for the cryogenic testing of bearings. The first facility designed could test six bearings simultaneously. The second test facility is simpler but holds only two bearings.

Six Bearing Test Facility. The first test apparatus, designed to enable the testing of six bearings simultaneously, is shown in Figure 4.22. The motor is mounted at the warm end of the facility and drives the bearings which are located in the cold end. This facility design reduces the overall heat input to the liquid helium by about 50 percent because the motor power is not dissipated into the cryogenic environment. The bearings are loaded into a precision bore with 0.0005 inch radial clearance with a precision turned and lapped shaft with 0.0005 inch radial clearance to the bearing I.D. The preload on the bearings is set by a spring and cup system with shims alternately between the inner and outer races such that the inner and outer races are alternately loaded and all bearings are preloaded to the same value. The preload on the bearings is setup warm so that it will be 8.88 N cold, with thermal contraction and the change in the modulus of the spring taken into account. The shaft is driven through a flexible bellows coupling by a brushless d.c. motor. Heat leak from the motor to the bearings is limited to about 2 watts by the thin-wall bellows and shaft length. The bearing bore/housing is mounted on a thin-wall structural shell to isolate it from the warm mounting.

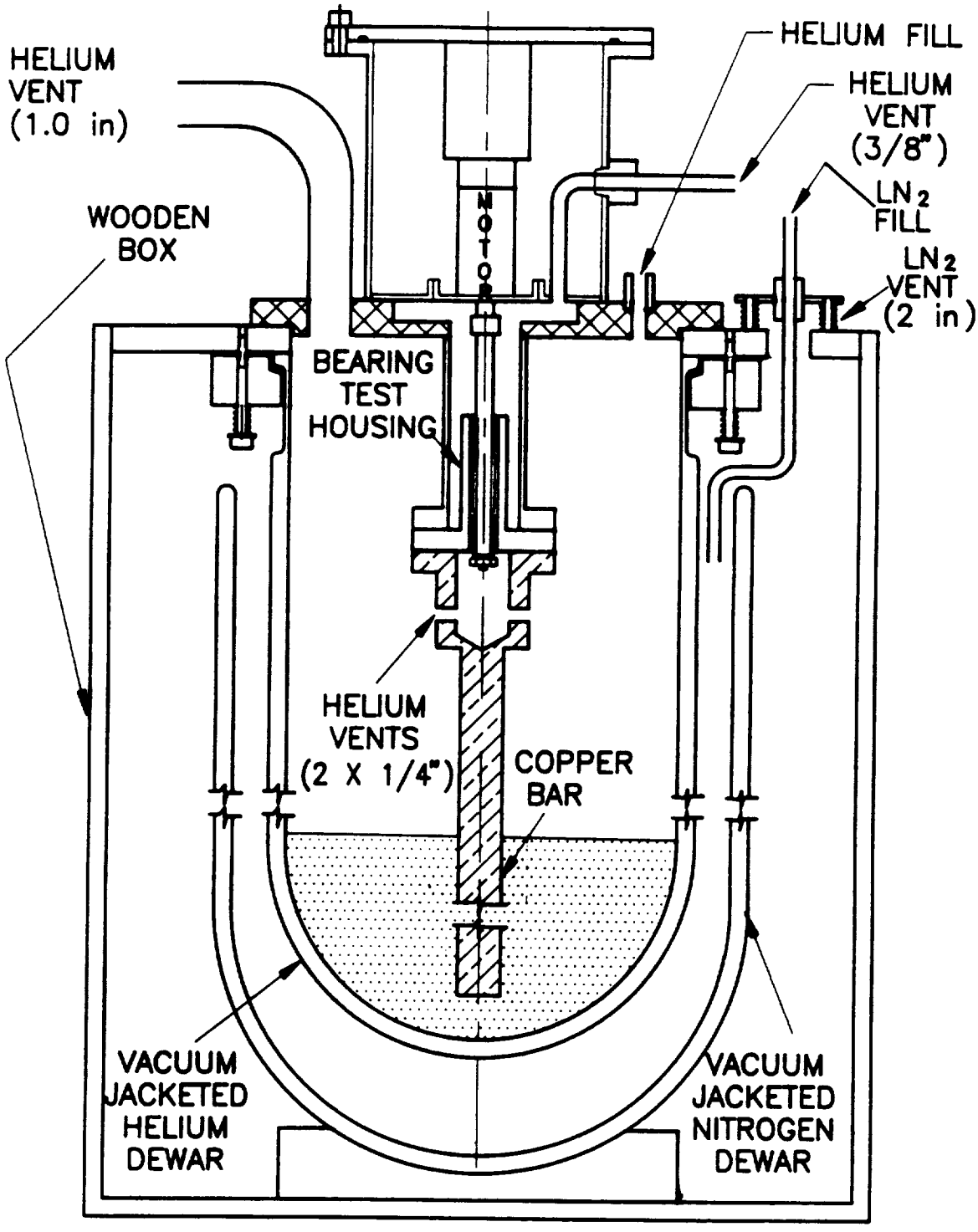

Figure 4.22. SKETCH OF TEST FACILITY NUMBER 1

The bearings are cooled by two mechanisms. The bore in which the bearings are mounted is thermally connected to the liquid helium by a solid bar of pure CDA110 copper. As the helium level drops during the test, the copper bar keeps the bearing housing cold by conduction. The boiloff vapor is channeled through ports in the bearing bore and through the center of the bearings. The clearance between the balls and the races and the cage is sufficient to allow the helium boiloff to pass through. This design was intended to permit all six bearings to operate at liquid helium temperature, in a gaseous helium environment.

Two Bearing Test Facility. The two bearing tester is shown in Figure 4.23. One of the pump motors was modified to allow the use of a controlled spring force to preload the bearings. Thus, the motor was assembled and operated normally except that a spring provided the 8.88 N preload instead of the pressure difference across a pump impeller. The motor was hung in the liquid helium by a thin stainless steel wire to limit heat leak. Heat generated in the motor caused a small amount of boiloff that created substantial convection in the motor that cooled the motor and flushed out debris generated by the bearings.

Test Procedures

The test procedures for both test facilities were essentially the same. Differences in detail arose from the different facility constructions. In both cases, the test facility was cleaned with a progression of solvents (acetone, alcohol, freon) to remove all traces of particulate and moisture. The bearings were installed in the housing and the preload set so that it would be 8.88 N when cooled to 4 K. The housing was installed into the dewar and all valves and seals installed. After an instrument check, the dewar was evacuated to a rough vacuum and back-filled with grade 6 helium at room temperature five or six times. After the dewar was purged with helium gas the motor was started and spun slowly. Then the liquid nitrogen jacket was filled, and the fill with liquid helium begun. Once the bearings reached operating temperature (LHe began to fill the dewar), the motor speed was increased to the full operating speed (21,000 for early tests, 12,000 for later tests).

Bearing tests were designed to run for approximately 24 hours. In the event of a bearing failure (the test facility seized) a test would be shortened. After 24-30 hours, the LHe in the supply dewar would generally run out. The motor would be turned off when the operating temperature began to rise. Bearings were removed from the facility and sent to MPB for inspection after the facility warmed to room temperature.

4.2.4 Test Results

Table 4.4 summarizes the six bearing tests that were run and the results of the tests. Of six tests, substantial retainer damage was identified in four cases. Clearly, the retainer is a weak link in the dry-lubricated cryogenic bearing. Similar observations have been made by others testing dry-lubricated bearings (Bhat, 1989; Kannel, et al.; Poole and Bursey; Devine and Kroll, 1964; Nosaka, et al., 1986; Wilson, et al., 1961; Vest, 1974).

Table 4.4 also gives a summary of the test results, and the final report by MPB (Jarvis, 1990) (attached as Appendix A) gives the details of their testing and results. The section below summarizes the analysis results.

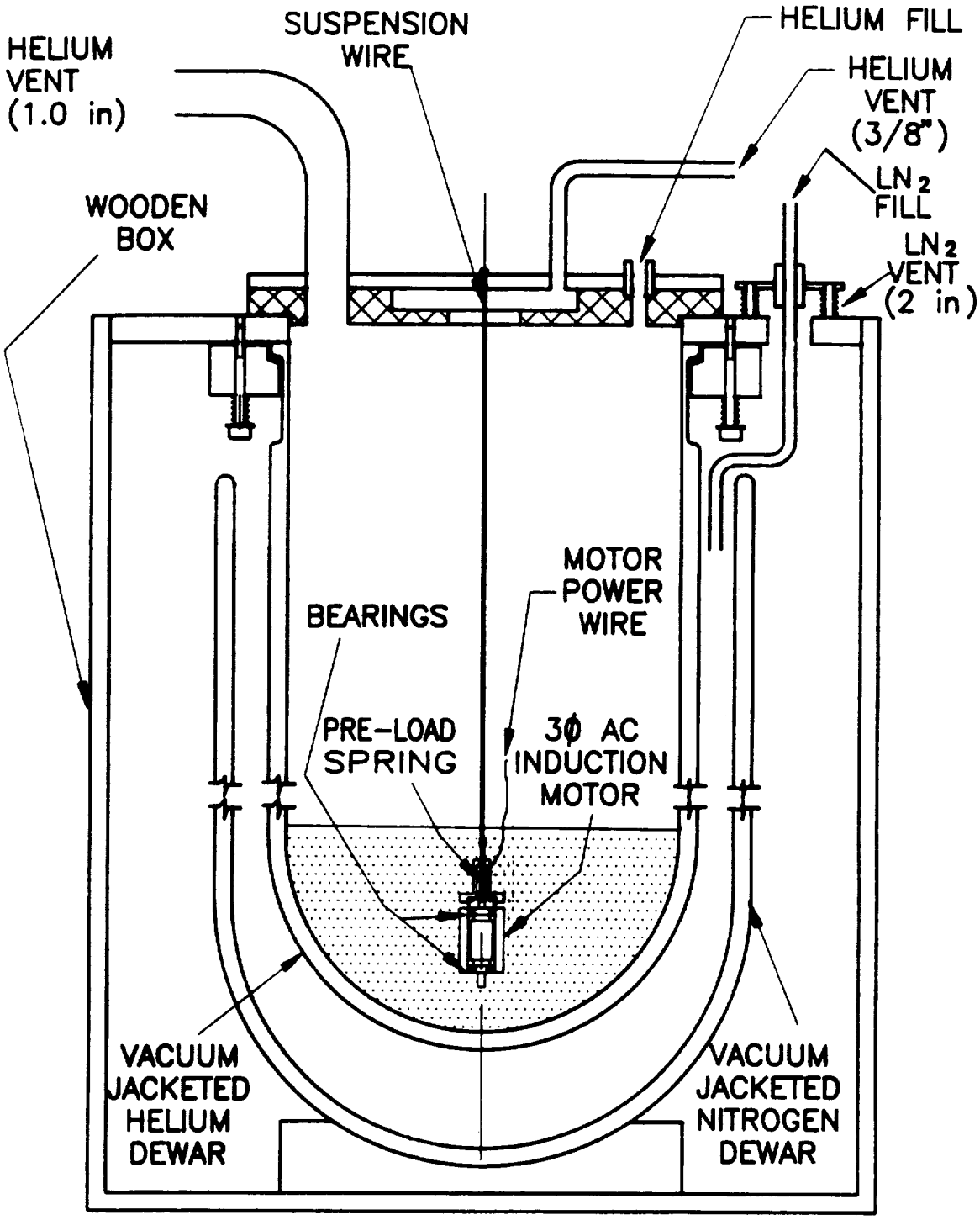

Figure 4.23. SKETCH OF TEST FACILITY NUMBER 2

Table 4.4. BEARING TEST LIST

Test	Source	Race Mat'l	Ball Mat'l	Retainer Material	Race Treatment	Speed rpm	Load lbs	No. Tested	Temp K	Duration Hours	Results
1	MBP	440C	440C	MCK (nylon, PTFE, glass composite)	None	21,000	2	6	4-40	24	1) bearings still running 2) bearings considered to be at imminent failure due to retainer debris
2	FAG	440C	440C	Vespel (SP-3) (Polyimide, 15% M_oS_2)	MoS_2 burnished on to races	21,000	2	6	4-20	3 1/2	1) bearings failed and seized due to retainer failure
3	Barden	440C	440C	Teflon/Glass/ M_oS_2	None	21,000	2	6	4-20	5	1) bearings intact at end of test 2) severe retainer debris buildup found inside shields 3) bearings considered to be at imminent failure
4	MPB	440C	Si_3N_4	Leaded Bronze	Lead Ion Plated	21,000	2	6	300	1/2	1) severe retainer wear and debris build-up found 2) imminent failure assumed
5	MPB	440C	Si_3N_4	Leaded Bronze	Lead Ion	12,000	2	2	4.2	25	1) substantial retainer wear 2) bearing still running at end of test
6	MPB	440C	440C	MCK	None	12,000	2	2	4.2	23.5	1) bearing still running at end of test

MPB SR3MCK7 Bearing. This bearing, as described above, is a standard bearing design with a nylon, glass, PTFE composite retainer design that is proprietary to MPB Corp. Two tests were conducted with this bearing design, one in each bearing tester. This bearing performed the best of all of the bearings because it showed the least damage and lowest torque values after the tests.

The bearings were first tested for 24 hours at temperatures from 4 to 40 Kelvin in Creare's six-bearing tester. After testing, all bearings showed retainer wear and debris from the retainer in the bearings. The retainers showed a burnishing of the ball pockets from contact with the balls and the bore of the retainer from contact with the inner ring of the bearing. The inner and outer rings of the bearings showed an accumulation of debris that, when cleaned, revealed undamaged raceways. The balls also showed debris on the surfaces that, when cleaned, revealed that the balls were undamaged. Figure 4.24a (Jarvis, 1990) is a 50x photo showing a view of the retainer with the burnishing of the retainer surface and figure 4.24b shows that the race appears undamaged after cleaning.

Another set of the MPB SR3MCK7 bearings were tested for 23.5 hours in Creare's second design tester. The retainer in this test showed no significant wear. Sinusoidal wear bands were found on the inner and outer raceways due to slight misalignment during assembly of the facility. Figure 4.25a shows the sinusoidal wear pattern on the inner race, caused by the misalignment. Figure 4.25b shows the displaced metal (2000x magnification) at the edge of the ball track. Local stresses were apparently so high because of the misalignment that the metal in the raceway smeared to the side of the path of the ball.

The torque measurement showed that these MPB bearings had the lowest post-test torque reading of the bearings tested (Jarvis, 1990). Figure 4.26 (Jarvis, 1990) shows the average running torque from the pre and post-test torque tests. These measurements confirm the inspection results that suggest that this bearing suffered the least wear.

FAG Bearing. Screening tests of the FAG bearings in the six bearing tester ended with catastrophic failure of the bearings. During testing, the motor power required to drive the bearings steadily increased and the noise level increased. After 3.5 hours the facility seized and would no longer run. Subsequent disassembly of the facility showed that there were broken retainer bits jammed into the bearings and that large quantities of retainer debris and probably the MoS_2 coating had flaked off and built up in and around the bearings. The bearings were also jammed into the housing because the vibration of the bearings in the bore causes the particulates to pack into the spaces around the bearings. Figure 4.27a (Jarvis, 1990) shows the ball wear groove in one of the retainer pockets. Figure 4.27b shows the inner ring wear showing pitting. The polyimide retainer apparently is not well suited to the liquid helium environment.

Barden "Bartemp" Bearing. The Barden bearings were run for only five hours due to the available liquid helium supply. The bearings were examined after the five hour run and found to have severe retainer wear and debris buildup. Figure 4.28a shows the contamination buildup on the raceway. It was the opinion of the examiners (Jarvis, 1990) that the rate of wear of the retainer and the quantity and nature of buildup on the raceway and balls indicated that these bearings were in the process of failing rapidly. Because of this, further testing was not performed. However, the lubrication mechanism for this bearing is the sacrificial wear of the retainer and deposition of that material onto the race. It is possible that the contamination

Figure 4.24a. VIEW OF MCK RETAINER SHOWING BURNISHING OF RETAINER POCKET (50x)

Figure 4.24b. VIEW OF INNER RACEWAY OF MPB SR3 MCK7 BEARING AFTER TESTING AND CLEANING (50x)

Figure 4.25a. INNER RACEWAY OF MPB SR3 MCK7 BEARING AFTER TESTING IN TEST FACILITY #2, SHOWING SINUSOIDAL WEAR BAND (20x)

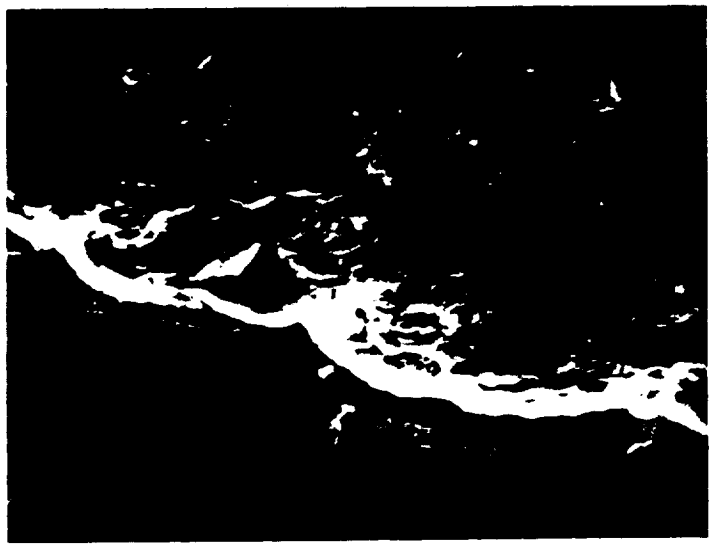

Figure 4.25b. INNER RACEWAY OF MPB SR3 MCK7 BEARING SHOWING DISPLACED METAL DUE TO EXCESS LOADING (2000x)

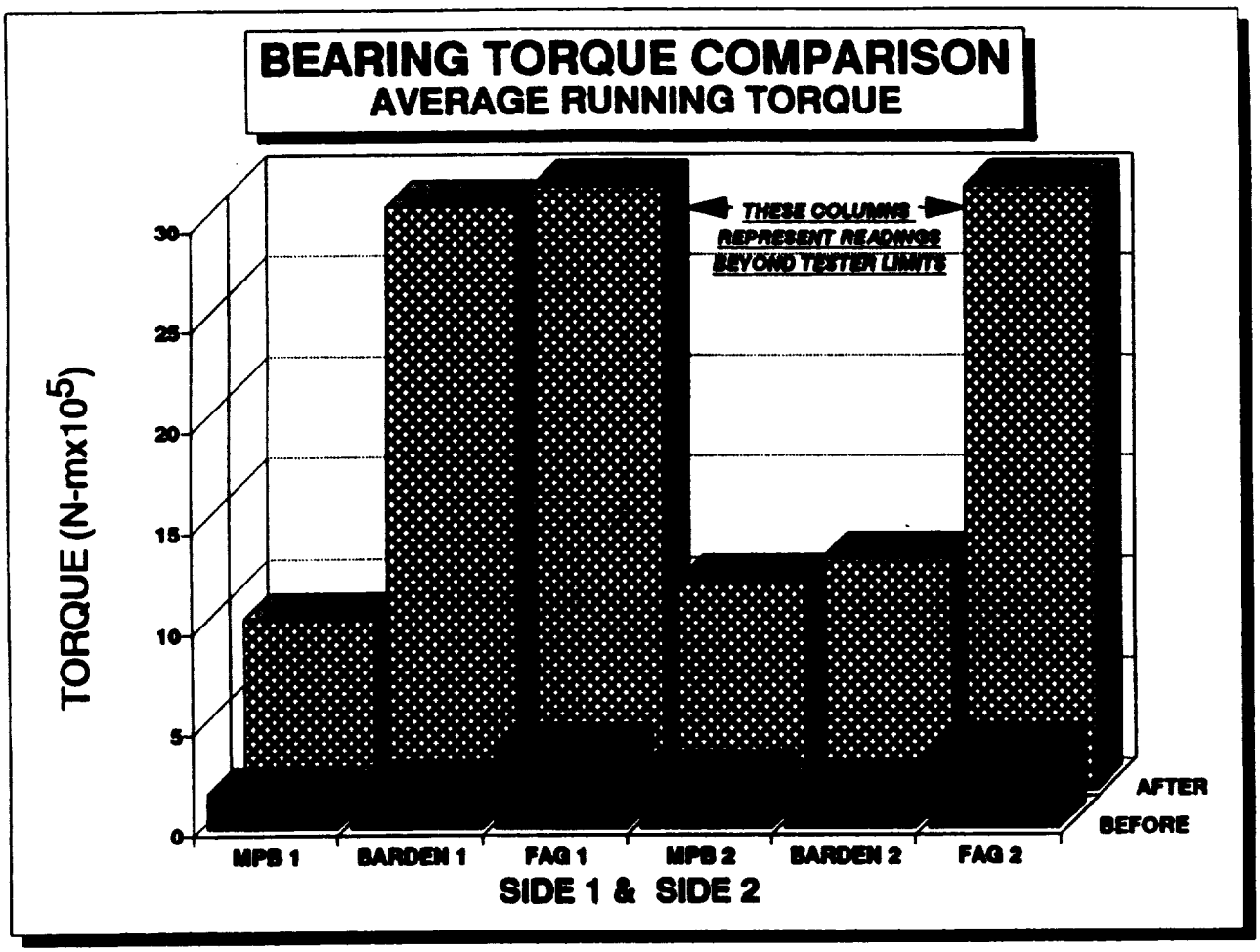

Figure 4.26. BEARING TORQUE COMPARISON

Figure 4.27a. VIEW OF POLYIMIDE RETAINER FROM FAG BEARING SHOWING WEAR TRACK IN BALL POCKET (20x)

Figure 4.27b. VIEW OF INNER RACEWAY OF FAG BEARING SHOWING PITTING SURFACE WEAR (50x)

Figure 4.28a. RETAINER POCKET OF BARDEN "BARTEMP" BEARING SHOWING RETAINER WEAR BAND (50x)

Figure 4.28b. INNER RACEWAY OF BARDEN BEARING SHOWING CONTAMINATION ON SURFACE (50x)

in Figure 4.28b is actually the beginning of the creation of the dry lubricating film. Without further testing, it is not possible to be certain whether rapid wear and contamination or sacrificial retainer wear and solid lubrication are occurring in this bearing.

MPB "K308 Bearing. The K308 bearing was run in two separate tests. In the first test, the bearings were run for 12 hours at 3.33 N preload at 12,000 rpm submerged in liquid helium in test facility number two. Examination of the bearings showed no significant degradation so they were returned for further testing. During the second test, the bearings were run for 25 hours at 12,000 rpm at an initial preload of 8.8-9.3 N in liquid helium. Upon examination of the bearing, it was found that the bearing internal parts were covered with bronze debris from the retainer. The retainers showed severe wear in the ball pockets and on the O.D. where they ride on the outer race. The raceway wear bands were coated with bronze debris, some of which was pressed onto the race material by the balls.

5. DISCUSSION OF RESULTS

The hydraulic efficiency of the transfer pump is limited by the performance of solid-lubricated ball bearings in liquid helium. A lower specific-speed impeller is required to increase bearing life. However, the difference in pump efficiency has little effect on the mass transfer efficiency. The pump performs well under NPSH conditions which simulate a liquid helium supply Dewar on orbit.

5.1 Comparison of Impeller Performance

Impeller 3 is somewhat less efficient than Impeller 2 because their specific speeds are different. The specific speed of Impeller 2 was selected to maximize hydraulic efficiency. The specific speed of Impeller 3 is less than Impeller 2 because the rotating speed of the pump was reduced to improve bearing life.

The maximum hydraulic efficiency measured for Impeller 3 is about 15% less than the maximum efficiency of Impeller 2. Efficiency data for Impeller 3 is illustrated in Figure 4.15b and the efficiency of Impeller 2 is shown in Figure 4.9. Impeller 3 reaches its maximum efficiency of 0.45 to 0.50 for flow coefficients in the range 0 to 0.2; Impeller 2 reaches maximum efficiencies in the range 0.5 to 0.6 for flow coefficients in the range 0.0 to 0.25.

The drop in hydraulic efficiency from Impeller 2 to Impeller 3 is due to a reduction in specific speed which was necessary in order to prolong bearing life. Early bearing tests at rotating speeds of 20,000 rpm have shown signs of rapid degradation, unacceptable for on-orbit helium transfer. As a result, the pump design has been altered to improve the performance of the bearings. Tests at 12,000 rpm have shown much less severe bearing wear, so that reliable operation through a complete transfer mission is highly likely. The design of Impeller 3 reflects the necessity of highly reliable operation. The drop in efficiency is expected.

The penalties for the loss in hydraulic efficiency are small. The mass transfer efficiency is insensitive to small changes in the pump efficiency, as illustrated in Figure 3.3. Thus, the reduction in pump efficiency results in a very small loss in mass transfer efficiency and implies that 15% more power is required to operate the pump during transfer. Since the amount of power is quite small in the first place (less than 10 W), the small penalties for slower speeds are small compared to the benefits of more reliable bearings.

5.2 Bearing Performance in Liquid Helium

Liquid helium is a severe environment for the operation of bearings. Polymers harden at cryogenic temperatures so the lubricating properties due to the softness of these materials may be lost. The same may be true of soft metals such as lead. This may be what happened to the polyimide retainer in the FAG bearing, causing it to abrade and wear rapidly. Liquid helium provides virtually no lubrication to the bearing and adds some drag to the rotating components, such as the retainer, and could increase the rate of wear of these parts.

The bearing which shows the most promise throughout the testing is the MPB SR3MCK7 bearing. This is the only bearing which has been tested in both test fixtures, because of its good performance in the first fixture. The MCK retainer of nylon, glass and teflon resists wear better at liquid helium temperatures than the other retainer materials. However, insufficient test time has been accumulated with these bearings to judge reliability after 500 hours. Further testing would be desirable.

The MPB K308 bearing with the silicon nitride balls and leaded bronze retainer showed some promise. But the leaded bronze retainer has worn too rapidly in 37 hours of cryogenic testing to give a high degree of confidence in the bearing. It is possible that the substitution of an MCK retainer would produce a more robust bearing.

The Barden Bartemp bearing also shows some potential. However, the wear of the retainer seems more rapid than would be acceptable in a long life bearing. With only five hours of test on the bearings, significant wear of the retainers is seen. Yet, the deposition of retainer/lubricant on the races is evident and might have led to a reduction in rate-of-wear.

The FAG bearing with polyimide retainer and MoS_2 coated races shows the least suitability to this application due to the rapid degradation of the retainers and subsequent seizure of the test bearings, after 3.5 hours of testing.

Data from these tests can guide future bearing development. In order to further develop these bearings, we recommend testing the SR3MCK7 bearing for a longer period of time (e.g., 100 hours). We also recommend testing a modified K308 bearing with the Si_3N_4 balls, 440C races and MCK retainers. Existing literature suggests that the silicon nitride balls should create a longer life bearing than unlubricated 440C on 440C. During our testing, no ball degradation was found even though the misalignment of the bearing caused significant raceway wear. If one of the bearings showed a clear advantage, a full statistical study could be pursued.

5.3 Pump Performance With Low Net Positive Suction Head

The transfer pump suffers no head degradation due to cavitation until the NPSH is very low. The pump is able to perform so well at low NPSH thanks to the thermodynamic and transport properties of liquid helium. In our tests, no head drop has been observed until the liquid level has fallen 13 cm below the tip of the inducer. Thus, the transfer pump is expected to perform well under similar NPSH conditions in an orbiting helium supply Dewar. These results confirm the hypothesis advanced in Phase I that the amount of head loss due to cavitation can be scaled based on the phenomenon of vapor pressure depression.

Liquid helium is not prone to severe cavitation because it has a high degree of vapor pressure depression. Formation of a vapor cavity on a pump impeller is a dynamic process which requires evaporation of liquid. Evaporation, in turn, requires heat which must be supplied by the liquid flowing through the impeller. Since heat must be conducted through the liquid directly adjacent to the vapor cavity, the liquid temperature at the vapor/liquid interface is less than the bulk liquid temperature. So the pressure in the vapor cavity, which is the saturation pressure corresponding to the interface temperature, is less than the vapor pressure which corresponds to the bulk fluid temperature. The difference in pressure between the cavity and the bulk vapor pressure is called the vapor pressure depression. If the vapor pressure depression is large, then a pump can operate at lower values of NPSH before a cavity can form on the impeller.

A scaling analysis of vapor pressure depression has been presented in the Phase I final report. An analysis based on thermodynamics and cavitating pump performance data shows that the vapor pressure depression is proportional to a "shift parameter," S:

$$\Delta h_v \propto S = \frac{\rho_g^2 h_{fg}^2}{\rho_f T k_f}$$

where Δh_v = vapor pressure depression (Pa),
ρ_g = density of vapor (kg/m^3),
ρ_f = density of liquid (kg/m^3),
h_{fg} = latent heat of evaporation (J/kg),
T = temperature (K), and
k_f = thermal conductivity of liquid (W/m-°C).

The units of S are s^{-1}.

Liquids with high S values tend not to cavitate readily, liquids with low S values tend to cavitate easily. Values of S have been calculated for several fluids and are tabulated in Table 5.1. Normal liquid helium has the highest value of all fluids analyzed. Superfluid helium, on the other hand, has the lowest S value (due to the high thermal conductivity) and is likely to be very prone to cavitation in centrifugal pumps. This analysis is consistent with the low-NPSH pump data for the transfer pump and with liquid helium pump data published by Ludtke and Daney (1987).

5.4 Pump Performance in Liquid Nitrogen

Several pump performance tests were run in which liquid nitrogen replaced liquid helium as the pumped fluid. These tests proved mechanical operation with a liquid cryogen. However, we were unable to successfully deduce the pump characteristics from the test data because of cavitation in the turbine flow meter.

Liquid nitrogen tests were run to prove pump operation in a liquid cryogen which was less expensive than liquid helium. The pump and all but one of the instruments were found to function properly in liquid nitrogen. However, the turbine meter was found to give erratic signals and would not indicate flows greater than about 480 L/hr.

We performed extensive calibration tests on the turbine meter with gases and liquids at ambient and cryogenic temperatures. We concluded that the turbine meter was probably cavitating in liquid nitrogen. Table 5.1 shows that LN_2 at atmospheric pressure is much more prone to cavitation than LHe. This diagnosis was confirmed when, in liquid helium tests of the transfer pump, the turbine meter functioned steadily and at all flow rates.

Table 5.1. CAVITATION PARAMETER CALCULATED FOR HELIUM AND OTHER FLUIDS

PROPERTY	FLUID/TEMPERATURE						
	Sat. HeII 1.8 K	Cold H_2O 300 K 1.21 bars	Sat. H_2O 378 K	Sat. LH 20 K	Sat. LN_2 77 K	Sat. LO_2 90 K	Sat. HeI 2.3 K
Vapor Density, ρ_v (kg/m^3)	0.44	0.015	0.60	0.09	4.5	4.0	1.43
Latent Heat, L (J/kg)	23×10^3	2450×10^3	2275×10^3	445×10^3	200×10^3	213×10^3	23×10^3
Liquid Density, ρ_ℓ (kg/m^3)	145	995	962	70.8	808	1,140	146
Thermal Cond., k (W/m K)	$\sim 10^4$	0.60	0.68	0.12	0.14	0.0084	0.003
Cavitation Parameter $\frac{\rho_v^2 L^2}{\rho_\ell T k}$ (sec^{-1})	$\sim 10^{-3}$	7.5×10^3	7.5×10^6	9.6×10^6	92×10^6	842×10^6	1.1×10^9

6. CONCLUSIONS

A centrifugal pump has been developed for helium transfer in space. The key characteristics of the pump are:

Performance. The pump provides a design-point flow rate of 800 L/hr at a head of 128 J/kg at a rotating speed of 12000 rpm. Head and flow correspond to the cold transfer requirements for refilling the SIRTF helium Dewar. Cooldown performance of 150 L/hr with a head of 184 J/kg is also met.

Bearings and reliability. Stainless steel ball bearings are used with nylon/teflon/fiberglass retainers which provide solid lubricant. These bearings have proven operation for 24 hours under simulated pumping conditions in liquid helium. Post test examination of these bearings shows some wear but no signs of imminent failure. Reliability for a single refill mission is high.

Resistance to cavitation. The transfer pump suffers no head degradation due to cavitation down to zero NPSH. So the pump will meet the SIRTF refill requirements for head and flow rate when pumping from an orbiting helium supply Dewar.

Efficiency. The overall efficiency of the transfer pump is 0.45. This corresponds to a mass transfer efficiency of 0.99 in the SIRTF refill mission.

Other broad conclusions and recommendations for further research and development are:

1) The pump hydraulic efficiency is limited by bearing performance. To achieve maximum pump efficiency, bearings are required which operate reliably at speeds of 20,000 rpm. However, the mass transfer efficiency is not very sensitive to the hydraulic efficiency and is still very high even at 12,000 rpm.

2) Bearing reliability is still unknown for very long operating lives. This is a key consideration for transfer pump applications in which bearings cannot be easily replaced (a space-based system, for example). In this case, endurance tests are recommended in which a large number of bearings are tested for long life in liquid helium. Test durations on the order of 500 hours are required if reliability is to be demonstrated for applications such as the Superfluid Helium On-Orbit Transfer (SHOOT) experiment. The tests performed in this project indicate which bearings have the most promise for extended life.

3) The true benefits of the inducer have not yet been determined. Pump performance is adequate for space helium transfer with or without the inducer. Cavitation tests in the present facility are unable to show head loss due to cavitation in the inducer because the pump is too close to the bottom of the test Dewar. The liquid level cannot reach a point far enough below the pump to cause significant cavitation in the inducer. It would be straightforward to modify the pump test facility to allow tests at lower NPSH. In this way, the effects of the inducer on cavitation performance could be measured.

REFERENCES

Abernathy, R.B., Breneman, J.E., Medlin, C.H., and Reinman, G.L.; Weibull Analysis Handbook; Aero Propulsion Lab., Air Force Wright Aeronautical Labs., Wright-Patterson AFB, OH, November, 1983.

Barden Engineering Data Sheet, B-3, Barden Corp., Danbury, CT, April, 1965

Bhat, B.N.; *Cryogenic Turbopump Bearing Materials*; Application of Advanced Material for Turbomachinery and Rocket Propulsion, AGARD, March, 1989.

Brew, D.E., Scibbe, H.W., and Anderson, W.J.; *Film-Transfer Studies of Seven Ball-Bearing Retainer Materials in 60°R (33 K) Hydrogen Gas at 0.8 Million DN Value*; NASA Lewis Research Center, OH, NASA TN-D-3730, November, 1966.

Daney, D. and Ludtke, P.; Personal Communication, 1987.

Devine, M.J. and Kroll, A.E.; *Aromatic Polyimide Compositions for Solid Lubrication*; Lubrication Engineering, June 1964.

Donsky, B.; *Complete Pump Characteristics and the Effect of Specific Speeds on Hydraulic Transients*; ASME Paper No., 61-Hyd-3, 1961.

Fletcher, E.E.; *Titanium Carbide Coatings for Aerospace Ball Bearings; Development Awareness Bulletin*, Iss. 198, Metals and Ceramics Information Ctr., Battelle, Columbus, OH, February, 1990.

Gould, S.G. and Roberts, E.W.; *The In-Vacuo Torque Performance of Dry-Lubricated Ball Bearings on Cryogenic Temperatures*; 23rd Aerospace Mechanisms Symp., Huntsville, AL, May, 1989.

Jarvis, E.W.; *Creare Cryogenic Test R3 Bearings*; Miniature Precision Bearings Engineering Lab., Report No. 90-18, December, 1990.

Kamath, P.S. and Swift, W.L.; *Two-Phase Performance of Scale Models of a Primary Coolant Pump*; EPRI NP-2578, Electric Power Research Inst., Palo Alto, CA, 1982.

Kamath, P.S., Tantillo, T.J., and Swift, W.L.; *An Assessment of Residual Heat Removal and Containment Spray Pump Performance Under Air and Debris Ingesting Conditions*; Creare TM-825, NUREG/CR-2792, US NRC, 1982.

Kannel, J.W., Merriman, T.L., Stockwell, R.D., and Dufrane, K.F.; Evaluation of Outer Race Tilt and Lubrication on Ball Wear and SSME Bearing Life Reductions; NASA Marshall Space Flight Ctr., AL, NASA-CR-170836, 1983.

Kannel, J.W., Dufrane, K.F., and Barber, S.A.; *Development of Improved Self Lubricating Cages for SSME HPOTP Bearings*; Battelle Columbus, Columbus, OH, NASA CP-3012, 1988.

Kittel, P.; *Liquid Helium Pumps for In-Orbit Transfer*; NASA Technical Memorandum 88239, 1986.

Lee, J.H., Ng, Y.S., and Brooks, W.F.; *Analytical Study of Helium II Flow Characteristics in the SHOOT Transfer Line*; NASA Ames Research Center, Presented at the Space Cryogenics Workshop, U. Wisconsin, June 21-23, 1987.

Ludtke, P.R.; *Performance Characteristics of a Liquid Helium Pump*; NBSIR 75-816, National Bureau of Standards, Boulder, CO, 1975.

NASA-Ames Research Center; *Request for Proposals for Development of a Superfluid Helium Centrifugal Pump Assembly for the Liquid Helium Transfer Flight Demonstration*; RFP2-33115(PSD), July 20, 1987.

Nosaka, M., Oike, M., Kamijo, K., Kikuchi, M., and Katsuta, H.; Experimental Study of Lubricating Performance on Self-Lubricating Ball Bearings for Liquid Hydrogen Turbopumps; ASLE Preprint, No. 86-TC-3E-1, October, 1986.

Poole, W.E. and Bursey, R.W., Jr.; Pratt & Whitney Cryogenic Turbopump Bearing Experience, Pratt & Whitney Gov. Engine Business, West Palm Bch., FL, May, 1988.

Spalvins, T.; *Coatings for Wear and Lubrication*; NASA Technical Memorandum, TM-78841, April, 1978.

Shepherd, D.G.; *Principles of Turbomachinery*; Macmillan Publishing Corp., NY, 1956.

Sixsmith, H. and Giarratano, P.; *A Miniature Centrifugal Pump; Review of Scientific Instruments*; 41(11), November 1970, pp. 1570-1573.

Steward, W.G.; *Centrifugal Pump for Superfluid Helium*; Cryogenics, 26 97, 1986.

Vest, C.E.; *Evaluation of Several Additional Dry Lubricants for Spacecraft Applications*; Lubrications Engrg., V.30(5), May, 1974.

Vlaming, D.J.; *Optimum Impeller Inlet Geometry for Minimum NPSH Requirements for Centrifugal Pumps*; Mech. Conference, 3rd Joint ASCE/ASME, La Jolla, CA, July 9-12, 1989.

Wiesner, F.J.; A Review of Slip Factors for Centrifugal Impellers; Trans. ASME, October, 1967.

Wilson, W.A., Martin, K.B., Brennan, J.A., and Birmingham, B.W.; *Evaluation of Ball Bearing Separator Materials Operating Submerged in Liquid Nitrogen*; ASLE Trans., 4, April, 1961.

APPENDIX A

CRYOGENIC TEST - R3 BEARINGS

MPB

Miniature Precision Bearings Engineering Laboratory Report

Title: CREARE CRYOGENIC TEST
R3 BEARINGS

Report No.: 90-18

Date: 21-DEC-90

Copies To: Robert Hasenbein
Creare, Hanover, N.H.

Written By: EW Jarvis

Approval:

BACKGROUND: The following will describe the test results of R3 bearings operating at cryogenic temperatures. The tests were conducted by Creare Inc. Hanover, NH. as part of a liquid helium pump development program for NASA. Bearing analysis was performed at MPB Corporation. The bearings in this program were run with no lubrication, a 1-2 lb preload, 22,000 and 12,000 RPM, at temperatures of 4°-20° Kelvin, submerged in liquid helium. The following bearings were evaluated:

MPB SR3MCK7 (R3 class 7 with molded nylon-fiberglass retainers) (Run 24 hrs)

Barden R3 "Bartemp" (Undefined internal bearing design) (Run 5 hrs)

FAG SR3.KE4.T5.C58.F. (Undefined internal bearing design) (Run 3.5 hrs)

MPB K308 R3 with lead-ion plated raceways, leaded bronze retainer and silicon nitride (Si_3N_4) balls. (Run 24 hrs)

CONCLUSIONS: It appears that operating at cryogenic temperature under the conditions of this test, created an environment for extraordinary bearing retainer wear. The wear debris accumulates in the ball pathway causing excessive bearing torque. Conclusions in this report are based on single tests, therefore judicious use of the data is advised.

1. The most successful of the bearings tested in this program is the MPB SR3MCK. Although this is the most generic of the bearings tested, the MCK retainer appeared to resist the abrasive environment better than all other materials evaluated. The MCK otherwise known as a Molded Minapar II retainer is a patented product exclusive to MPB.

2. The second choice is the K308 bearing. Of the many materials considered at the beginning of this program, this bearing included the features which we thought most likely to provide success. Debris resulting from wear on the leaded bronze retainer and the lead coated raceways created excessive rolling resistance in the bearings.

3. The third choice is the Barden "Bartemp" bearing which had severe retainer wear and dramatically increased torque after only five (5) hours.

4. The last is the FAG bearings which were totally unusable with severely worn and fractured retainers after (3.5) hours.

PROJECT APPROACH: Creare Inc., Hanover, NH has a contract to develop a Liquid Helium Pump for NASA. The pump assembly will be submerged in liquid helium which is at extremely low temperatures of about (4°) Kelvin. The motor bearings will be exposed to a flow of liquid and gaseous helium at a rotational speed of 22,000 RPM with axial preloads of 1 to 2 lb.. MPB was approached to supply some bearings for test and to provide post service analysis for these and bearings recommended and supplied by Barden and FAG. Pre-run torque tests and post-run analysis will be conducted at MPB, all cryogenic testing was performed at Creare in Hanover. Due to technical and financial constraints, the actual run-time at temperature was restricted to (24) hours and limited to single tests of each bearing design.

TEST METHOD: The test method used to expose the bearings to liquid helium fall into two categories. Considering the high cost of materials and test maintenance, the first approach (test fixture 1) was intended to gain maximum information from each (24) hour supply of liquid helium. In this test (6) bearings were stacked in a single housing, preloaded and run at 22,000 RPM in a vertical orientation. After a series of tests were run with this fixturing it was determined that severe retainer wear introduced too much debris to the lower bearings in the stack. The excessive debris made bearing removal from the fixture very difficult and clouded the details of any refined Post Service Bearing Analysis.

Using information from the first test series, a second fixturing system was established (test fixture 2). In an effort to duplicate as close as possible the final bearing application, this new fixture located (2) bearings horizontally, were run at 12,000 RPM, in a flow of liquid helium. Debris from retainer wear will now most likely be flushed out of the bearings.

As a result of (6) bearings per test, the bulk of our data was derived from test fixture (1). If the failure mode was subtle, contamination from bearings in this system could have made failure analysis difficult. However damage to the retainers was so severe, direct comparison of bearing performance can be made with a reasonable degree of confidence. For example, torque comparisons in this report were made with values after running bearings with test fixture (1).

The two bearing designs performing best in test fixture (1) were run in fixture (2). Refer to MPB SR3MCK and MPB K308.

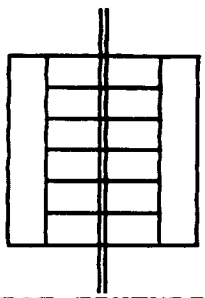

TEST FIXTURE 1

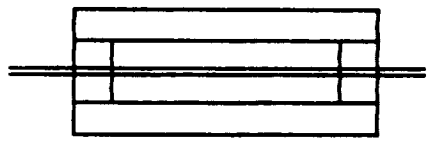

TEST FIXTURE 2

EARING DESCRIPTIONS:

PB BEARINGS: MPB has the capability to provide a great number of bearing aterials and coatings which could enhance bearing performance and life. The ost recent innovations of bearing technology were considered for this pplication. Because of the limited funding for this program MPB supplied he following two bearing designs for test:

308: The first was the K308 bearing incorporating features which, according o available test data, would provide the best chance for success in this pplication. The K308 bearing is a complex design employing a process eveloped and produced by the European Space Tribology Laboratory (ESTL), isley, Warrington, England. The ring material is 440C stainless steel, etainers were machined from a special composition of leaded bronze and the alls were AFBMA Grade 5 manufactured from silicon nitride (Si_3N_4). The earing components were manufactured at MPB and sent to ESTL for processing. heir very tightly controlled process includes lead plating of the raceways nd a run-in of the assembled bearings.

The leaded bronze retainer and the raceway lead coating of pproximately 0.5 microns by ESTL were selected based on extensive, uccessful, bearing performance evaluation at cryogenic temperatures by STL. Information from these tests was presented at the 32nd Aerospace echanisms Symposium, May 3-5 1989, Huntsville, Alabama {1}. This material nd process is also used extensively in the European Space Programs.

SR3MCK: The second recommendation by MPB was an SR3MCK which is the most economical design in which we had a high confidence factor. The SR3MCK is a standard catalog bearing using 440C stainless steel rings and balls with a molded Minapar II retainer. The retainer is an MPB proprietary nylon/fiberglass composite. This material was developed to resist wear and to provide a controlled release of Teflon as a lubricant for marginally lubricated conditions. To insure adequate clearance while operating at 4° Kelvin, the standard MCK retainer bore was increased by .004".

Experimentally, the SR3MCK bearing has proved quite successful under a variety of temperature and starved lubricant conditions. Although we have confidence in the MCK retainer operating at low temperatures, we had no data at the cryogenic range of liquid Helium.

BARDEN BEARING: Barden's recommendation for this application is an R3 bearing with 440C rings and balls with a "Bartemp" retainer. Essentially "Bartemp" is a Barden trade name for Duroid which represents a sacrificial self-lubricating retainer material intended to operate in extreme temperature applications.

FAG BEARINGS: FAG recommendation for this application is an (SR3.KE4.T5.C58.F) bearing. The retainer for this bearing is made of Vespel which is also a sacrificial self-lubricating material for extreme temperature applications. Bearing internal surfaces had a bead-blasted appearance which was probably a wear resistance coating.

EXAMINATION RESULTS:

FAG: Six FAG bearings were evaluated after running for 3.5 hours in test fixture (1). Included with these six test bearings from Creare was a packet of debris removed from the fixture with the bearings. Included also were the two motor bearings used to drive the test bearings. These motor bearings were run for 3.5 hours but at the higher temperature of 220 Kelvin.

The following conditions were found in the eight bearings tested:

1. Outside diameters and raceways of inner rings, inside diameters and raceways of outer rings and balls that were not destroyed, are covered with a rough, bead-blasted appearance. If this represents a surface treatment for wear resistance, it did not seem to accomplish much in this application.

2. All retainer pockets were badly worn, some to a point where the retainer came out of the bearing and became lodged between the balls of two adjacent bearings. In this position rotating balls generated wear grooves in the retainer faces. Refer to photographs on page #17. In some bearings the retainers fractured into many pieces.

3. Major debris throughout the system was the result of extensive retainer wear accelerated by the rough surfaces.

4. Test bearings #1,2,3,4, and motor bearings #7 and #8 had about the same degree of damage described above. Bearings #5 and #6 were much more severely damaged with gross wear and spalling on raceways and balls. This damage was most probably caused by a break-down of the metal surface treatment including exceptional stress generated by an abundance of retainer debris from the bearings located above. Refer to photographs on page #18.

5. Bearing torque after the run test was greater than the capacity of our torque tester, therefore no "after" torque readings are available.

BARDEN: Six Barden bearings with "BARTEMP" retainers were evaluated after running for 5.0 hours in test fixture (1). The following conditions were found in the six bearings tested:

1. All bearings contained a substantial amount of debris resulting from excessive retainer pocket wear. Refer to photographs on page #19 and #20.

2. Bearing #6 contained the least amount of retainer debris yet had the most severe damage (contamination brinelling) to the raceway wear band. Refer to photographs on page #21.

Bearing #6 also had a sinusoidal wear band which indicates a misalignment of the inner ring to the rotational path of the balls. This inner misalignment had no influence on other bearings, considering the concentric wear bands found on all other bearings from this fixture.

3. Bearing torque values after the run test of (5) hours were much higher than expected. Refer to charts and graphs on page #9,10,11,12,13 & 15.

PB SR3MCK - TEST FIXTURE #1: The six SR3MCK bearings were evaluated after unning for 24 hours in test fixture (1). The following conditions were ound in the six bearings tested:

1. All bearings contained a layer of fine retainer debris in differing mounts. The retainer ball pockets were burnished from contact with the otating balls. This burnish appears to have compressed the material in a arrow band near the retainer O.D. The retainer bore was also burnished from ontact with the inner ring O.D. Refer to photographs on page #22.

2. Inner and outer ring "wear bands" have an accumulation of loose etainer debris. After cleaning, the raceways appear to be undamaged. Refer o photographs on page #23.

3. Balls have loose contamination on the surface. Close examination shows o detectable damage. Refer to photographs on page #24.

4. Torque values after the (24) hour run-test increased less than other earings evaluated. Refer to charts and graphs on page #9,10,11,12,13 & 14.

IPB SR3MCK - TEST FIXTURE #2: Two SR3MCK bearings (#13 & 14) were evaluated ifter running in test fixture (2), for 23 hours at 12,000 RPM, with an .nitial preload of 2.0 to 2.1 pounds, at 4.2° Kelvin. The following conditions were found in both bearings tested:

1. Inner and outer rings from both bearings have sinusoidal wear bands. This is an indication of misalignment between the rings and rotational axis of the bearing pair. Compared to bearings in alignment, this condition will cause much higher bearing internal stresses. Extremely high stresses were apparent in both bearings represented by a smooth wear band with displaced metal in the direction of the low contact angle. These are not typical wear bands in which abrasive contact stresses erode raceway material away. They appear to be caused by the cyclic stress created by excessive preload, imprinting rotating balls into the inner and outer raceways. Refer to photographs on page #25.

2. Retainers show no sign of wear or burnish. There are however slight traces of dark debris in some pockets and the bores. In one area of the retainer from bearing #14, there appears to be a small amount of embedded metallic debris. Refer to photographs on page #26.

3. Balls have a single wear band which is sign of a single, constant loading which prevents random ball rotation. Refer to photographs on page #27.

MPB K308 - TEST FIXTURE #1: Six K308 bearings were mounted for test in test fixture (1) and run for ½ to 1 hour at 5,000 to 12,000 RPM at room temperature with an initial preload of about two pounds. When the test fixture was disassembled to correct an instrument malfunction, the bearings were found to be loaded with fine black and bronze colored dust. This debris also jammed the bearings into the bore of the test cartridge. As a result of this finding, these bearings were not run additionally at cryogenic temperature and had torque values beyond the tester capacity. The following information resulted from the room temperature test:

1. All bearings were contaminated with relatively large amounts of debris, primarily from retainer wear. This debris within the bearings caused excessive stress and over heating the ring wear bands as represented by a variety of colors from straw to dark blue. Refer to photographs on page #28.

2. Balls were covered with debris but after cleaning, appeared to be undamaged. Refer to photographs on page #28.

3. Retainers were severely worn where the O.D. contacted the outer ring bore and in all ball pockets. Refer to photographs on page #29.

MPB K308 - TEST FIXTURE #2: As a result of findings from test fixture (1), it was determined to re-design the test bed to more realistically replicate the final bearing application. The following information resulted from the first test performed on the re-designed fixture (2):

In the first phase of this test the bearings were run for 12 hours, at 12,000 RPM, 0.75 pound preload, at 4.2° Kelvin, submerged in liquid helium. At this point the bearings were examined at MPB for obvious problems and none were found. General observations were made on assembled bearings only because disassembly could have changed the orientation of components and destroyed the bearing integrity. The bearings were then returned to Creare for additional run-test time.

In the second test phase, the bearings were run for 25 hours, at 12,000 RPM, with an initial preload of 2.0 to 2.1 pounds, at 4.2° Kelvin, submerged in liquid helium. After running for 25 hours the bearings in the fixture had lost preload and loosened to a .001" free end play. The bearing which is required to slide to maintain preload was jammed with debris and unable to move. The following information was found in the disassembled bearings:

1. All bearing internal components were covered with retainer debris. Inner and outer raceway wear bands from both bearings were covered with a thick bronze colored flaking film. Considering the gross retainer wear, it is obvious that this film is retainer wear debris which has been pressed onto the raceways. Refer to photographs on page #30.

2. Retainers show severe wear in all ball pockets and where the O.D. contacts the outer ring bore. Refer to photographs on page #31.

3. Balls were covered with retainer debris but appeared to be un-damaged. Refer to photographs on page #30.

ISCUSSION:

etainer Wear: The most serious problem found in the bearings evaluated was etainer wear. Balls rotating within the bearing push against the retainer ockets causing the retainer to spin about the bearing axis. Any conditions hat would cause resistance to the retainer movement could exaggerate riction and wear. The wear points would be at the ball to retainer pocket nterface and at the contact point between the retainer and the bearing ing. These wear points were apparent in nearly every bearing evaluated in his program.

Where some bearings have successfully operated at cryogenic emperatures in other applications, the following extreme conditions of this est must be considered:

1. (4°) Kelvin (liquid helium) is an extremely low cryogenic temperature.

2. Operating submerged in liquid which has low lubricity.

3. 12,000 and 22,000 RPM is a rather high speed for running in liquid.

This report presents the results of single tests only. To determine he specific cause of failures will involve extensive additional testing.

'AG: Based on Vespel material recommendations, the FAG bearings were xpected to perform well in this application. Pre-run torque tests indicated omewhat higher values compared to other bearings tested. Refer to torque alue charts and graphs on page 9,10,11,12,13 & 16. Both inner and outer aceways appeared to be treated with a substance which left a very rough bead blast) surface which was probably a wear resistance coating. All earings failed with gross retainer wear after only 3.5 hours.

Barden: Barden "Bartemp" retainers are basically Duroid material which is lso recommended for cryogenic operation. The conditions of this test were pparently too severe for this bearing design with retainer failure after nly 5 hours.

MPB K308: The K308 bearing incorporated features which MPB thought would rovide the best chance for success in this application. Much work done by ESTL has shown that leaded bronze retainers, with 440C rings processed with heir proprietary lead coating, performs very well in space applications at ryogenic temperatures.

Comparative conditions representing ESTL research which were presented at the 23rd Aerospace Mechanism Symposium in May 1989 {1} and this test program conducted by Creare are as follows:

	ESTL	Creare
1. Temperature	: 20° Kelvin	4° Kelvin
2. Speed (RPM)	: 100 / 200	12,000
3. Environment	: Vacuum	Liquid Helium

MPB K308 (cont'd: Results show the conditions of the Creare test (fixture 2) to have generated an extremely abrasive environment causing gross retainer wear. Retainer debris in the ball pathway then created extremely high bearing torque. The following conditions could have contributed to this unexpected excessive wear in the ball pocket and retainer outside diameter:

1. Increased speed.
2. Decreased temperature.
3. Running in liquid rather than a vacuum.

The (6) bearings run for ½ to 1 hour in test fixture (1), at room temperature, created about the same degree of retainer wear. More testing would be required to develop a reasonable failure scenario for this test.

MPB SR3MCK: There does not seem to be any question about retainer wear being the primary cause of failure in all other bearings tested in this program. The MCK retainer material seems to resist wear better than the other materials under the conditions of this test.

In the most severe test (fixture 1) at 22,000 RPM, the MCK retainer showed a slight depression in the ball pockets that appeared to be a combination of wear and compression of the basic material.

In fixture (2) which simulates the final application at 12,000 RPM, the retainer shows no wear at all.

In fixture (2) there seems to be a serious alignment/preload problem. Both rings of both bearings have extremely heavy sinusoidal wear bands. These wear bands clearly show a misalignment of the raceways to the rotational axis of the ball train. A review of the fixture bearing mounts could explain the cause of this misalignment.

Misalignment will cause excessive cyclic loading of the bearings, however the condition of these raceways indicate a more serious problem. The fixture preload system should be reviewed for the cause of this extreme overloading.

One must be concerned about making serious judgments without the benefit of repetitive tests to establish confidence by statistical evaluation. Under the conditions of this program we can only make recommendations based on the limited available data. With this in mind, it appears that a standard MPB MCK retainer resists wear better than other materials tested and there seems to be no problem with good quality 440C basic bearings.

REFERENCES:

{1} S.G. Gould and E.W. Roberts; "The in-vacuo torque performance of dry-lubricated ball bearings at cryogenic temperatures", 23RD Aerospace Mechanisms Symposium, May 3-5, 1989, Huntsville, Alabama.

S.G. Gould and E.W. Roberts; "The performance of PTFE, Lead and MoS_2 as lubricant films for ball bearings operating in vacuum at 20°K", ESTL, AEA Technology, Risley, Warrington, WA3 6AT, UK.

)RQUE TESTING: Torque testing at low speed (2-RPM), has been shown to be ıe most effective way to evaluate the internal quality of an instrument ɜaring. In general torque testing measures the rolling resistance between ıe rotating bearing inner ring and the fixed outer ring. In this program ɔrque traces of the bearings were made before and after exposure to the ɜst conditions as one means of evaluating the effect of running at ɾyogenic temperatures. Torque limitations or the need for them in this ɔplication have not been established, therefore torque values in this ɜport should be used for reference comparison only.

The bearings were torque tested at two (2) RPM, under a 400 gm axial ɔad, one rotation clockwise and one rotation counterclockwise. The torque n FAG bearings after cryogenic exposure, was too great for the torque ɜster, as a result no "after" readings are available. K308 bearings were ent directly to Creare in the sealed packages as received from ESTL herefore no detailed "before" torque data is available. A single K308 earing was tested to establish general torque values in the "before" ategory for reference only.

INTERPRETING TORQUE TRACES FROM THE RT2C

The RT2C produces an actual trace of a bearing's torque characteristics in addition to calculating its basic torque values. Further analysis of a torque trace may reveal other conditions.

THE QUANTITATIVE PARAMETERS OF
THE
RUNNING TORQUE OF A BEARING
(MIL-STD-206)

PEAK RUNNING TORQUE = X
AVERAGE RUNNING TORQUE = Y/2
MAXIMUM HASH WIDTH = Z
AVERAGE HASH WIDTH = Z_1

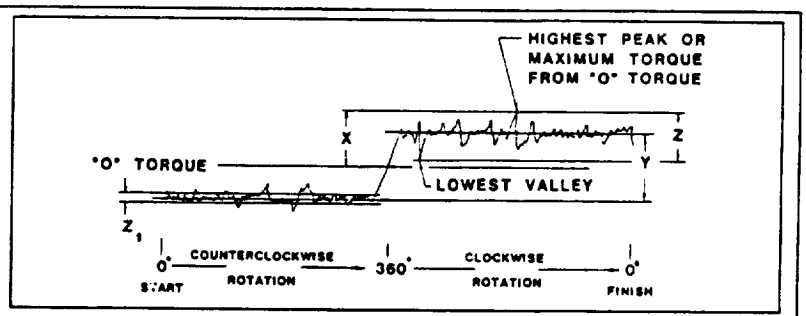

CONSOLIDATED TORQUE VALUES (Detailed Results Later In This Report)

			SIDE # 1				SIDE # 2			
:O.	BRG	TEST SEQ.	ART	PRT	AHW	MHW	ART	PRT	AHW	MHW
:==	===	=======	======	=======	======	=======	======	=======	==========	==========
ɜARD	AV.	BEFORE	2125	5750	1083	6150	2000	7167	1083	5467
ıPB	AV.	BEFORE	1788	3813	1031	5094	2605	6408	966	7971
'AG	AV.	BEFORE	3922	39916	17818	68038	3916	39832	19318	68333
:308	REF	BEFORE	17542	64403	14229	87906	----	----	----	----
ɜARD	AV.	AFTER	29019	82714	16881	149147	11485	71878	22132	150852
ıPB	AV.	AFTER	8628	36076	14974	60908	10427	42147	15853	66591
'AG	AV.	AFTER	----	----	----	----	----	----	----	----
ɜARD	AV.	DIFF.	26894	76964	15798	142997	9485	64711	21048	145385
ıPB	AV.	DIFF.	6840	32263	13942	55814	7822	35739	14887	58610
'AG	AV.	DIFF.	----	----	----	----	----	----	----	----

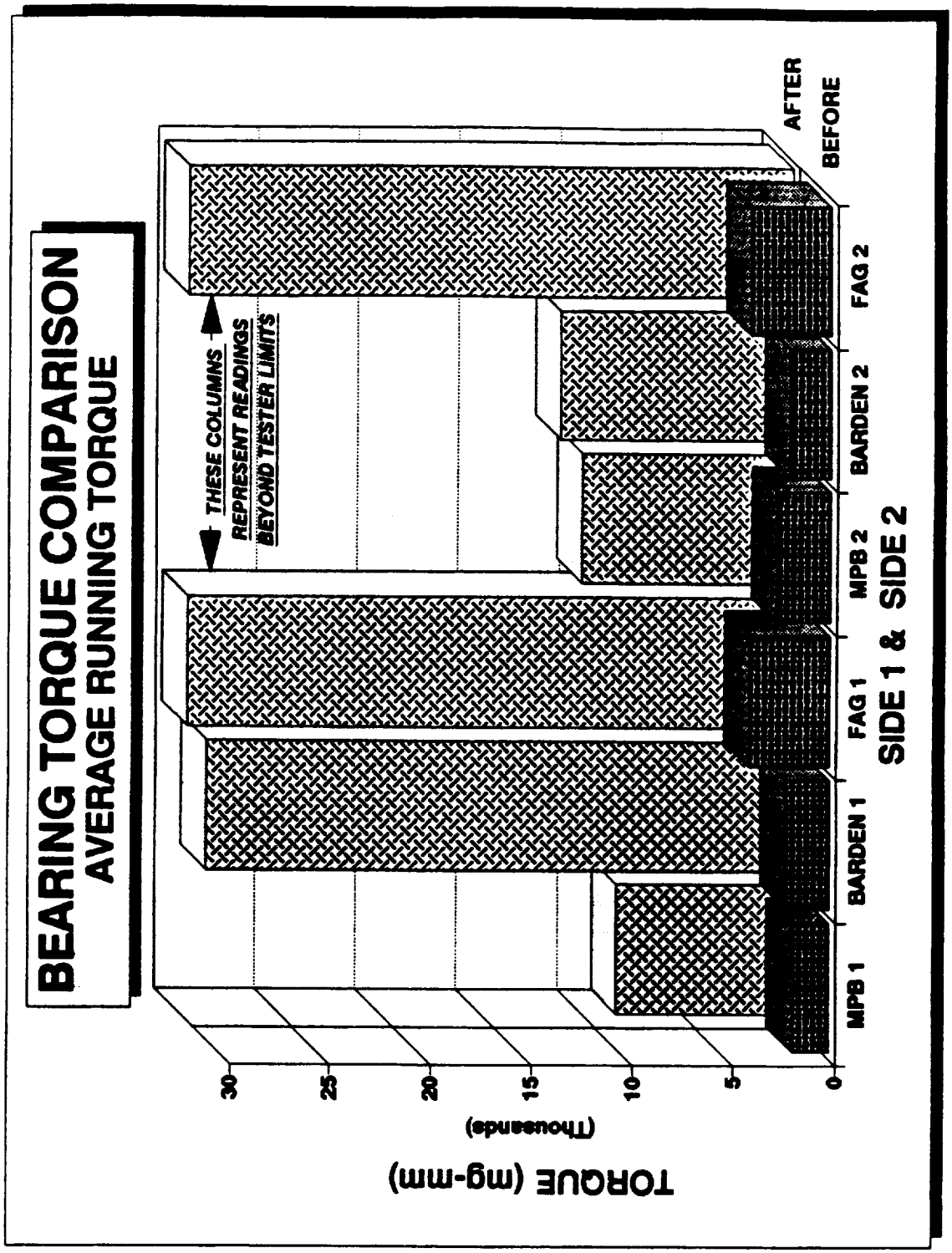
BEARING TORQUE COMPARISON
AVERAGE RUNNING TORQUE
THESE COLUMNS
REPRESENT READINGS
BEYOND TESTER LIMITS
AFTER
BEFORE
TORQUE (mg-mm)
(Thousands)
30
25
20
15
10
5
0
MPB 1
BARDEN 1
FAG 1
MPB 2
BARDEN 2
FAG 2
SIDE 1 & SIDE 2

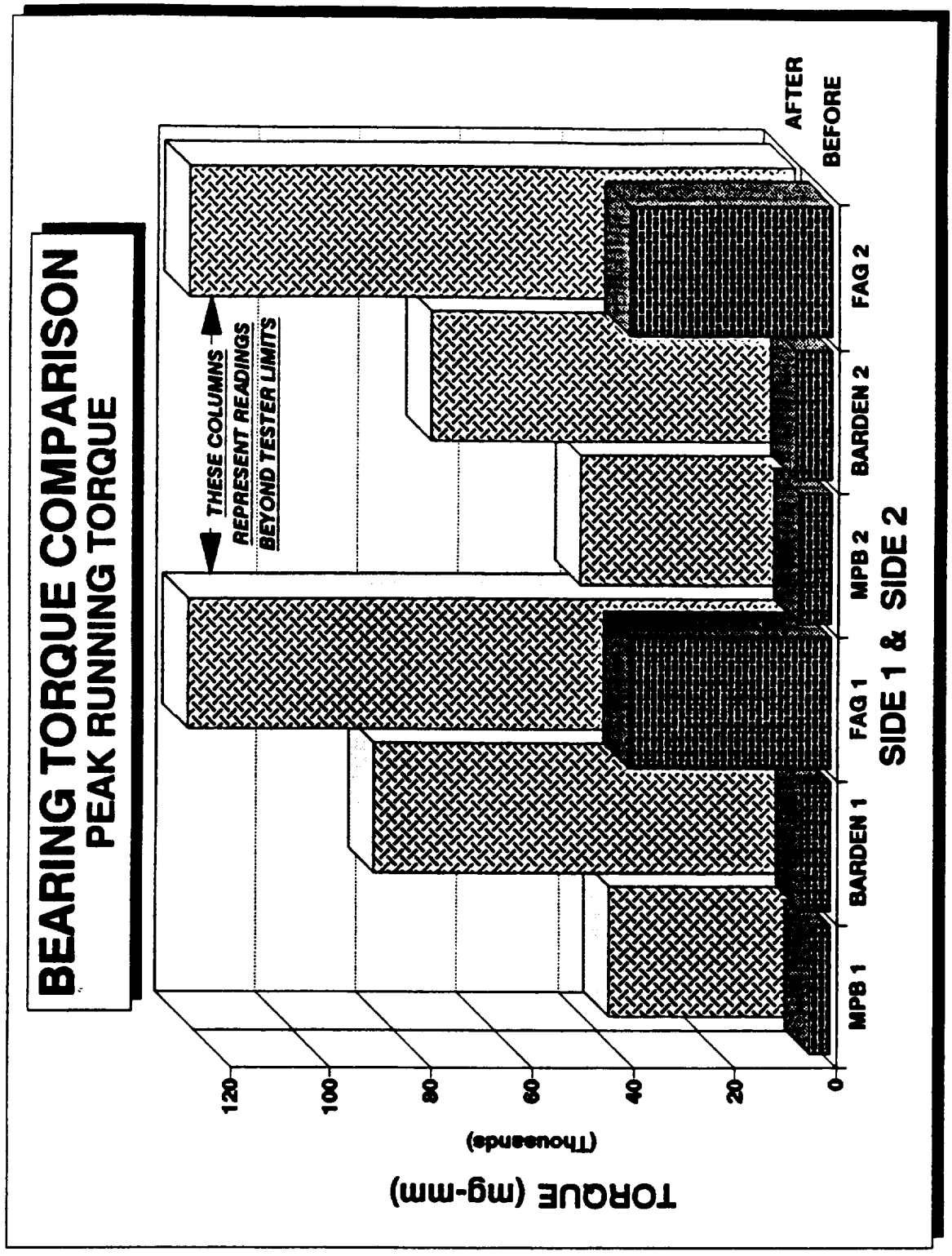
BEARING TORQUE COMPARISON
PEAK RUNNING TORQUE
THESE COLUMNS REPRESENT READINGS BEYOND TESTER LIMITS
AFTER
BEFORE
TORQUE (mg-mm)
(Thousands)
120
100
80
60
40
20
0
MPB 1
BARDEN 1
FAG 1
MPB 2
BARDEN 2
FAG 2
SIDE 1 & SIDE 2

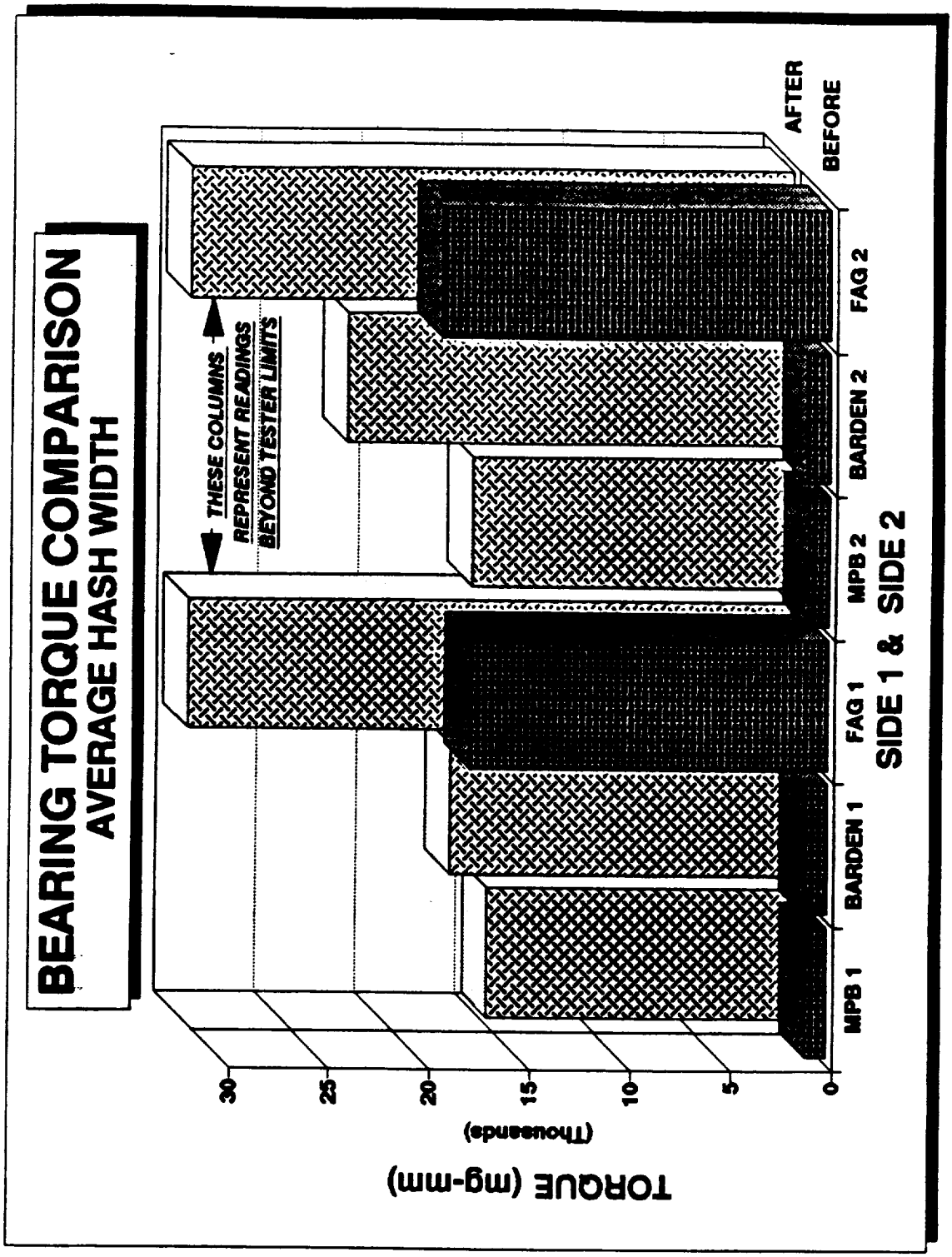
BEARING TORQUE COMPARISON
AVERAGE HASH WIDTH
THESE COLUMNS REPRESENT READINGS BEYOND TESTER LIMITS
AFTER
BEFORE
TORQUE (mg-mm)
(Thousands)
0
5
10
15
20
25
30
MPB 1
BARDEN 1
FAG 1
MPB 2
BARDEN 2
FAG 2
SIDE 1 & SIDE 2

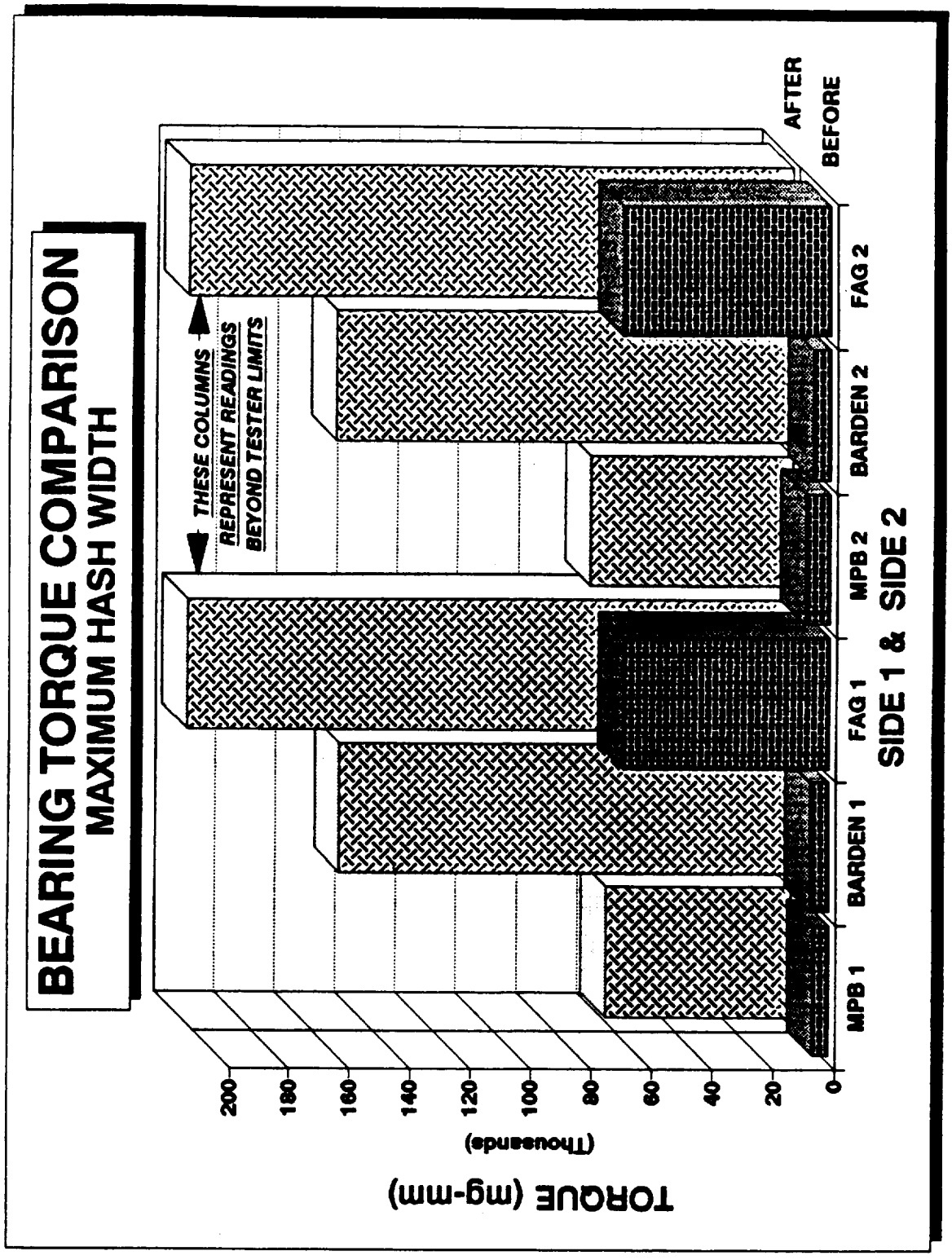
BEARING TORQUE COMPARISON
MAXIMUM HASH WIDTH
THESE COLUMNS
REPRESENT READINGS
BEYOND TESTER LIMITS
AFTER
BEFORE
TORQUE (mg-mm)
(Thousands)
200
180
160
140
120
100
80
60
40
20
0
MPB 1
BARDEN 1
FAG 1
MPB 2
BARDEN 2
FAG 2
SIDE 1 & SIDE 2

MPB TORQUE VALUES

CO.	BRG	TEST SEQ.	SIDE # 1 ART	SIDE # 1 PRT	SIDE # 1 AHW	SIDE # 1 MHW	SIDE # 2 ART	SIDE # 2 PRT	SIDE # 2 AHW	SIDE # 2 MHW
MPB	1	AFTER	7581	40663	17539	72954	21358	49205	25845	86250
MPB	1	BEFORE	1633	4299	1215	6792	4005	12442	1151	19811
MPB	1	DIFF.*	5948 *	36364 *	16324 *	66162 *	17353 *	36763 *	24694	66439
MPB	2	AFTER	11766	38447	13868	51477	12002	46833	11799	67159
MPB	2	BEFORE	1345	3329	877	4811	4523	12422	878	13301
MPB	2	DIFF.*	10421 *	35118 *	12991 *	46666 *	7479 *	34411 *	10921	53858
MPB	3	AFTER	6609	2678	8716	41590	6146	28623	9595	49431
MPB	3	BEFORE	1379	2411	883	3396	1900	3054	890	2547
MPB	3	DIFF.*	5230 *	267 *	7833 *	38194 *	4246 *	25569 *	8705	46884
MPB	4	AFTER	7095	46635	12420	66818	7286	43551	16083	70568
MPB	4	BEFORE	2528	4998	1111	5094	1699	3433	1005	3679
MPB	4	DIFF.*	4567 *	41637 *	11309 *	61724 *	5587 *	40118 *	15078	66889
MPB	5	AFTER	10635	47287	19434	70909	7394	39194	14028	54545
MPB	5	BEFORE	1934	4070	1045	5660	1737	3575	978	4528
MPB	5	DIFF.*	8701 *	43217 *	18389 *	65249 *	5657 *	35619 *	13050	50017
MPB	6	AFTER	8087	40751	17869	61704	8380	45478	17771	71590
MPB	6	BEFORE	1911	3770	1058	4811	1768	3519	893	3962
MPB	6	DIFF.*	6176 *	36981 *	16811 *	56893 *	6612 *	41959 *	16878	67628
MPB AV.		AFTER	8628	36076	14974	60908	10427	42147	15853	66591
MPB AV.		BEFORE	1788	3813	1031	5094	2605	6408	966	7971
MPB AV.		DIFF.*	6840 *	32263 *	13942 *	55814 *	7822 *	35739 *	14887 *	58610

* CALCULATED DIFFERENCE = (AFTER - BEFORE)

BARDEN TORQUE VALUES

O.	BRG	TEST SEQ.	SIDE # 1 ART	PRT	AHW	MHW	SIDE # 2 ART	PRT	AHW	MHW
ARD	1	AFTER	15973	87341	23026	110795	9470	65515	22204	97159
ARD	1	BEFORE	2500	4000	1000	8000	2000	10000	1000	4500
ARD	1	DIFF.*	13473 *	83341 *	22026 *	102795 *	7470 *	55515 *	21204 *	92659
ARD	2	AFTER	56323	121652	12476	282954	19244	103788	44238	294886
ARD	2	BEFORE	2500	5500	1000	6500	2500	6500	1000	8000
ARD	2	DIFF.*	53823 *	116152 *	11476 *	276454 *	16744 *	97288 *	43238 *	286886
ARD	3	AFTER	15633	81526	26793	114204	16811	87156	19943	110795
ARD	3	BEFORE	2750	9500	1500	1400	2500	8500	1500	1300
ARD	3	DIFF.*	12883 *	72026 *	25293 *	112804 *	14311 *	78656 *	18443 *	109495
ARD	4	AFTER	10820	36188	12652	42613	7071	26178	8965	37500
ARD	4	BEFORE	2000	6500	1000	7000	1000	5000	1000	7000
ARD	4	DIFF.*	8820 *	29688 *	11652 *	35613 *	6071 *	21178 *	7965 *	30500
ARD	5	AFTER	63811	124965	7802	277840	5546	89905	17811	281250
ARD	5	BEFORE	1500	4500	1000	6000	2000	5000	1000	6000
ARD	5	DIFF.*	62311 *	120465 *	6802 *	271840 *	3546 *	84905 *	16811 *	275250
ARD	6	AFTER	11556	44617	18540	66477	10772	58731	19632	83522
ARD	6	BEFORE	1500	4500	1000	8000	2000	8000	1000	6000
ARD	6	DIFF.*	10056 *	40117 *	17540 *	58477 *	8772 *	50731 *	18632 *	77522
ARD	AV.	AFTER	29019	82714	16881	149147	11485	71878	22132	150852
ARD	AV.	BEFORE	2125	5750	1083	6150	2000	7167	1083	5467
ARD	AV.	DIFF.*	26894 *	76964 *	15798 *	142997 *	9485 *	64711 *	21048 *	145385

* CALCULATED DIFFERENCE = (AFTER - BEFORE)

FAG TORQUE VALUES

CO.	BRG	TEST SEQ.	SIDE # 1 ART	SIDE # 1 PRT	SIDE # 1 AHW	SIDE # 1 MHW	SIDE # 2 ART	SIDE # 2 PRT	SIDE # 2 AHW	SIDE # 2 MHW
FAG	1	AFTER	----	----	----	----	----	----	----	----
FAG	1	BEFORE	3609	41436	17215	74705	3549	45856	19466	74705
FAG	1	DIFF.	----	----	----	----	----	----	----	----
FAG	2	AFTER	----	----	----	----	----	----	----	----
FAG	2	BEFORE	3776	40054	18712	63529	4173	39659	18628	65294
FAG	2	DIFF.	----	----	----	----	----	----	----	----
FAG	3	AFTER	----	----	----	----	----	----	----	----
FAG	3	BEFORE	3904	46432	18423	74117	3991	35763	20950	64117
FAG	3	DIFF.	----	----	----	----	----	----	----	----
FAG	4	AFTER	----	----	----	----	----	----	----	----
FAG	4	BEFORE	4340	39474	18306	63529	4014	36584	18430	61764
FAG	4	DIFF.	----	----	----	----	----	----	----	----
FAG	5	AFTER	----	----	----	----	----	----	----	----
FAG	5	BEFORE	4178	43077	18090	80000	3907	45757	20414	85294
FAG	5	DIFF.	----	----	----	----	----	----	----	----
FAG	6	AFTER	----	----	----	----	----	----	----	----
FAG	6	BEFORE	3727	29025	16166	52352	3867	35377	18022	58823
FAG	6	DIFF.	----	----	----	----	----	----	----	----
FAG AV.		AFTER	----	----	----	----	----	----	----	----
FAG AV.		BEFORE	3922	39916	17818	68038	3916	39832	19318	68333
FAG AV.		DIFF.	----	----	----	----	----	----	----	----

No "After" values are available because broken and dislocated retainers created torque readings beyond the capacity of MPB Torque Testers.

FAG RETAINER

FACE WEAR FROM RETAINERS
LODGED BETWEEN THE BALLS OF TWO ADJACENT BEARINGS

Wear Groove - Ball Pocket - 50X

Wear Groove - Retainer Prong - 20X

Wear Groove - Back Face - 20X

Wear Groove - Back Face - 50X

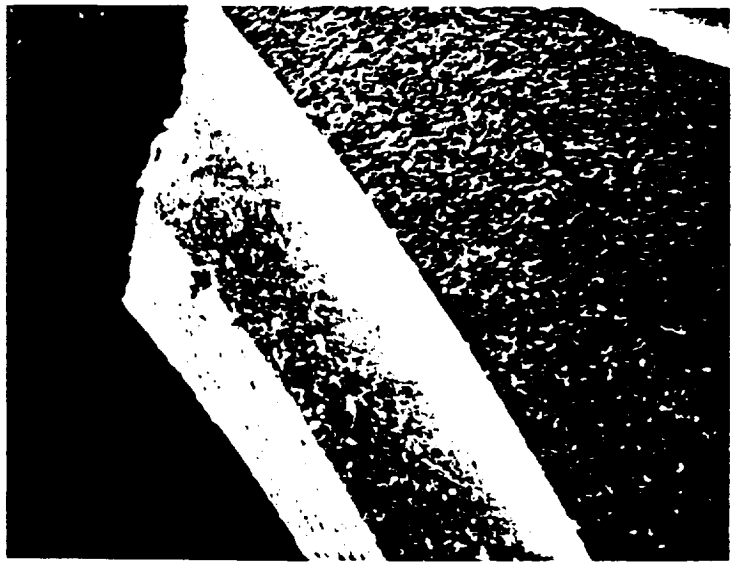

FAG BEARING

INNER RING WEAR
BALL WEAR

Inner Ring Wear - 20X

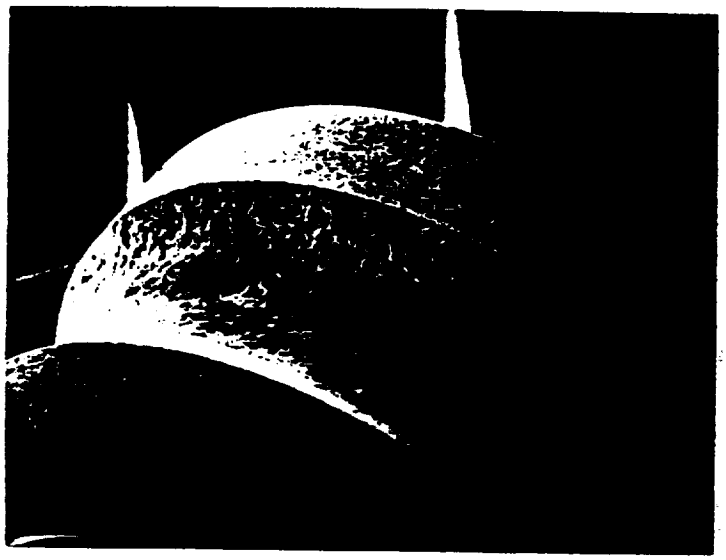

Inner Ring Wear - 50X

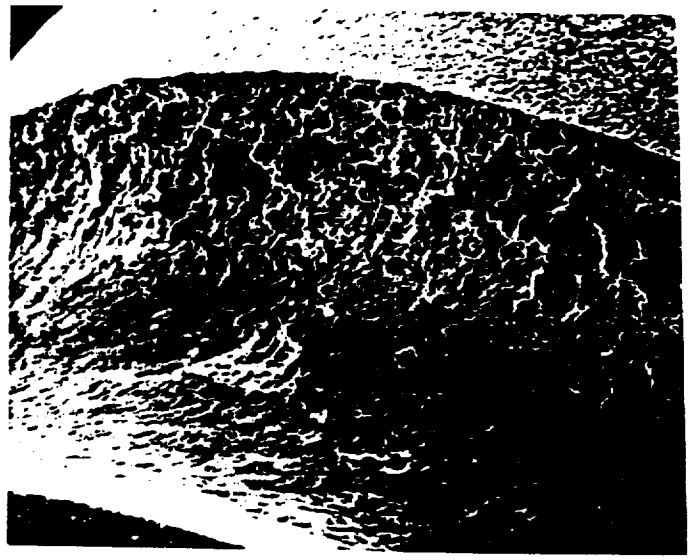

Severe Ball Wear - 20X

Severe Ball Wear - 50X

BARDEN BEARINGS

RETAINER POCKET WEAR

Retainer Pocket Wear - 20X

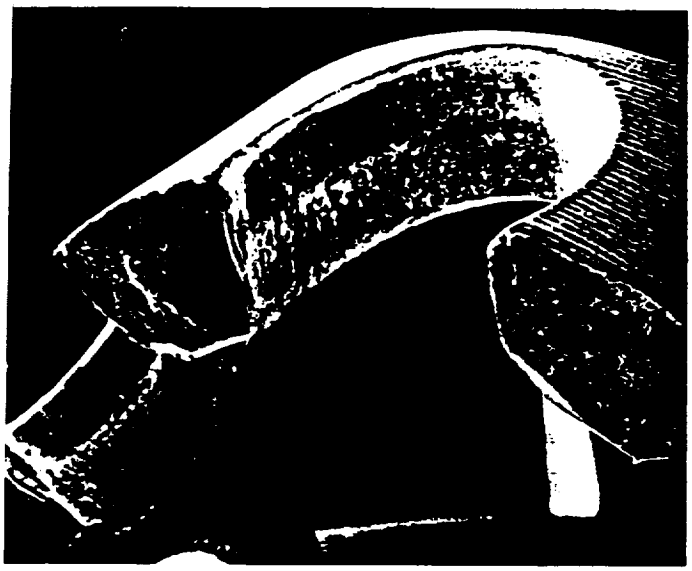

Retainer Pocket Wear - 50X

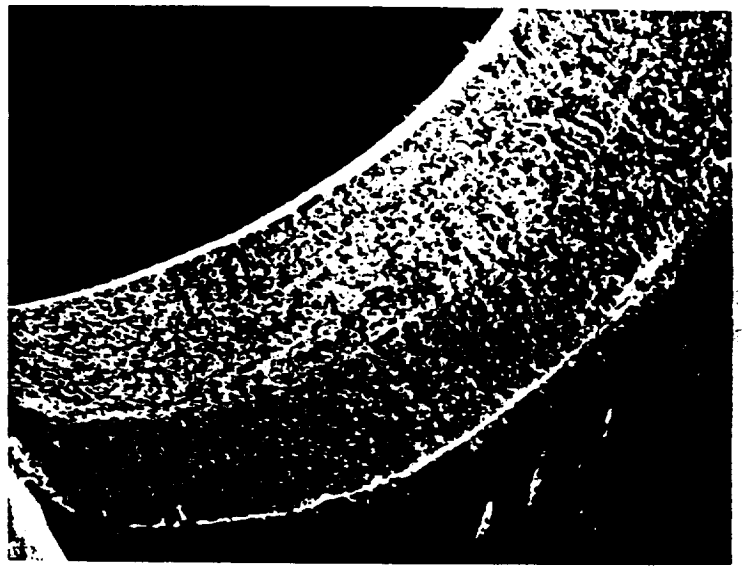

BARDEN BEARING

BALL AND RACEWAY CONTAMINATION WITH RETAINER DEBRIS

Ball Contamination - 20X

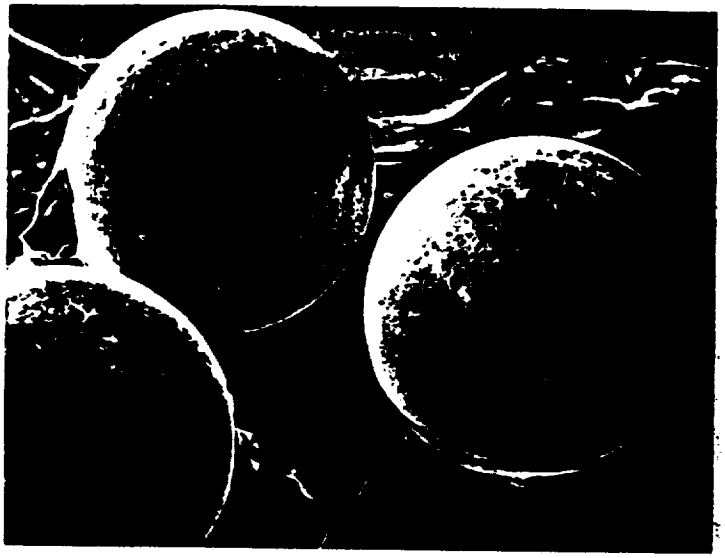

Ball Contamination - 50X

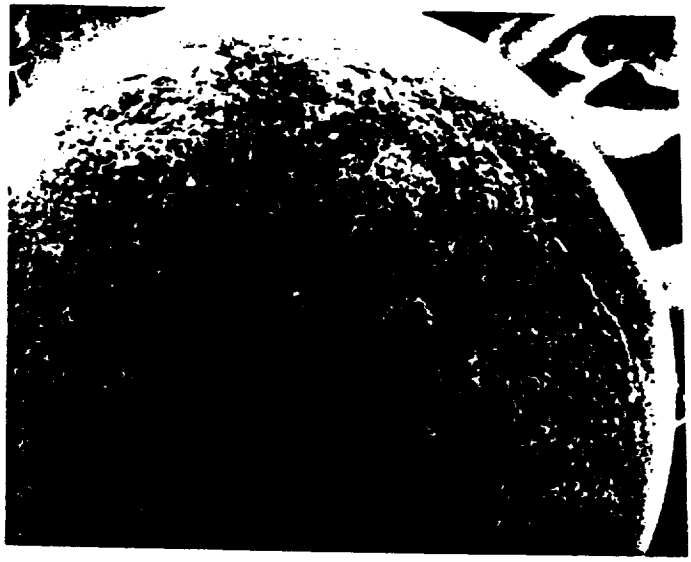

Inner Raceway Contamination - 20X

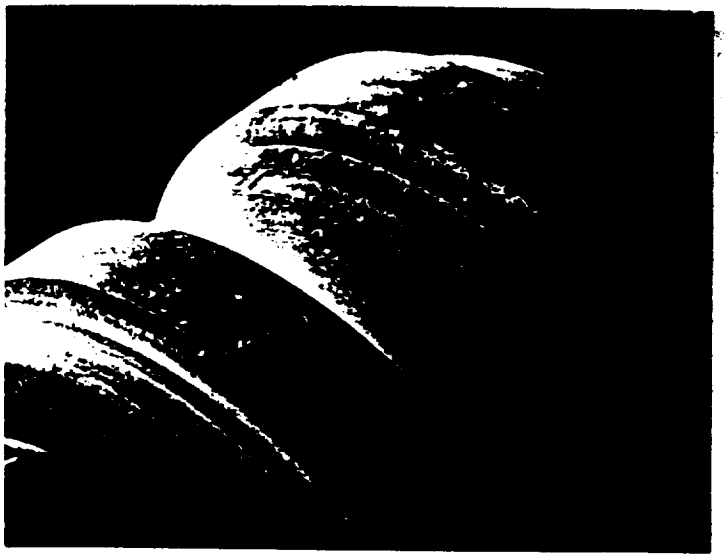

Inner Raceway Contamination - 50X

BARDEN BEARING

BEARING #6 - SINUSOIDAL WEARBAND WITH CONTAMINATION BRINELLING (DENTS)

Bearing #6 Inner Raceway - 20X

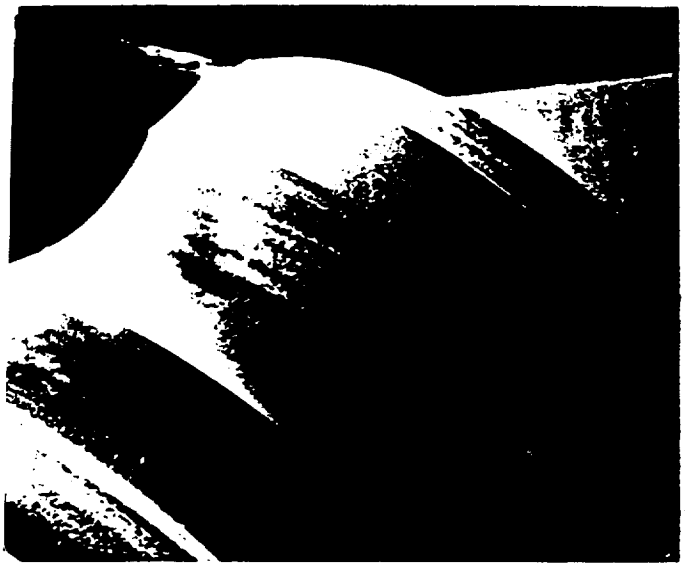

Bearing #6 Inner Raceway - 50X

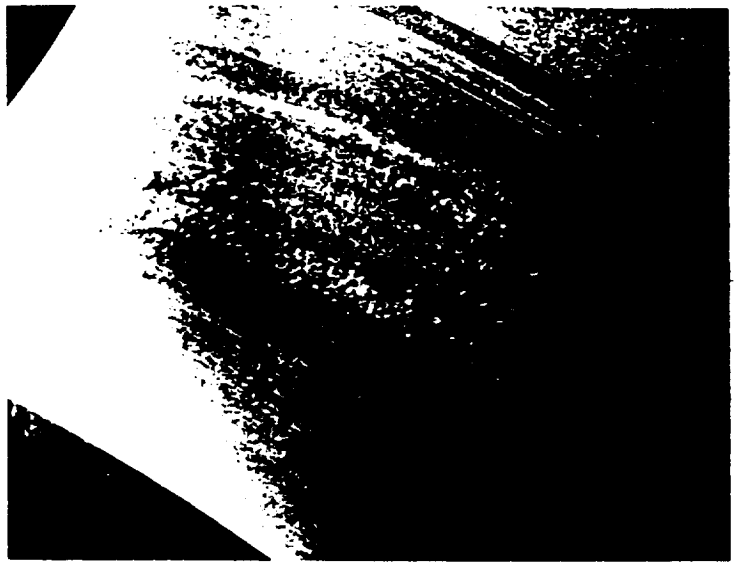

Bearing #6 Inner Raceway - 500X

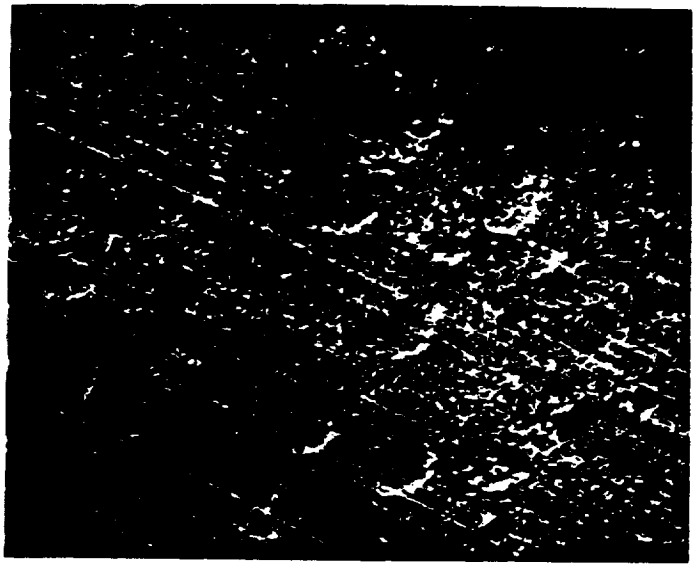

Bearing #6 Inner Raceway - 1KX

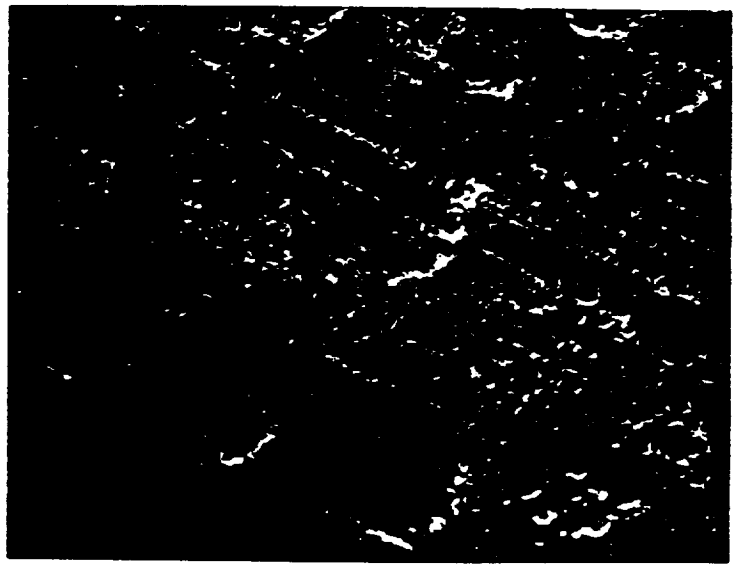

MPB BEARING

SR3MCK TEST FIXTURE #1
RETAINERS

Retainer Pocket Burnish (wear) - 50X

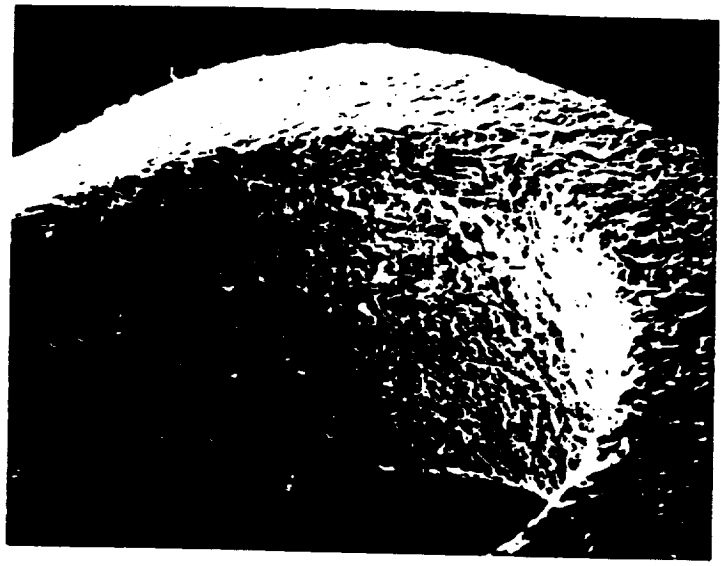

Retainer Pocket Burnish (wear) - 20X

Retainer Pocket Burnish (wear) - 50X

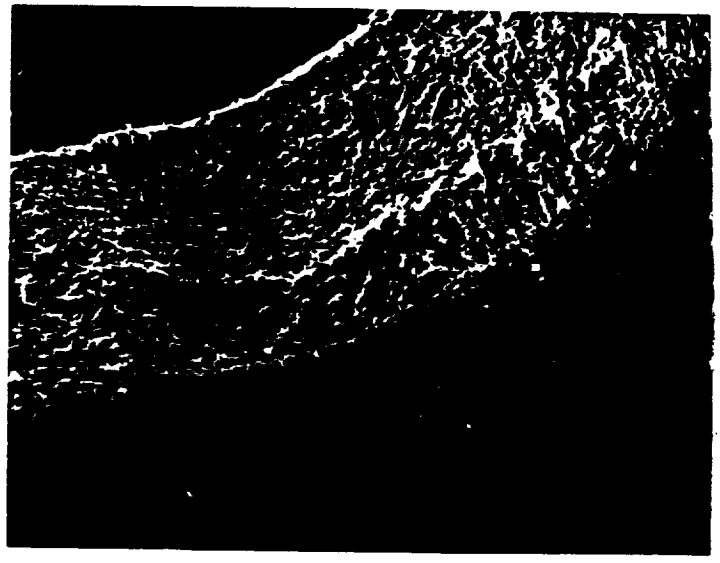

MPB BEARING

SR3MCK TEST FIXTURE #1
INNER RINGS

Inner Raceway Before Cleaning - 200X

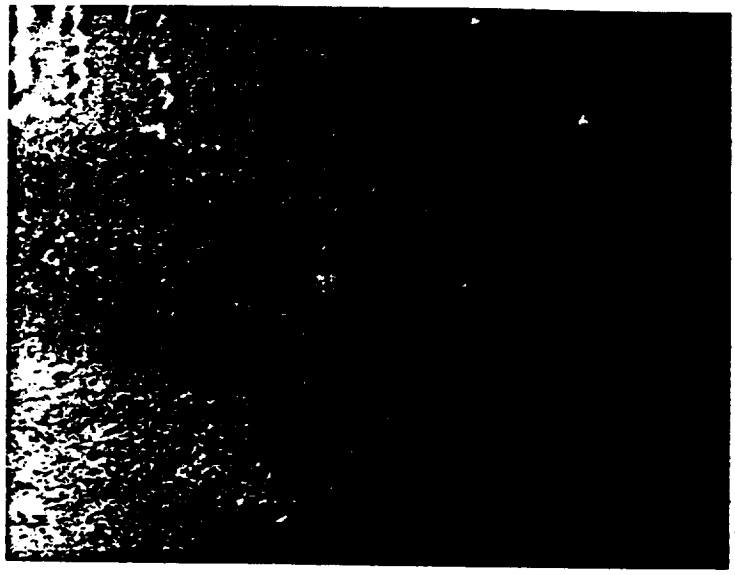

Inner Raceway After Cleaning - 20X

Inner Raceway After Cleaning - 50X

MPB BEARING

SR3MCK TEST FIXTURE #1
BALLS

Balls - 20X

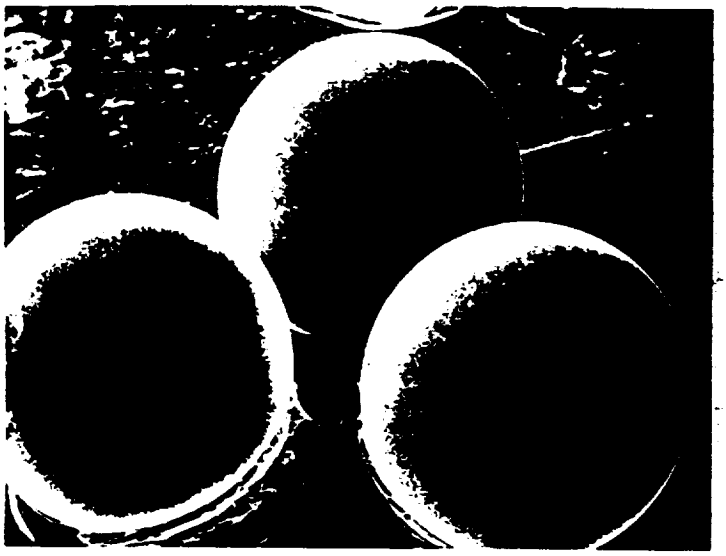

Ball Before Cleaning - 50X

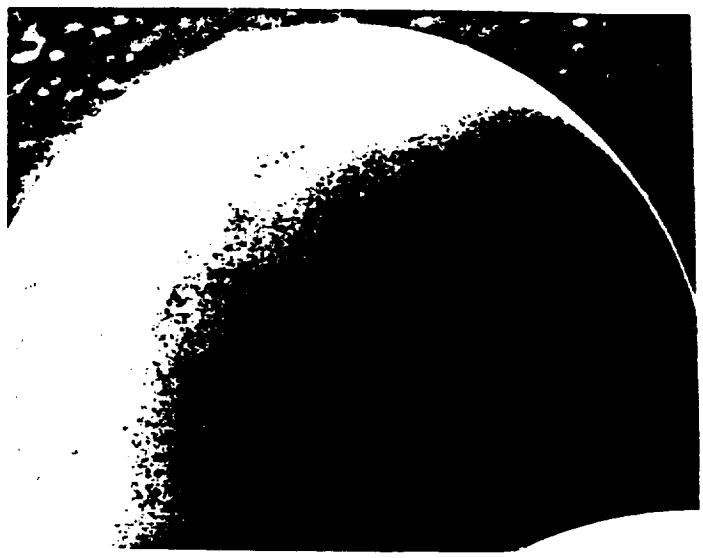

MPB BEARING

SR3MCK TEST FIXTURE #2
INNER RACEWAY

Inner Raceway - 20X

Inner Raceway - 50X

Inner Raceway Displaced Metal - 500X

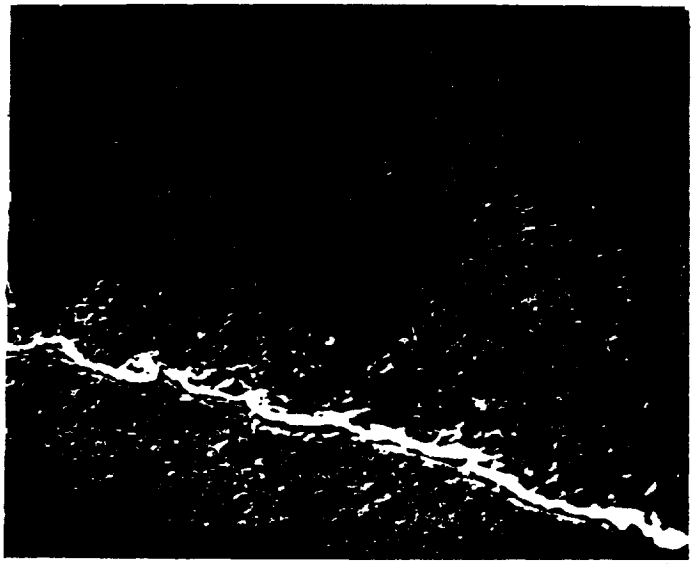

Inner Raceway Displaced Metal - 2KX

MPB BEARING

SR3MCK TEST FIXTURE #2
RETAINER

Retainer Ball Pocket (no wear) - 20X

Retainer Ball Pocket (no wear) - 50X

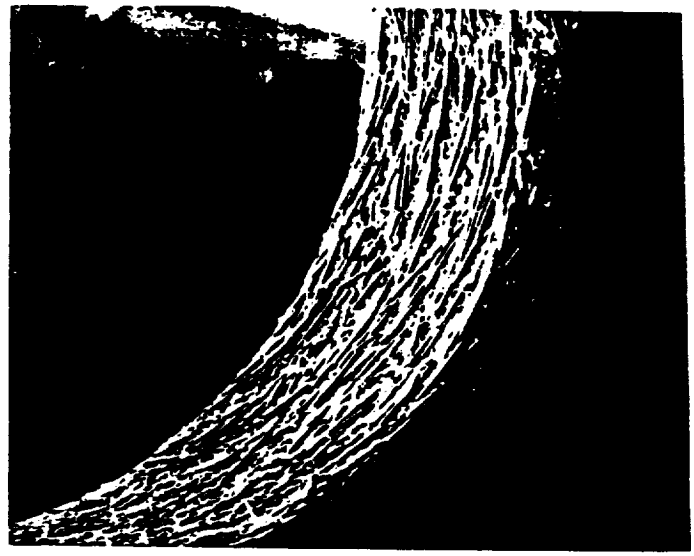

MPB BEARING

SR3MCK TEST FIXTURE #2
BALL SURFACE

Ball Surface - 20X

Ball Surface - 50X

Ball Wear Band - 500X

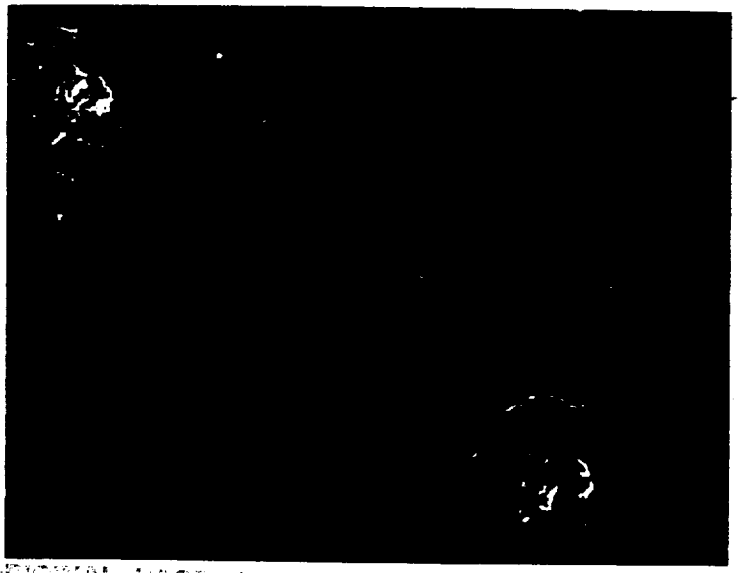

MPB BEARING

K308 TEST FIXTURE #1
INNER RING AND BALLS

Inner Raceway Wear Band - 20X

Inner Raceway Wear Band - 50X

Balls (no wear) - 20X

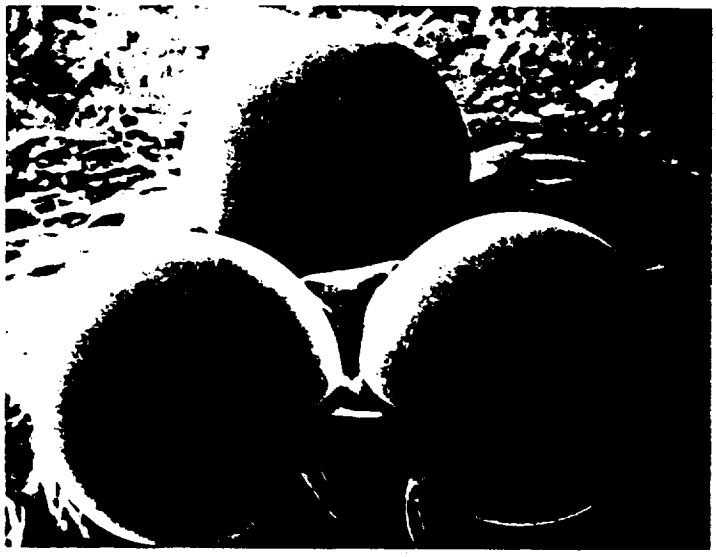

Ball (no wear) - 50X

MPB BEARING

K308 TEST FIXTURE #1
RETAINER

Retainer O.D. Wear - 20X

Retainer O.D. Wear - 50X

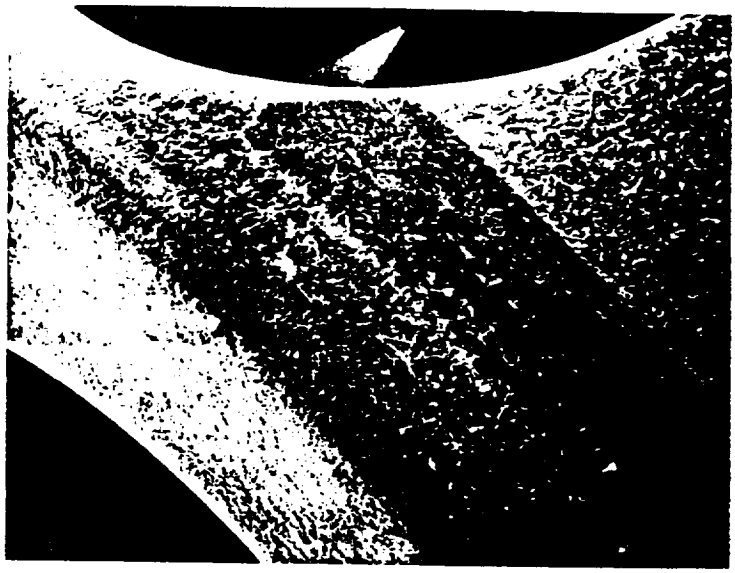

Retainer Pocket Wear - 20X

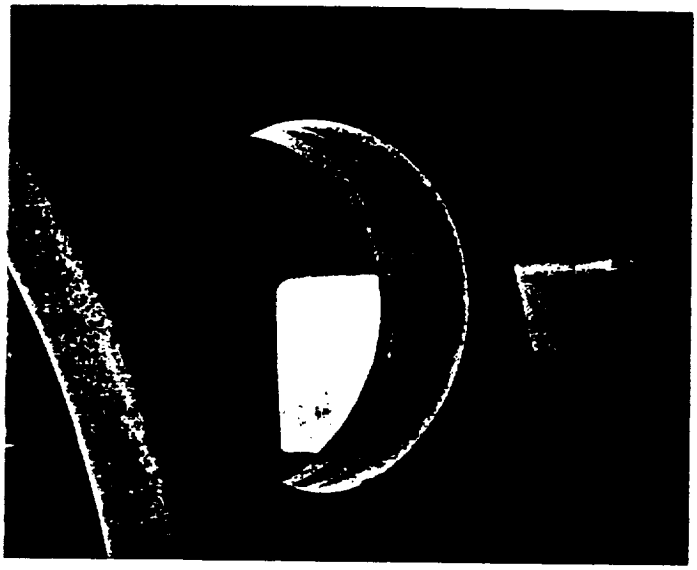

Retainer Pocket Wear - 50X

MPB BEARING

K308 TEST FIXTURE #2
BALLS AND INNER RING

Balls (cleaned - no damage) - 20X

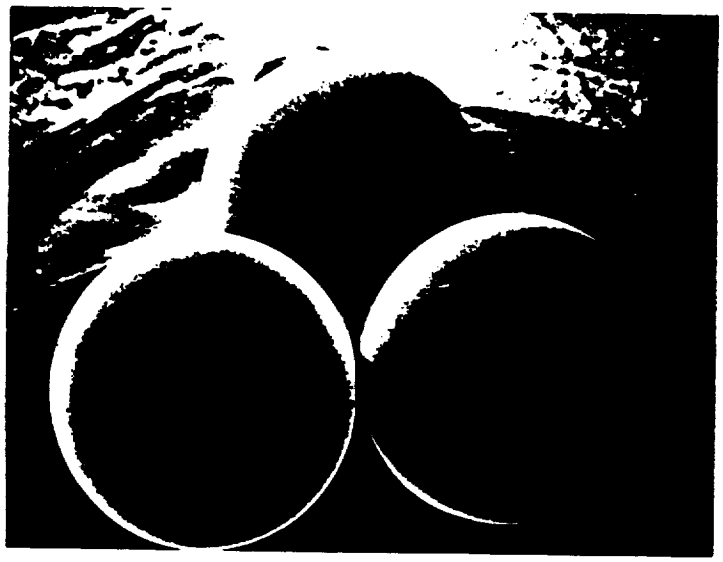

Balls (cleaned - no damage) - 50X

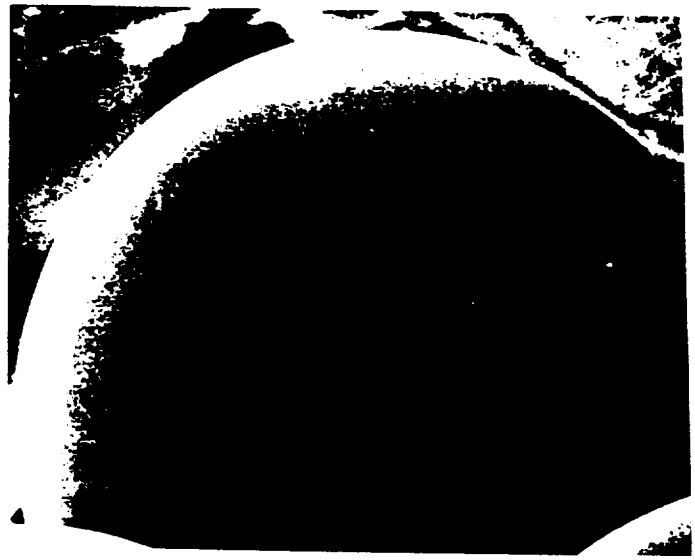

Inner Raceway Wear Band - 50X

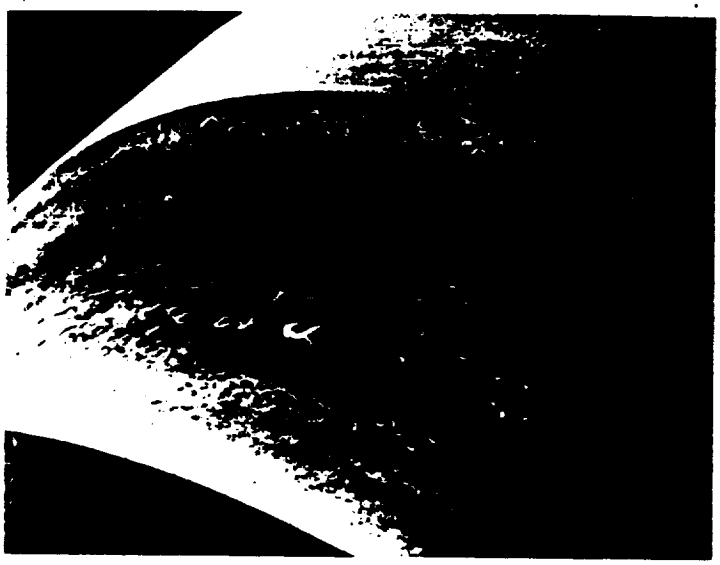

Inner Raceway Bronze Colored Debris - 1KX

MPB BEARING

K308 TEST FIXTURE #2
RETAINER

Retainer O.D. & Pocket Wear - 20X

Retainer O.D. Wear - 50X

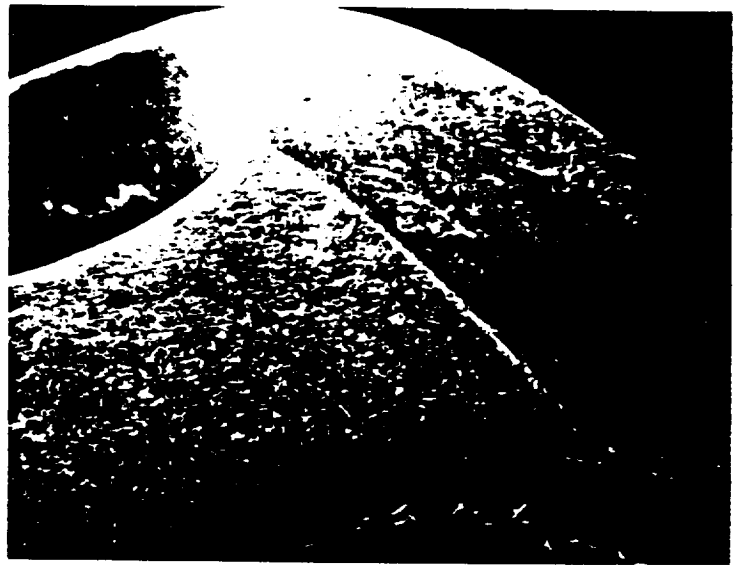

Retainer O.D. & Pocket Wear - 20X

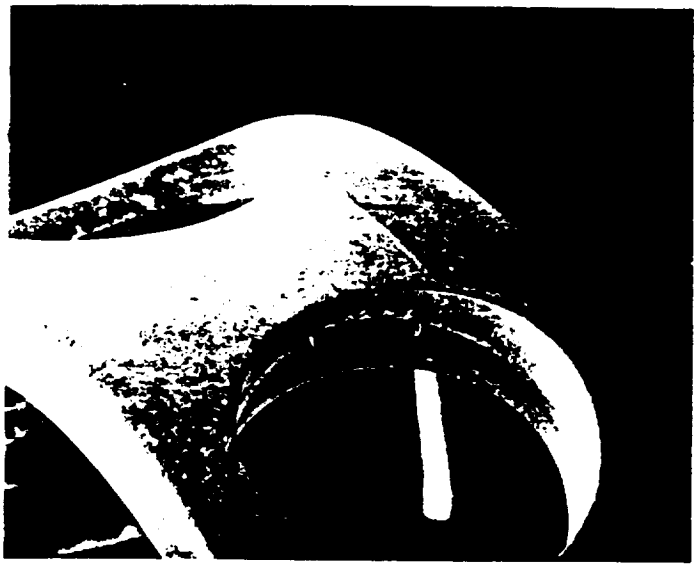

Retainer Pocket Wear - 50X

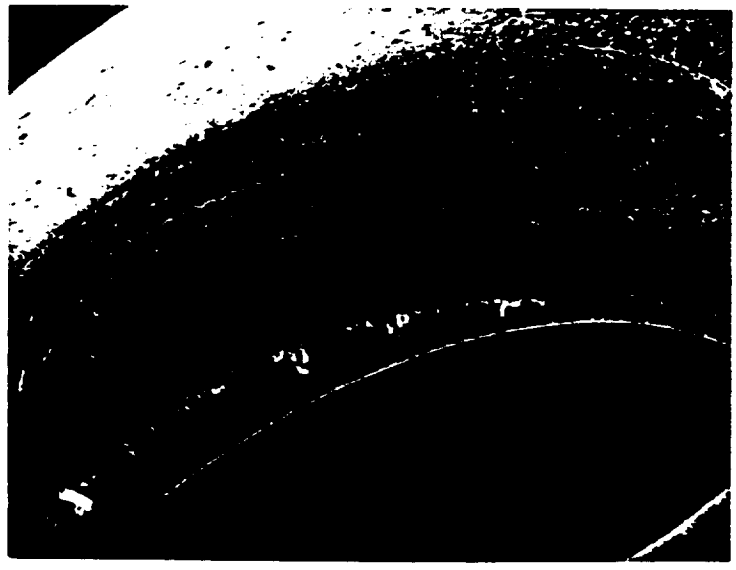

REPORT DOCUMENTATION PAGE

Form Approved
OMB No. 0704-0188

1. AGENCY USE ONLY *(Leave blank)*	2. REPORT DATE	3. REPORT TYPE AND DATES COVERED
	December 1991	Contractor Report

4. TITLE AND SUBTITLE

High Efficiency Pump for Space Helium Transfer

5. FUNDING NUMBERS

NAS2-12950

6. AUTHOR(S)

Robert Hasenbein, Michael G. Izenson, Walter L. Swift, and Herbert Sixsmith

7. PERFORMING ORGANIZATION NAME(S) AND ADDRESS(ES)

Creare Inc.
P. O. Box 71
Hanover, NH 03755

8. PERFORMING ORGANIZATION REPORT NUMBER

A-92050

9. SPONSORING/MONITORING AGENCY NAME(S) AND ADDRESS(ES)

Ames Research Center
Moffett Field, CA 94035-1000

10. SPONSORING/MONITORING AGENCY REPORT NUMBER

NASA CR-177595

11. SUPPLEMENTARY NOTES

Point of Contact: Peter Kittle, Ames Research Center, MS 244-10, Moffett Field, CA 94035-1000; (415) 604-4297 or FTS 464-4297

12a. DISTRIBUTION/AVAILABILITY STATEMENT

Unclassified — Unlimited
Subject Category 37

12b. DISTRIBUTION CODE

13. ABSTRACT *(Maximum 200 words)*

A centrifugal pump has been developed for the efficient and reliable transfer of liquid helium in space. The pump can be used to refill cryostats on orbiting satellites which use liquid helium for refrigeration at extremely low temperatures. The pump meets the head and flow requirements of on-orbit helium transfer: a flow rate of 800 L/hr at a head of 128 J/kg. The overall pump efficiency at the design point is 0.45. The design head and flow requirements are met with zero net positive suction head, which is the condition in an orbiting helium supply Dewar. The mass transfer efficiency calculated for a space transfer operation is 0.99. Steel ball bearings are used with gas fiber-reinforced teflon retainers to provide solid lubrication. These bearings have demonstrated the longest life in liquid helium endurance tests under simulated pumping conditions. Technology developed in the project also has application for liquid helium circulation in terrestrial facilities and for transfer of cryogenic rocket propellants in space.

14. SUBJECT TERMS	15. NUMBER OF PAGES
Centrifugal, Pumps, Liquid helium, Space transfer	99
	16. PRICE CODE: A05

17. SECURITY CLASSIFICATION OF REPORT	18. SECURITY CLASSIFICATION OF THIS PAGE	19. SECURITY CLASSIFICATION OF ABSTRACT	20. LIMITATION OF ABSTRACT
Unclassified	Unclassified		